Linköping Studies in Science and Technology
Dissertation No. 2127

On Subscale Flight Testing

Cost-Effective Techniques for Research and Development

Alejandro Sobron

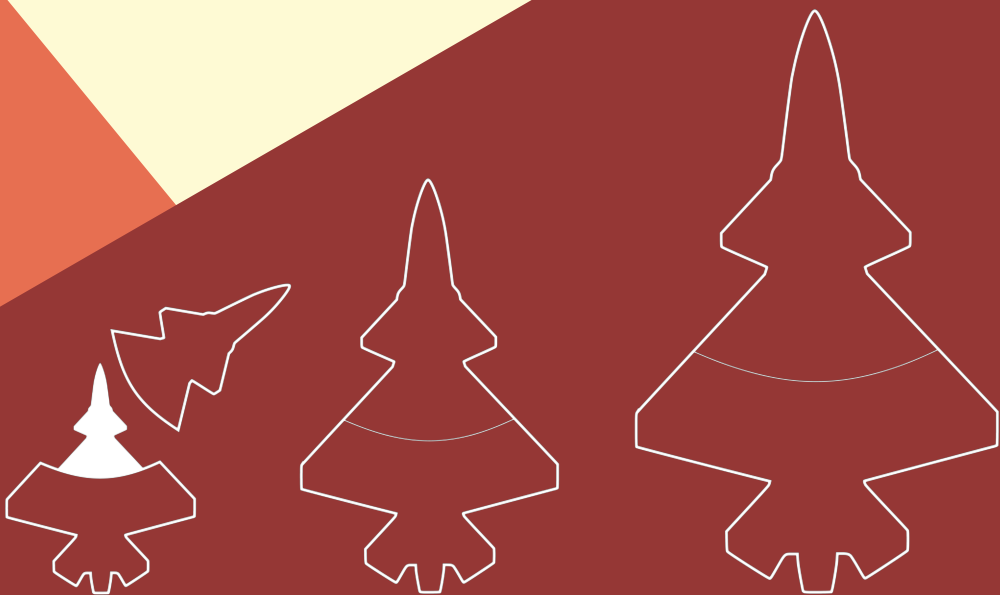

LINKÖPING UNIVERSITY

Linköping Studies in Science and Technology
Dissertations No. 2127

On Subscale Flight Testing

Cost-Effective Techniques for Research and Development

Alejandro Sobron

LINKÖPING UNIVERSITY

Division of Fluid and Mechatronic Systems
Department of Management and Engineering
Linköping University, SE–581 83 Linköping, Sweden

Linköping 2021

On Subscale Flight Testing
Cost-Effective Techniques for Research and Development

ISBN 978-91-7929-691-9
ISSN 0345-7524

Cover: Alejandro Sobron, 2021

Distributed by:
Division of Fluid and Mechatronic Systems
Department of Management and Engineering
Linköping University
SE-581 83 Linköping, Sweden

Printed in Sweden by LiU-Tryck, Linköping 2021.

To my family

> La experiencia, madre de las ciencias todas.
> (Experience, the mother of all knowledge.)

Don Quixote by Miguel de Cervantes (1605),
often quoted by my father when something
went unexpectedly wrong.

Abstract

Experiments with downscaled or subscale physical models have traditionally been an essential source of information in aerospace research and development. Physical models are very effective at revealing unforeseen issues and providing confidence in design predictions or hypotheses. While computational methods are predominant nowadays, experimental methods such as wind-tunnel testing still play a critical role as verification and calibration tools. However, wind-tunnel testing is often too expensive, too slow or unavailable during aircraft conceptual design or the early development of immature technologies. It is here that testing free-flight subscale models – referred to as subscale flight testing (SFT) – could be an affordable and low-risk complementary method for obtaining both qualitative and quantitative information.

Disruptive technological innovations have significantly altered both the cost and the capabilities of SFT during recent decades. Such innovations include the price performance of miniaturised electronics and communication systems, advances in rapid prototyping techniques and materials, the availability of specialised components from the booming drone market and the rapid development of open-source software and hardware, allowing for sophisticated and capable test platforms at a fraction of the cost compared to a few decades ago. It is therefore necessary to re-evaluate the benefits and limitations of SFT, as well as its role in contemporary aircraft design and technology development processes.

This dissertation aims to contribute to knowledge on the use of the SFT method for research and development, focusing on low-cost, time-efficient solutions that are particularly suitable for small organisations and limited resources. The method's challenges, needs and limitations are identified through a critical study of the physical similarity principles, an in-depth review of the experiences of other organisations, and practical field experiments with different subscale models in real conditions. Some of the proposed solutions include a low-cost data acquisition system with custom-made instruments, a novel method for automatic execution of excitation manoeuvres, specific techniques and parameter-identification methods for flight testing in confined airspaces, and a set of tools for the analysis and visualisation of flight data. The obtained results may serve as proof of the current possibilities to evaluate and demonstrate new technology through SFT using very limited economic and human resources.

Populärvetenskaplig sammanfattning

Flygprov med nedskalade prototyper

Kostnadseffektiva lösningar inom forskning och utveckling

Experiment med nedskalade fysiska modeller har traditionellt sett varit en ovärderlig källa av information inom flyg- och rymdforskning. Fysiska modeller är mycket användbara för att upptäcka oförutsägbara problem och för att styrka trovärdigheten i beräkningar och antaganden. I en tid då datorbaserade simuleringar är ledande spelar fortfarande vindtunnelprov en avgörande roll som kalibrerande och verifierande verktyg. Dock är vindtunnelprov en kostsam, tidskrävande och ofta otillgänglig metod i ett konceptuellt designstadium. Det är här användningen av nedskalade fysiska modeller kommer till användning. Flygprov med nedskalade prototyper, mer specifikt kallade ”Subscale Flight Testing” (SFT), kan erbjuda en mindre kostsam och riskabel testmetod som komplement till övriga metoder. Detta kan bidra med både kvalitativ och kvantitativ kunskap.

Nya teknologiska framsteg har markant förändrat både kostnaden och möjligheterna med SFT. Många faktorer har bidragit till detta; bland annat prestandan i förhållande till kostnaden inom miniatyriserad elektronik och kommunikationssystem, framstegen inom att snabbt framställa prototyper inom teknik och material, tillgängligheten till specialiserade komponenter inom den växande marknaden runt drönare samt den markanta utvecklingen av opensourcetillgänglig hård- och mjukvara. Alla dessa faktorer bidrar till möjligheten att skapa sofistikerade och användbara plattformar för enbart en bråkdel av kostnaden som dessa tekniker skulle ha erfordrat några årtionden tillbaka i tiden. Det är därför viktigt att åter utvärdera för- och nackdelarna med SFT, samt dess roll inom utvecklingsprocessen inom modern flygplanskonstrution och teknologi.

Den här avhandlingen syftar till att bidra med kunskaper runt användning av SFT inom forskning och utveckling. Fokus ligger på kostnads- och tidseffektiva lösningar inom små organisationer eller där kostnaderna måste begränsas. Metodens utmaningar, behov och begränsningar identifieras genom en kritisk studie av de fysiska likhetsprinciperna, en djupdykning inom erfarenheter från andra organisationer samt genom praktiska fältexperiment med olika typer av nedskalade fysiska modeller i riktiga förhållanden. Några av de föreslagna lösningarna innefattar ett kostnadseffektivt datainsamlingsprogram med specialanpassade instrument, en ny metod för att automatiskt utföra testmanövrar, specifika tekniker och parameteridentifikationsmetoder inom flygtestning i begränsat luftrum, samt en samling av verktyg för att analysera och visualisera flygdata. De samlade resultaten kan fungera som bevis för de nuvarande möjligheterna att utvärdera och demonstrera ny teknologi genom SFT under begränsade resurser; både ekonomiska och mänskliga.

Acknowledgements

There is not enough space here to name everyone to whom I am deeply grateful, but I would like to mention at least some of them.

A big thank you to my present, former and visiting colleagues at the Division of Fluid and Mechatronic Systems (Flumes) at Linköping University, a truly unique environment where I had the joy of carrying out this work. Thanks for letting me absorb a little bit of your vast expertise and for all the enriching conversations, both professional and off-topic.

I am especially grateful to my supervisors Professor Petter Krus and Dr David Lundström, who trusted me with this task and placed full confidence in my abilities. Thanks for your guidance and your unfailing commitment through the good times and the less good times. David, in addition to being quite generous with his time, has also played a fundamental role in all the many practical experiments.

This project would definitely not have been the same without the support, inspiration and enlightening input from Dr Christopher Jouannet at Saab Aeronautics. I must also acknowledge the valuable contributions from Dr Roger Larsson and Dr Ingo Staack. It has been a great pleasure working with all of you.

Despite the support of all these knowledgeable researchers, not a single plane would have taken off or a page been written without the invaluable help from the university's skilled workshop and administrative staff. A very special mention goes to Rita Enquist, who is always glad to guide me out of any bureaucratic difficulties.

My sincere gratitude also goes to the students that I had the pleasure to supervise during their thesis work. Some of you made significant contributions to this project, and in all cases the learning experience was mutual.

I would also like to extend my gratitude to the Swedish National Aeronautics Research Programme (NFFP), the Swedish Aerospace Research Centre (SARC) and the Swedish-Brazilian Research and Innovation Centre (CISB) for their financial support, training opportunities and for giving me the opportunity to carry out part of this work at the Instituto Tecnológico de Aeronáutica (ITA) in Brazil. It was there that I learnt what hospitality and generosity mean.

A special mention to Professor Luiz Góes, Professor Roberto Gil A. da Silva and Leonardo Nepomuceno. Obrigado!

Along this journey, some of my fellow PhD students have become true friends and have given me unforgettable memories. Thanks in particular to Viktor Larsson, Robert Hällqvist, Athanasios Papageorgiou, Alexandra Oprea, Katharina Baer, Raghu Chaitanya and Jörg Schminder.

No words can truly express how much I appreciate the everlasting patience and understanding of my little family: Gabrielle and Kasper. I recognise that this thesis stole much of the time that should have been yours. The least I can do is to dedicate it to you.

Finally, my deepest gratitude goes to my parents José María and Emma. Your love and unconditional encouragement, even from afar, have always pushed me forward. This thesis is also yours.

Linköping, April 2021

Alejandro Sobron

Abbreviations

ADC	analog-to-digital converter
AGL	above ground level
ALAN	Aircraft Log Analysis
AOA	angle-of-attack
AOS	angle-of-sideslip
BFF	body freedom flutter
BVLOS	beyond visual line of sight
BWB	blended wing body
CAD	computer-aided design
CFD	computational fluid dynamics
CG	centre of gravity
COTS	commercial off-the-shelf
EKF	extended Kalman filter
EVLOS	extended visual line of sight
FCS	flight control system
FLUMES	Division of Fluid and Mechatronic Systems
GFF	Generic Future Fighter
GNSS	Global Navigation Satellite System
HPA	human-powered aircraft
I/O	input/output
IMU	inertial measurement unit
MEMS	micro-electro-mechanical system
NASA	National Aeronautics and Space Administration of the United States
PCB	printed circuit board
R/C	radio control
RPA	remotely piloted aircraft
RPAS	remotely piloted aircraft system
SFT	subscale flight testing
STOL	short take-off and landing
TOM	take-off mass
TRL	technology readiness level

UAS	unmanned aircraft system
UAV	unmanned aerial vehicle
VLM	vortex lattice method
VLOS	visual line of sight
VTOL	vertical take-off and landing

Nomenclature

A	Area	[m^2]
a	Linear acceleration	[m s^{-2}]
α	Angle of attack	[$^\circ$ or rad]
α'	Generalised aircraft attitude relative to airstream	[$^\circ$ or rad]
AR	Aspect ratio	[-]
β	Angle of sideslip	[$^\circ$ or rad]
c	Speed of sound (in the pertinent fluid)	[m s^{-1}]
D	Drag force	[N]
δ	Control surface deflection angle	[$^\circ$ or rad]
E	Modulus of elasticity	[Pa]
e	Span efficiency factor	[-]
EI	Bending stiffness	[N m^2]
F	Force	[N]
Fr	Froude number	[-]
g	Acceleration due to gravity	[m s^{-2}]
GJ	Torsional stiffness	[N m^2]
I	Mass moment of inertia	[kg m^2]
L	Lift force	[N]
l	Characteristic linear dimension	[m]
m	Mass	[kg]
M	Mach number (context dependent)	[-]

M	Moment (context dependent)	[N m]
μ	Dynamic (absolute) viscosity	[Pa s]
ν	Kinematic viscosity	[m^2 s$^-1$]
Ω	Generalised angular rate	[rad s^{-1}]
ω	Frequency of oscillation	[rad s^{-1}]
$\dot{\Omega}$	Generalised angular acceleration	[rad s^{-2}]
$\bar{p}$	Static pressure	[Pa]
Re	Reynolds number	[-]
ρ	Mass density (of the pertinent fluid)	[kg m^{-3}]
σ	Surface tension per unit length	[N m^{-1}]
t	Time	[s]
τ	Time constant or reduced-time factor	[-]
V	Linear velocity	[m s^{-1}]
W	Weight force	[N]
$_\infty$	Indicates free-stream reference value	
$_{fs}$	Indicates full-scale value	
$_m$	Indicates model value	

Papers

The work presented in this thesis is based on the papers listed below, which will be referred to by their Roman numerals throughout the text. These papers, appended in chronological order, are reproduced in their original state with the exception of minor formatting changes. A short summary of each paper and the author's role in it is presented in Chapter 9.

[I] Alejandro Sobron, David Lundström, Ingo Staack, and Petter Krus. "Design and Testing of a Low-Cost Flight Control and Data Acquisition System for Unstable Subscale Aircraft". In: *30th Congress of the International Council of the Aeronautical Sciences*. Daejeon, South Korea, 2016.

[II] David Lundström, Alejandro Sobron, Petter Krus, Christopher Jouannet, and Roberto Gil Annes da Silva. "Subscale Flight Testing of a Generic Fighter Aircraft". In: *30th Congress of the International Council of the Aeronautical Sciences*. Daejeon, South Korea, 2016.

[III] Alejandro Sobron, David Lundström, Roger Larsson, Petter Krus, and Christopher Jouannet. "Methods for efficient flight testing and modelling of remotely piloted aircraft within visual line-of-sight". In: *31st Congress of the International Council of the Aeronautical Sciences*. Belo Horizonte, Brazil, 2018.

[IV] Roger Larsson, Alejandro Sobron, David Lundström, and Martin Enqvist. "A Method for Improved Flight Testing of Remotely Piloted Aircraft Using Multisine Inputs". In: *Aerospace* 7.9 (2020), p. 135. DOI: 10.3390/aerospace7090135.

[V] Alejandro Sobron, David Lundström, and Petter Krus. "A Review of Current Research in Subscale Flight Testing and Analysis of Its Main Practical Challenges". In: *Aerospace* 8.3 (2021), p. 74. DOI: 10.3390/aerospace8030074.

[VI] Leonardo Nepomuceno, Alejandro Sobron, Roberto Gil Annes da Silva, David Lundström, and Petter Krus. “Estimation of Lift Characteristics of a Subscale Fighter using Low-Cost Experimental Methods”. In: *Aircraft Engineering and Aerospace Technology* (2021). Submitted, under peer review.

This thesis is a continuation of the author’s licentiate thesis, titled “On Subscale Flight Testing: Applications in Aircraft Conceptual Design” (Linköping University, 2018). Publishing a licentiate thesis and obtaining a licentiate degree (120 ECTS credits) can be considered a step towards obtaining a doctoral degree (240 ECTS credits) in the Swedish postgraduate education system. The composition and subject of a licentiate thesis is typically similar to that of a doctoral thesis, and its aim is to summarise the author’s progress at the point where at least some of the research questions can already be tentatively answered. This doctoral thesis builds on the previously presented licentiate work and, therefore, reuses a significant part of the previously published information.

Other publications

The following publications are not directly included in this thesis, although they constitute an important part of the background.

[VII] Christopher Jouannet, David Lundström, Petter Krus, Alejandro Sobron, Roberto Gil Annes da Silva, Fernando Catalano, and Paulo Greco. “Aerodynamic database of a subscale demonstrator”. In: *35th AIAA Applied Aerodynamics Conference*. Denver, CO, USA, 2017.

[VIII] Alejandro Sobron, David Lundström, Petter Krus, Christopher Jouannet, and Luiz C. S. Góes. “Flight test design for remotely-piloted aircraft in confined airspace”. In: *6th CEAS Air and Space Conference, Aerospace Europe*. Bucharest, Romania, 2017.

[IX] Diego de Matos Monteiro, Leonardo Murilo Nepomuceno, Roberto Gil Annes da Silva, Marcos da Silva e Souza, Flávio José Silvestre, Petter Krus, and Alejandro Sobron. “Subscale Flight Test Model Development and Testing as a Tool for Unconventional Aircraft Design”. In: *6th CEAS Air and Space Conference, Aerospace Europe*. Bucharest, Romania: CEAS, 2017.

[X] Ingo Staack, Alejandro Sobron, and Petter Krus. “The whole truth about electric-powered flight for civil transportation : From Breguet to operational aspects”. In: *7th CEAS Air and Space Conference, Aerospace Europe Conference 2020*. Bordeaux, France: CEAS, 2020.

[XI] Alejandro Sobron, Ingo Staack, and Petter Krus. “The Role of Electric-Powered Flight in Real-World Commercial Operations”. In: *Making Aviation Environmentally Sustainable, 3rd ECATS Conference, Book of Abstracts*. Vol. 1. Gothenburg, Sweden, 2020.

[XII] Ingo Staack, Alejandro Sobron, and Petter Krus. “The Potential of Full-Electric Aircraft for Civil Transportation”. In: *CEAS Aeronautical Journal* (2021). Submitted, under peer review.

Contents

Appended Papers

1 Introduction

Experimental techniques have been the backbone of aeronautical technology ever since its birth. Aircraft are complex machines that also make use of complex natural phenomena which, in some cases, were anticipated and exploited long before they were completely understood. Some problems, such as the inherent nonlinearity of the Navier-Stokes equations that govern fluid dynamics, still remain unresolved and their study requires a combination of experimentation and numerical approximation.

Downscaled physical models, also referred to *subscale* models, have played an essential role in our attempts to understand the complex physics of flight. Aviation pioneers, such as the Wright brothers, performed systematic tests with subscale models during the early days of aircraft design [1]. Later on, placing captive subscale models inside wind tunnels became the main source of information for technological aerodynamics and aeronautical applications; a methodology that remained unchallenged until the recent disruption of numerical simulation [2].

Computational methods are slowly pushing experimental techniques towards a secondary role as verification or calibration tools, but real testing of physical models is still undoubtedly effective at providing confidence, validating estimations and even revealing issues that were not correctly identified in the *virtual domain*. In the words of Kress: "[Physical models] may even spade up potential problems you wish you had never seen!" [3]. In some cases, testing physical prototypes might not only be a cost-effective complement to other design tools, but might also expedite the development process [4, 5].

Wind-tunnel testing is probably one of the most established experimental methods in this field, but it sometimes fails to satisfy the requirements of modern aeronautical research and development: modern wind tunnel facilities are a scarce and costly resource, and are therefore not efficient for quick or iterative explorations of the design space during the initial stages of aircraft development. Further, their testing volume and capabilities are sometimes too limited to evaluate the integration of novel or immature technologies at low technology readiness levels (TRLs). On the other hand, flight testing of full-scale, manned vehicles is, at this stage, often prohibitive in terms of both cost and risk.

In some cases, testing of free-flight subscale models – often referred to as subscale flight testing (SFT) – could offer an affordable and low-risk alternative for gathering both qualitative and quantitative information beyond the inherent physical limitations of a wind-tunnel rig. The cost and capabilities of SFT have changed significantly thanks to factors such as the miniaturisation of mechatronic and communication systems, advances in rapid-prototyping and manufacturing techniques, and the availability of both software and hardware from the booming drone market. Sophisticated test objects can now be developed across a wide range of scales, even by organisations with limited resources. As a result, the practical threshold for engaging in scientific free-flight experiments is lower than ever before.

It is therefore necessary to re-evaluate the role of SFT and its potential to complement other digital techniques within the contemporary aircraft research and development process. This dissertation explores these possibilities and aims to contribute to knowledge on the practical use of the SFT method, focusing on low-cost, time-efficient solutions that are particularly suitable for small organisations and limited resources.

1.1 Background

The National Aeronautics and Space Administration of the United States (NASA) has historically been one of the most frequently mentioned actors in the field of SFT. Chambers [6] presents an extensive historical review of NASA's research activities involving subscale models from the 1940s to 2008. Free-flying models, both remotely controlled and uncontrolled, have been used in low-speed tests that are considered to be high risk, such as studying the dynamics of high angle-of-attack (AOA), stall, departure, post-stall and spin regimes. These studies typically comprised four different techniques: (1) small free-spinning models inside vertical wind tunnels, (2) free flight inside large low-speed wind tunnels, (3) unpowered models dropped from manned aircraft and (4) remotely piloted models with their own propulsion system.

The use of small, unpowered and uncontrolled subscale models without instrumentation inside vertical wind tunnels was a common technique for researching developed spin as early as in the 1930s. Figure 1.1 shows a typical spin test, and a detailed description can be found in [7]. Although it requires very specialised facilities, this relatively simple technique has remained in use until modern times, as seen in programmes such as the *X-31* [8], *F-18* [9] and *F-22* [6].

Free-flight testing of models inside a wind tunnel usually requires a test section of considerable dimensions, such as the large, open section of the *full-scale tunnel* at NASA's Langley Research Center [10]. According to Chambers,

Figure 1.1 *A subscale model of the Northrop XB-35 during a free-spinning test inside a vertical wind tunnel at the NASA Langley Research Center in 1943. Courtesy of NASA (L-34796).*

free-flight tests at this facility were common, providing aerodynamic data and predictions of high-AOA behaviour for every high-performance military aircraft developed in the USA during the 1970s and 1980s [10]. Figure 1.2 shows the preparation of two typical dynamically scaled models used in early free-flight tests. Besides military programmes, free-flight tests inside wind tunnels were also used to investigate wake encounters [11], and new civil concepts such as the blended wing body (BWB) *X-48B*, which – with a 3.8-meter wingspan – was not only the largest but also the last free-flight model to be tested in the Langley Full-Scale Tunnel before its closure [10].

In order to increase the freedom for manoeuvring outside the limitations of a wind tunnel and the size of the subscale models, unpowered models dropped from manned aircraft have also been used in several military and research programmes. Examples where post-stall dynamics have been studied using these susbcale *drop models* include the *X-31* [12, 8], the *F-4*, *F-14*, *F-15* and *B-1* [6], and the *F/A-18E/F* [13]. This technique has also been used to study space vehicles such as the NASA-Ames *M2-F1* vehicle [6], the Lockheed Martin *X-38* and the Japanese *HOPE-X* [14].

More advanced platforms emerged as progress was made in the fields of materials, electronics, computer science, power storage and communications. Modern subscale aircraft are often powered by their own internal propulsion systems and operate as conventional remotely piloted aircraft systems (RPASs). Two early examples of using this kind of vehicle for research and technology demonstration are the Rockwell *HiMAT* [15] and the multiple radio control (R/C) models of conceptual V/STOL aircraft tested by Grumman [3]. More recent technology demonstration projects include the NASA/McDonnell Douglas *X-*

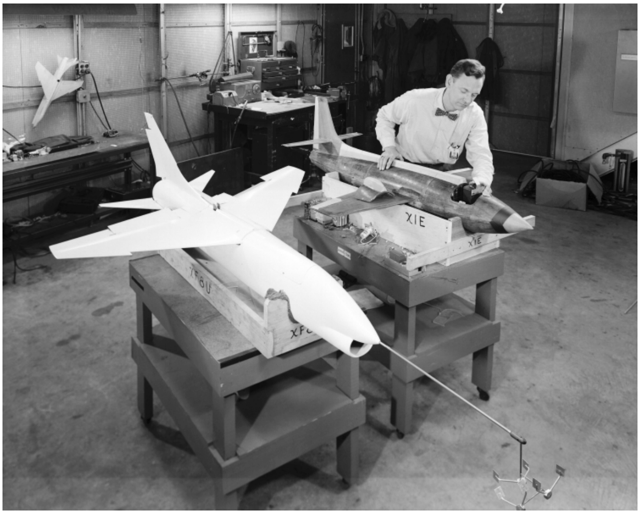

Figure 1.2 *A technician prepares dynamically scaled, free-flight models of the Bell X-1E and the Vought XF-8U Crusader for wind tunnel testing at the NASA Langley Research Center in 1957. Courtesy of NASA (LRC-1957-B701_P-00660).*

36 [16], the NASA/Boeing *X-48B/C* BWB [17] and the BAE Systems research programme *FLAVIIR*, in which the subscale model *Eclipse* [18] was built and evaluated before developing the final *Demon* demonstrator [19]. A common factor in all these cases is that the proposed configurations and flight control solutions are highly unconventional, and hence there is an aim to demonstrate their feasibility and acquire more data without the high cost and risk associated with a manned, full-scale vehicle.

Alongside military and industrial developments, other contemporary projects also use SFT as an airborne test facility for civil research purposes. A notable example is the NASA *AirSTAR* research programme [20], in which dynamically scaled models are used to explore an extended flight envelope and novel control laws for civil transport aircraft. The NASA *FASER* project uses low-cost models instead for research and demonstration of advanced dynamic modelling and control design concepts [21]. In fact, the closure of some of NASA's wind-tunnel facilities contrasts with the recent establishment of a dedicated *Subscale Research Lab*. Another example of a civil research project with partners from both academia and industry is the NACRE *Innovative Evaluation Platform* (IEP), in which a modular, dynamically scaled aircraft is built to study environmental and safety issues [22, 23].

Various academic and research projects involving SFT have also been carried out recently by different universities, often with much lower budgets than those of the previously mentioned programmes. In most cases, the platforms used in these projects are derived from hobbyist R/C equipment and the models are usually not accurately scaled. Some examples of different implementations can be found in references [24, 25, 26, 27, 28, 29, 30].

1.1.1 Subscale Flight Testing in Sweden

In Sweden, the first notable examples of using subscale models can be found in the development of the Saab 35 *Draken*. With its double delta wing with very small aspect ratio, it was certainly a radical design when first proposed in 1949. In order to reduce the uncertainties and the scepticism around this configuration, practical experiments were initially conducted with paper models, followed by numerous powered line-control models built to various scales and in various configurations. Dorr et al. [31] describe these experiments in detail. The line-control models, weighing about 6 kg and powered by pulsejet engines, were flown in a circular trajectory with a 19-metre radius for approximately two minutes. The flight tests were filmed from the pilot's position, and the information obtained was mostly a qualitative assessment of low-speed behaviour and controllability with different tail configurations and centre of gravity (CG) locations. Figure 1.3 shows one of these models, in this case with a distinct nose intake design. According to Dorr et al., these experiments provided a significant insight into the double delta's flight characteristics and they also verified the conclusions reached by the engineering team, proving that such a design was feasible.

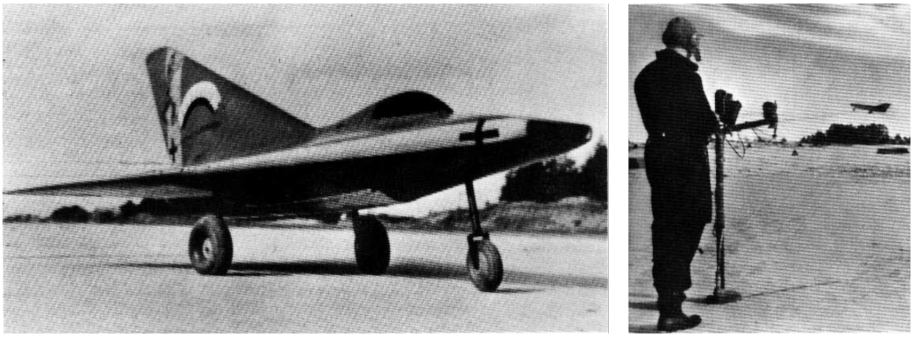

Figure 1.3 *One of the line-control subscale models used during the initial development of the Saab 35 Draken, c. 1949. Courtesy of Saab.*

Another subscale test-bed was built immediately afterwards. The Saab 210 *Lilldraken* ("little *Draken*") was a manned aircraft approximately half the size of the final *Draken*, powered by a small turbojet engine. Developed solely as an experimental platform and first flown in 1952, the *Lilldraken* performed more than 1000 tests during the test programme and played an important role in the evolution of the final design [31].

Furthermore, a subscale drop model was used for spin testing during the Saab 37 *Viggen* test programme in the 1960s, as described by Henriksson [32]. Later on, subscale platforms were used as technology demonstrators in the Saab *SHARC* and *FILUR* projects during the 2000s [33, 34].

1.1.2 Previous Research at Linköping University

At Linköping University, building and testing subscale demonstrators has traditionally been a distinctive part of the aeronautical education offered by the Division of Fluid and Mechatronic Systems (FLUMES). According to Jouannet et al., this activity provides aeronautical students with a fundamental holistic view of the entire design cycle of an aircraft, as well as valuable experience of practical, applied work [35]. Numerous demonstrators have been designed and built during the last two decades, although most of these remained unpublished as local academic projects. Two exceptions are the demonstration of an *ECO-Sport* aircraft design [36] and the dynamically scaled demonstrator of a light business jet named *RAVEN*, a project which is described by Jouannet and Lundström in references [37, 38]. This demonstrator was equipped with an in-house data acquisition system, and it was tested on top of a moving car using a specially designed rig with three degrees of freedom, as shown in Figure 1.4. Indications of a possible stability problem prevented further flight testing.

Amadori et al. manufactured and flight-tested a series of automatically designed micro air vehicles between 2008 and 2010 [39], a project that included the noteworthy achievement of carrying out the first documented flight test of an entirely 3D-printed aircraft. A short summary of the SFT research activities at Linköping University around the year 2010 is given by Staack et al. in [40]. The research platforms available at that time included a 13%-scale, commercial off-the-shelf (COTS) model of a Dassault *Rafale* fighter aircraft, used mainly as a test-bed for systems and procedures. This model is shown in Figure 1.5. Lundström has been one of the main contributors to research into SFT and rapid prototyping at Linköping University in recent years. His participation in these and other projects up until 2012 is summarised in [41].

A special mention should be made of the Generic Future Fighter (GFF) project, launched in 2006 as a research collaboration between Saab Aeronautics, the Swedish Defence Research Agency (FOI), Volvo Aero, Linköping University and the Royal Institute of Technology (KTH). This project involved the conceptual design of a hypothetical next-generation fighter aircraft with stealth, super-cruise and long-range capabilities. The production of a 14%-scale remotely piloted demonstrator was awarded to Linköping University in 2009. The development of this jet-powered model, shown in Figure 1.6, is described in detail in references [42, 43].

The GFF subscale demonstrator was flown a few times between 2009 and

Figure 1.4 *RAVEN, the subscale demonstrator of a light business jet described in [38], mounted on a custom-made rig for car-top testing in 2008. Courtesy of David Lundström, Linköping University.*

Figure 1.5 *Jet-powered, commercial model of a Dassault* Rafale *fighter at a 13%-scale, often used at Linköping University to test systems and procedures.*

Figure 1.6 *Demonstrator of the GFF, surrounded by most of its developers, soon after its completion in 2009. Courtesy of FLUMES, Linköping University.*

2010, but no formal flight-testing campaign was conducted at that time and the integration of a data acquisition system fell outside the scope of the initial project. Still one of the most advanced research platforms at Linköping University, the GFF demonstrator has become a perfect test-bed for an important part of the work presented in this thesis: First, it represents a contemporary and relevant problem for the industry in which an unconventional configuration needs to be explored during the conceptual design phase. Second, the small size and relatively low cost of this platform fits well with the range of complexity on which this investigation intended to focus, i.e. considering the use of SFT in small companies or organisations with limited resources. Last, this platform is capable of integrating different types of equipment and is therefore well-suited to demonstrating new technologies and methods.

1.2 Aim and Research Questions

The overall aim of this thesis is to contribute to knowledge on the use of the SFT method for research and development, focusing on low-cost, time-efficient solutions that are particularly suitable for small organisations and limited resources.

The different aspects explored in this effort can be condensed into four research questions, as follows:

RQ1: What are the main opportunities, challenges and limitations for the cost-efficient use of SFT within contemporary aircraft research and development?

RQ2: To what extent can low-cost platforms, equipment and instrumentation fulfil flight testing requirements and be used to gather useful information?

RQ3: Which flight-testing techniques and infrastructure are suitable for a small organisation in order to safely perform SFT at low cost?

RQ4: What is a suitable approach to the analysis and interpretation of flight data gathered during SFT experiments?

1.3 Delimitations

The following delimitations should be taken into account:

- Different interpretations of the similarity principles allow for a wide variety of scaling approaches and use cases, but a general discussion on scaling is beyond the scope of this thesis. The analysis of scaling methods and the applicable physics is here limited to a context of aircraft flight characteristics.
- The border between unmanned aerial vehicle (UAV) development and SFT is often ambiguous. While the former can be considered similar to 'full-scale' development and hence not of interest here, using remotely piloted aircraft (RPA) or UAV to integrate and test a simplified version of technologies or solutions that are intended for a 'larger' system can indeed be considered SFT. Therefore, the inclusion or exclusion of certain projects from the literature review may be subject to discussion.
- This thesis focuses on the implementation of SFT in contexts where both human and economic resources are limited. There is therefore a sharp focus on low-cost solutions and time-efficient implementations.
- Where possible, the use of COTS components has been favoured for similar reasons.

- The experiments carried out here were primarily aimed at verifying feasibility and functionality. In some cases, data fidelity has therefore been of secondary importance. In fact, this may represent an appropriate level of fidelity for those cases in which the design is not frozen yet, as in early aircraft development stages. In addition, calibrating and validating the obtained data might not be possible if no full-scale aircraft or additional experimental data are available.

- The empirical case study presented here is limited to a small number of platforms.

- The flight-testing methods proposed here are in part a consequence of the local regulations for civil air operations at the time that this work took place. Different conditions may apply at different times or in other areas of the world.

1.4 Methodology

The presented research is primarily based on hypothetico-deductive principles [44], as illustrated in Figure 1.7. In addition, the process of evaluation or falsification has been largely empirical.

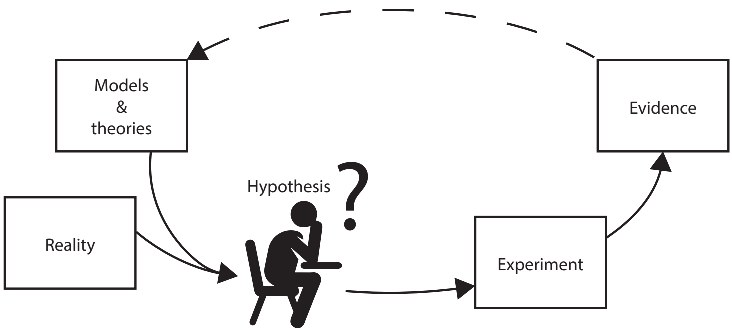

Figure 1.7 *An empirical, hypothetico-deductive cycle.*

The methodology used to conduct this work can be described in terms of three main domains:

- *Theory*, involving the established theories, rules and laws, and the predictions that can be made by observing reality.
- *Technology*, involving the methods, procedures, tools and devices needed to make an activity possible.
- *Experimentation*, involving the evaluation of such technology and proposed theories, as well as exploring new phenomena.

Starting from an initial idea or hypothesis, the knowledge-forming process can be described as an iterative cycle of synthesis, adaptation and analysis performed across these three domains at various hierarchical levels, similar to the iterative process described by Brandt et al. [45] and by Hochwallner [46]. Figure 1.8 attempts to illustrate this cycle as a spiral that leads to a final solution.

The *theory* domain is approached by means of a review of the published information within this field, as well as an analysis of the physical laws that govern the similarity principles. This analysis could easily be generalised over a wide range of scenarios and applications, but unfortunately this is not the case for the technological and experimental domains.

The approach to *technology* and *experimentation* is, in this case, largely empirical. It is therefore impossible to cover a sufficiently wide range of cases, scenarios and applications. These two aspects are approached with a case study, selected as a representative example of the scenarios of interest: relatively small,

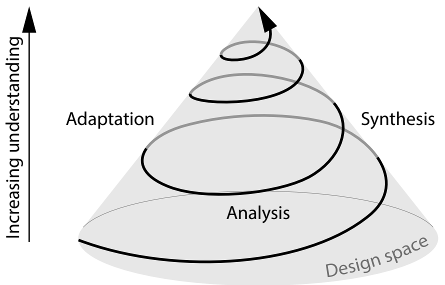

Figure 1.8 *Design spiral conceived as an iterative cycle of synthesis, adaptation and analysis. Adapted from [45].*

low-cost SFT projects carried out by small organisations in a short time. The published papers appended to this thesis deal mainly with these two aspects.

The process of using SFT to gain knowledge about certain design problem can be fundamentally described by the hypothetico-deductive cycle depicted in Figure 1.7. The method's theoretical principles are used to formulate an hypothesis or model that is evaluated experimentally by means of flight testing and the analysis of gathered data. This experiment requires three essential elements: a test platform, a flight testing method and a data analysis tool. The gathered information or evidence, seen through the theoretical principles and limitations, can then be used to gain knowledge about the initial design problem. Figure 1.9 illustrates this process and indicates what phases and domains the research questions refer to.

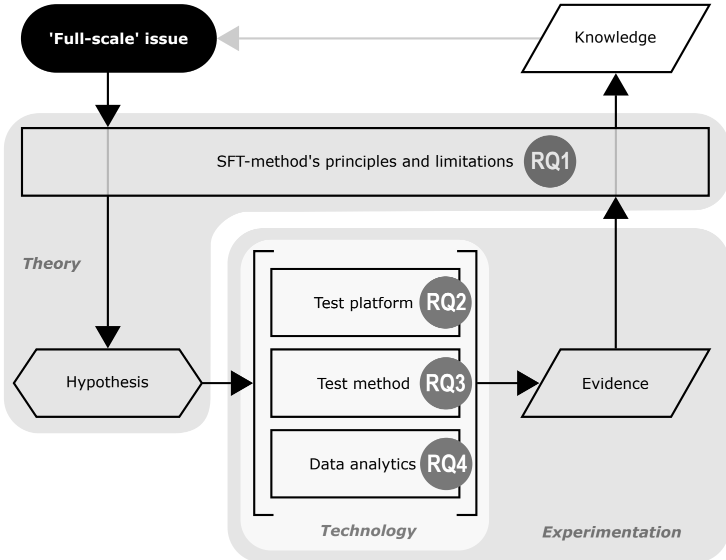

Figure 1.9 *The process of gaining knowledge through SFT can be considered an hypothetico-deductive cycle. The specific aspects studied in this thesis are demarcated by the research questions 'RQ'.*

1.5 Contribution

This thesis should be seen as an integration effort rather than a specific development. It involves both theoretical and practical work in disciplines as diverse as mechatronics, measurement techniques, flight testing, data analytics, modelling and simulation.

The SFT method's challenges, needs and limitations are identified through a critical study of the physical similarity principles, an in-depth review of the experiences of other organisations, and practical field experiments with different subscale models in real conditions. Some of the proposed solutions include a low-cost data acquisition system with custom-made instruments, a novel method for automatic execution of excitation manoeuvres, specific techniques and parameter-identification methods for flight testing in confined airspaces, and a set of tools for the analysis and visualisation of flight data. The obtained results may serve as proof of the current possibilities to evaluate and demonstrate new technology through SFT using very limited economic and human resources.

1.6 Thesis Outline

The order in which the analysis and contributions are presented in this dissertation is approximately the same as that of the SFT process, as illustrated in Figure 1.9. Chapter 2 provides the context for the application of SFT. Chapter 3 presents a review of current research and identifies the main characteristics and challenges of the SFT method (RQ1). Chapter 4 focuses on the development and integration of a suitable instrumentation and data acquisition system (RQ2). Chapter 5 presents the development and application of a suitable flight testing strategy (RQ3). Chapter 6 summarises the tools and methods developed for the analysis and visualisation of data (RQ4). Chapter 7 discuses the impact and validity of these findings. Conclusions in relation to the research questions are drawn in Chapter 8.

The appended papers are presented in chronological order and do not cover the research questions in the same order. Table 1.1 indicates the approximate relationship between these papers, the research questions and the respective domains covered. A short review of each paper is given in chapter 9.

Table 1.1 *Overview of the domains and research questions covered in the appended papers.*

Paper	[I]	[II]	[III]	[IV]	[V]	[VI]
Domain						
Theory					X	
Technology development	X	X	X	X	X	
Experimentation	X	X	X	X	X	X
Research question						
RQ1			X		X	X
RQ2	X	X			X	X
RQ3			X	X	X	
RQ4	X	X	X	X	X	X

2
Opportunities in Aircraft Conceptual Design

Modern aircraft are tremendously complex products. Their development process involves high risks and presents some unique characteristics. This chapter offers a brief overview of the initial phases of such a process in order to provide a context for further discussion, and focuses on identifying the challenges and opportunities for SFT.

2.1 Characteristics of the Aircraft Development Process

From a general product development perspective and according to the definitions offered by Ulrich et al. [4], aircraft can be categorised as both high-risk products and complex systems: The high risk of failure originates from the technical and market uncertainties as well as the high non-recurring costs. As a system, its extreme complexity is usually managed by decomposition into several subsystems and components that are often designed and developed in parallel.

In order for such a development process to succeed, it is therefore critical to identify the risks and track the propagation of uncertainty from the earliest time possible. In fact, early testing and validation are often conducted at subsystem level without waiting for final integration in order to reduce the degree of uncertainty. However, very little information is usually available during the earliest design phases.

As a consequence of the product's high degree of complexity, the uncertainty of the performance estimation methods and the usually sequential decision-making strategy, the aircraft design process typically suffers from a paradoxical disparity between available knowledge and design freedom, as well as committed cost [47, 48], as illustrated in Figure 2.1. Unfortunately, important decisions affecting the total life-cycle cost of the aircraft are often taken under a high degree of uncertainty during the early design stages.

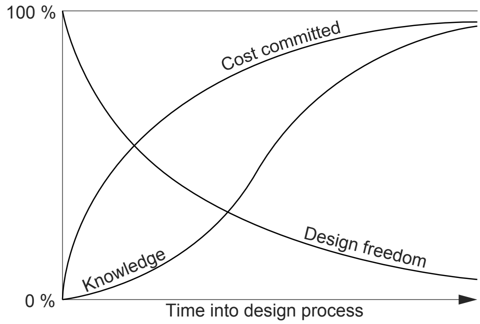

Figure 2.1 *Traditional design paradox in the aircraft development process, based on [47] and [48].*

These factors contribute to aeronautics being a relatively conservative industry in which empirical experience gathered from previous programmes plays a central role in any new project. However, empirical experience is often configuration-specific and hence does not contribute to reducing the risk of radical or non-evolutionary designs [2]. It may therefore be deduced that one of the principal keys to innovation in aircraft development is the capability to estimate the performance of the final product in a reliable and competitive manner, based on a limited set of information.

2.2 The Aircraft Conceptual Design Phase

As a consequence of the factors described above, there is significant interest in researching cost-effective methods to reduce uncertainty and to increase the available knowledge during the early phases of aircraft design. The specialist literature includes several different interpretations of what can be considered a typical aircraft development programme, although most sources agree on dividing the main design activities – from initial project planning to production ramp-up – into three major phases: conceptual, preliminary and detail design [45, 47, 49, 50]. The first of these, conceptual design, is characterised by:

- exploring of the design space,

- estimating operational effectiveness and life-cycle costs,
- synthesising technical requirements and technology needs,
- and analysing market opportunities and competitors.

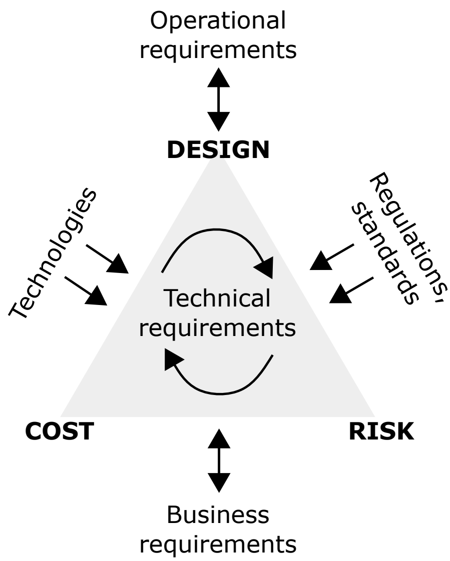

Figure 2.2 *Aircraft conceptual design can be conceived as the process of finding a technical solution that optimally balances requirements and drivers of very different nature. Adapted from Christopher Jouannet, Saab Aeronautics.*

Figure 2.2 represents some of the aspects and forces that drive this process. Aircraft conceptual design is thus a complex multidisciplinary effort that aims to propose a technical solution which, within certain levels of certainty, will comply with the desired functional requirements while balancing business, regulatory and other multiple aspects. In this context, SFT could be used iteratively to acquire additional information and reduce uncertainty with low risk and cost.

Despite resembling the full-scale product in terms of external appearance, subscale models used in SFT are not intended to fulfil the same prototyping functions as full-scale test aircraft. The latter are tremendously expensive, carefully planned prototypes which are not appropriate for design iterations, and their use is generally confined to the final stages of development when large-scale, comprehensive verification of product performance is required. According to the classification proposed by Ulrich et al. [4], the models used in SFT can be described as highly focused physical prototypes, at a similar level to those used in wind-tunnel testing. Figure 2.3 illustrates these characteristics.

The reader should note that, unless specifically stated, the meaning of the term *model* is context dependant. The term *model* is, however, used throughout this thesis in most cases to designate a physical representation of a true object, generally of a different size but interconnected by some type of similarity.

According to Staack [51], the aircraft conceptual design phase is characterised as being:

- "**efficient**", in terms of time, finances and human resources;
- "**flexible**", in terms of quick adaptability;
- "**transparent**", in terms of favouring the comprehensibility and general understanding of the design problem;
- and "**multi-modal**", in terms of enabling and making use of both manual and automated design modes.

These characteristics also indicate the different features that would be required from the tools and methods used during this design phase. In these terms, modern SFT could potentially offer:

- **Efficiency**: It offers low cost thanks to tremendous improvements in the price-performance ratio of miniaturised electronics. It also offers quick development times thanks to rapid prototyping methods. This method can be carried out by a reduced team and it is also suitable for outsourcing.

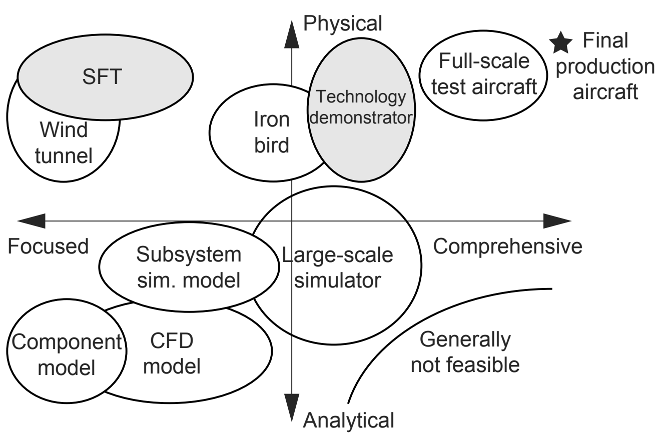

Figure 2.3 *Characteristics of SFT models and technology demonstrators according to the prototype classification proposed by Ulrich et al. [4].*

- **Flexibility**: The low cost and short time required for design-build-test iterations make this method relatively flexible in comparison with other traditional experimental techniques such as wind-tunnel testing.
- **Transparency**: Physical prototypes, such as subscale models, are especially valuable for learning design features and communicating knowledge as well as being useful for detecting unanticipated phenomena [4].
- **Compatibility with automation**: While this method may generally require manual and focused sub-design tasks to perform complete iterations, some parts of the process can be effectively automated and may be suitable for optimisation. For instance, reference [39] is a good example of an agile framework for flight testing of automatically designed and 3D-printed micro air vehicles.

2.3 The Cost-Benefit Principle

Considering that numerous examples of successful applications of SFT in aircraft research and development have already been given in Section 1.1, the reader might question the need for further research. However, recent disruptive innovations justify a re-evaluation of SFT and its potential applications; the progress made in the fields of electronics, computer science, manufacturing, power storage and communications during the last two decades have totally altered the *cost-benefit* ratio for developing of small, flying vehicles such as subscale models.

The cost reduction in capable microprocessors and solid-state sensors and the increased availability of *open-source* software have been especially disruptive in many markets, such as mobile telephony and other consumer electronics. These enabling technologies are also partially responsible for the explosive growth in consumer unmanned aerial vehicles (UAVs), the so-called *drone revolution* [52]. Figure 2.4, based on data and predictions from various sources, illustrates some of these trends.

As with many other processes, the cost-benefit principle also applies in aircraft conceptual design. Here, the main objective is to maximise the information obtainable with very limited money, time and human resources. Within these limits, any tool or method that provides more value than it consumes would be desirable.

In this context, inexpensive models of very low complexity could still provide valuable information with respect to the invested resources. For physical aircraft prototypes in particular, as illustrated in Figure 2.5, the cost often escalates significantly with complexity and hence exhaustive prototypes are only valuable if real-world performance validation can be obtained. While having a limited impact in high-end systems, the improvements in enabling technologies discussed previously help to maximise the utility and the cost-benefit ratio of the lower end, such as in the case of the relatively simple models used in SFT.

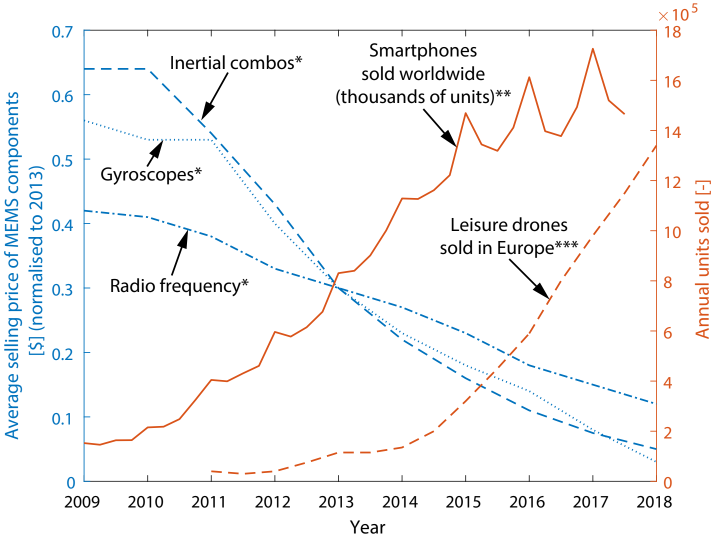

Figure 2.4 *Cost trend and sales volume of various electronic devices during recent years. *Data on Micro-Electro-Mechanical System (MEMS) components provided by [53]. **Data on smartphone sales provided originally by Gartner and retrieved from [54]. ***Data on drone sales provided by [55].*

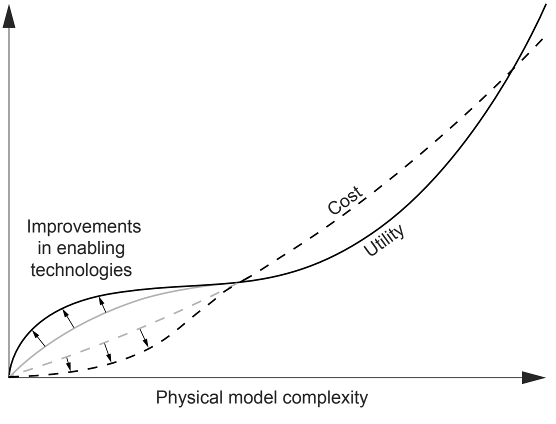

Figure 2.5 *A conceptual representation of the evolution of the cost-benefit ratio for unmanned aircraft prototypes. Utility and complexity behave as in typical simulation models [56], while new technological developments, such as low-cost microprocessors and solid-state sensors, help to improve the cost-benefit ratio – an effect that is especially noticeable with relatively simple prototypes.*

3 Analysis of the SFT Method

Experiments with scaled test articles are rarely expected to reveal the desired full-size characteristics directly, instead producing a set of data from which the desired full-scale characteristics can be estimated. A deep understanding of the phenomenon of interest and the physical laws behind it are essential in order to design the experiment appropriately. This chapter discusses the similarity principles that govern the most common scaling methods from a practical perspective.

3.1 Definition of Important Concepts

Some of the terms used in this analysis may have different interpretations and uses in other contexts. For the sake of clarity, some important concepts will be defined here.

Subscale flight testing (SFT) is defined here as an experimental method in which a downscaled, unmanned aerial vehicle is free-flown in the open atmosphere to obtain qualitative or quantitative information about a larger vehicle, a more complex system or a technology of interest.

This definition may differ slightly from other more open interpretations as it implies the following:

1. The test object is flown unconstrained in the open atmosphere, which excludes flight inside wind-tunnel facilities.

2. The test object does not have any crew on-board, independently of its control method.

3. The test object represents a significantly larger, more complex system or technology and is therefore far from a final product, which excludes conventional flight testing of UAVs but does not exclude technology demonstrators.

Model Downscaled UAVs are sometimes referred to as *scaled models* or even *model aircraft*. Note that, unless stated otherwise, the term *model* is used throughout this paper to designate a physical representation of an object, generally of a different size but connected by some type of similarity.

Similarity In this context, the concept of *similarity* or *similitude* represents an equivalence of properties or behaviour between two systems that are described by the same physics. Hence, it is a condition that depends on the nature of the physical phenomenon of interest and that can be defined via dimensional analysis [57, 58]. In a purely mechanical interpretation at a general level, there are three types of physical similarity of relevance in this analysis:

- **geometric similarity**, which implies equivalence in shape and proportions;
- **kinematic similarity**, which implies equivalence in motion;
- and **dynamic similarity**, which implies equivalence in motion and forces.

Both geometric and kinematic similarity are typically used in aircraft development for communication and knowledge exchange, such as in technical drawings, flow visualisation tools or computer-aided design computer-aided design (CAD) environments. The quantitative analysis of behaviour and performance of an aircraft involves the synthesis of multiple forces and motions and therefore dynamic similarity is generally required. This is the case of aerodynamics, flight mechanics, and propulsion, among other disciplines.

Scale factor The word *scale* or *scale factor* is generally used in this context to represent the proportional ratio of linear dimensions of the model with respect to the corresponding characteristics of the original object, i.e. it refers commonly to the correlation of characteristic physical dimensions assuming proportional geometric similarity:

$$\frac{l_{model}}{l_{full-scale}} = scale\ factor \tag{3.1}$$

In engineering applications, and particularly in aeronautics, the scale factor of physical models used for research and development is often less than the unity, meaning that the model is smaller than the original object being studied. In this case, the term *subscale* is commonly applied. Figure 3.1 is a simple example of geometric similarity in which each model presents a different scale factor.

Figure 3.1 *A traditional Russian Matryoshka doll: an example of geometric similarity in which the various models present different scale factors.*

3.2 Similarity Requirements for Flight Mechanics

Non-dimensional or *dimensionless parameters*, derived from dimensional analysis, are commonly used in engineering to ensure that the dependence between the different physical quantities involved a the experiment is equal for the subscale and full-scale articles [57]. The number of non-dimensional parameters required to define these dependences for given phenomenon can be expressed as:

$$\binom{\text{Nr. nondimensional}}{\text{parameters}} = \binom{\text{Nr. physical}}{\text{quantities}} - \binom{\text{Nr. fundamental}}{\text{units}} \tag{3.2}$$

Conforming to dimensional analysis, complete similarity for a specific phenomenon can only be achieved by fulfilling all the conditions defined by all the non-dimensional parameters. In practical applications, however, these conditions can be often reduced to the most relevant parameters and disregard those who have little effect on the case of interest [7].

The non-dimensional parameters that govern a specific scaling problem are commonly referred to as *similarity parameters*, *scaling parameters*, or more generally *scaling laws*. The derivation of similarity parameters with useful applications in aircraft development is discussed extensively in references [7] and [59].

Focusing on the mechanical analysis of aircraft behaviour and performance in a typical atmospheric flight, the forces and moments are generally a function of the aircraft and fluid properties, the characteristics of the motion, and gravitational effects:

$$F,\ M = f(\overbrace{\rho, \mu, c}^{\substack{\text{fluid}\\ \text{prop.}}}, \overbrace{l, \delta, m, I, EI', GJ'}^{\text{aircraft prop.}}, \overbrace{\alpha', V, a, \Omega, \dot{\Omega}, \omega}^{\text{motion charact.}}, \overbrace{g, t}^{\substack{\text{gravity,}\\ \text{time}}}) \tag{3.3}$$

All these seventeen physical quantities involve three fundamental units (*mass*, *length*, and *time*), which according to Equation (3.2), leads to fourteen different non-dimensional parameters defining similarity for flight dynamics. Following the dimensional analysis done in [7] and assuming fluid compressibility, these parameters take the following form:

$$C_F,\ C_M = f\left(\overset{(a)}{\frac{\rho V l}{\mu}}, \overset{(b)}{\frac{V}{c}}, \overset{(c)}{\delta}, \overset{(d)}{\frac{m}{\rho l^3}}, \overset{(e)}{\frac{I}{\rho l^5}}, \overset{(f)}{\frac{EI'}{\rho V^2 l^4}}, \overset{(g)}{\frac{GJ'}{\rho V^2 l^4}}, \overset{(h)}{\alpha'}, \overset{(i)}{\frac{al}{V^2}}, \overset{(j)}{\frac{\Omega l}{V}}, \overset{(k)}{\frac{\dot{\Omega} l^2}{V^2}}, \overset{(l)}{\frac{\omega l}{V}}, \overset{(m)}{\frac{V^2}{lg}}, \overset{(n)}{\frac{tV}{l}}\right) \tag{3.4}$$

where C_F and C_M are now also non-dimensional aerodynamic coefficients in the usual form of $\left(\frac{F}{(1/2)\rho V^2 l^2}\right)$ and $\left(\frac{M}{(1/2)\rho V^2 l^3}\right)$ respectively.

The similarity parameters from Equation (3.4) are described as it follows:

(a) *Reynolds number*: $Re = f\left(\frac{Fluid\ inertial\ force}{Fluid\ viscous\ force}\right) = \frac{\rho V l}{\mu} = \frac{Vl}{\nu}$

(b) *Mach number*: $M = f\left(\frac{Fluid\ inertial\ force}{Fluid\ pressure\ (elastic)\ force}\right) = \frac{V}{c}$

(c) Control surface angular deflection: $\delta_a, \delta_e, \delta_r, ...$

(d) Relative density or mass ratio: $f\left(\frac{Vehicle\ weight\ force}{Aerodynamic\ force}\right) = \frac{m}{\rho l^3} = \frac{W}{\rho g l^3}$

(e) Relative mass moment of inertia: $f\left(\frac{Vehicle\ inertial\ force}{Aerodynamic\ force}\right) = \frac{I}{\rho l^5}$

(f) Aeroelastic-bending parameter: $f\left(\frac{Bending\ force}{Aerodynamic\ force}\right) = \frac{EI'}{\rho V^2 l^4}$

(g) Aeroelastic-torsion parameter: $f\left(\frac{Torsion\ force}{Aerodynamic\ force}\right) = \frac{GJ'}{\rho V^2 l^4}$

(h) Aircraft attitude relative to the airstream: α, β

(i) Reduced linear acceleration: $\frac{al}{V^2}$

(j) Reduced angular velocity: $\frac{\Omega l}{V}$

(k) Reduced angular acceleration: $\frac{\dot{\Omega} l^2}{V^2}$

(l) Reduced oscillatory frequency (*Strouhal number*): $\frac{\omega l}{V}$

(m) *Froude number*: $Fr = f\left(\frac{Inertial\ force}{Gravitational\ force}\right) = \frac{V^2}{lg}$

(n) Reduced-time parameter: $\tau = \frac{tV}{l}$

This theory implies that, in order to achieve complete dynamic similarity for the aerodynamic coefficients and their respective derivatives, it would be necessary to design an experiment in which all these parameters are equal in both model and full-scale aircraft, i.e. $(parameter_m)/(parameter_{fs}) = 1$ for all the terms detailed above. As a consequence of the diversity of requirements, physical limitations and technological limitations (for example, the gravitational field cannot be adjusted), it is generally impossible to design a subscale experiment in which all these similarity requirements are met simultaneously [6, 7, 59]. Instead, subscale experiments can be designed to achieve a balance between fulfilling a subset of relevant parameters and relaxing others, depending on the phenomenon of interest. A particular approach to this similarity problem and the considerations around a specific scaled experiment are here referred to as a *scaling method*.

3.3 Common Scaling Methods

An extensive literature review was carried out with a focus on subscale experiments performed in the context of aircraft research and development. It was observed that most experiments with subscale models could generally be categorised into four different scaling methods, according to their main focus and the degree to which they fulfil similarity conditions. These are listed in Table 3.1.

Table 3.1 *The most common scaling methods used in SFT experiments can be grouped into four different types.*

Method	**Focus**	**Relevant similarity parameters**
Aerodynamic scaling	Similarity of the flow field, disregarding similarity of the aircraft self-motion	(a)(b)(c)(h)(j)(l)(n)
Dynamic scaling	Similarity of the rigid aircraft motion as well as the aerodynamic loads that cause it	(a)(b)(c)(d)(e)(h) (i)(j)(k)(l)(m)(n)
Aeroelastic scaling	Builds on dynamic scaling and includes similarity for vehicle deformations	All (a) to (n)
Demonstrative scaling	Scaled demonstration of a particular technology, system, or capability; partially or fully disregarding the vehicle's similarity conditions	Variable

This general classification is indicative and by no means unequivocal. The boundaries between these methods are not always clearly defined, since many of the phenomena involved are closely interrelated. Some cases might fall partially in between or even outside these categories, although most subscale experiments can be related to at least one category. The following sections explore in more detail what are the characteristics and issues of each one of these four scaling methodologies.

3.4 Aerodynamic Scaling

The complexity of aircraft geometries and the innate nonlinearity of the flow-governing Navier-Stokes equations have traditionally forced aerodynamicists to rely heavily on empirical experiments to acquire information and to verify their estimations.

The ultimate goal of an aerodynamic study with subscale articles is generally to estimate the properties of the equivalent, real-world flow field around the full-scale vehicle. Therefore, the focus here is exclusively on the flow dynamics for a given set of conditions and a particular state of the vehicle. Thus, it is possible to disregard the vehicle motion and to transform the original problem to a flow-similarity problem. For instance, in order to study the flow around the wing at a specific attitude it is not necessary to take into account the mass properties of the aircraft. Although this approach may seem most appropriate for static tests, dynamic tests are also possible, for example by inducing flow curvature and rotating or oscillating models.

Two major side effects come from disregarding vehicle dynamics. First, models are assumed to be rigid, or at least, to be in a static deformation state. Thus, the *real* aerodynamics resulting from the interaction between flow and aircraft structure would not be identified in the experiment. Second, the only way of conducting these experiments is by externally forcing the model to hold the desired attitude, since freedom of movement would produce dissimilar responses. This can be achieved by mounting the model on static or dynamic test rigs inside a closed test section, as in wind tunnels [10], or in the open atmosphere, as in car-top testing [38]. Using this scaling method in subscale flight testing (SFT) is therefore difficult, and additional means (for example, thrust vectoring) would be required to force a free-flying model into the desired motion. Nevertheless, aerodynamic scaling is probably the most widely established scaling method in aircraft development, and its use in wind tunnels is extensively covered in the literature.

Wind tunnels: a typical example of aerodynamic scaling

Historically, wind tunnel testing has been one of the main sources of information for technological aerodynamics and aeronautical applications [2]. Mounting subscale or even full-scale models inside tunnels where the moving-flow properties can be modified is a way of enabling designers to study flow behaviour in a laboratory environment. A general description of this method can be found in [60].

As a result of the progress in computational capability and numerical simulation, as well as the high costs of operating such complex facilities, the role of wind tunnel testing is changing. In many cases, its function is shifting from a primary estimation tool to a source of calibration and verification for numerical simulations, which are instead used as the primary estimation method [2]. Furthermore, traditional wind-tunnel testing cannot always meet all the requirements of modern aeronautical research and development. Internal testing rigs often have limited degrees of freedom and constrain the analysis of dynamic phenomena and unconventional manoeuvres. Achieving appropriate flow conditions to cover the extensive flight envelope of modern aircraft requires highly specialised facilities. Additionally, the similarity parameters often prescribe conditions that – depending on the scale factor and reference state – are very difficult to balance. This issue becomes even more challenging for tests in an open environment, such as in open-section wind tunnels and car-top testing, since it is generally impossible to manipulate the atmospheric conditions and the flow properties.

3.4.1 Aerodynamic Scaling Parameters

In order to achieve similar aerodynamic force and moment coefficients, the flow field around the subscale model should be equivalent to that of the full-scale counterpart. Note that, although it is commonly assumed that this implies an accurate geometric similarity between the two articles, this is not necessarily required as long as the flow field produced is equivalent. To identify the pertinent scaling parameters, it is necessary to take a step back and perform a dimensional analysis as described in Section 3.2, focusing in this case on the motion equations of the fluid.

The Navier-Stokes equations indicate that fluid motion is primarily governed by viscous, pressure, inertial and gravity forces. For a compressible fluid, this will lead to the following similarity parameters already obtained in Equation (3.4): terms (a), (b) and (m) for static tests, and terms (j), (l) and (n) for dynamic flow tests. Observe that if the flow is incompressible, the term accounting for the ratio between pressure and inertial forces (b) will take a slightly different form: the *Euler number* will be used instead of the *Mach number* [59].

An additional similarity parameter, known as the *Weber number*, will appear if surface-tension forces are considered [59].

Furthermore, the laws of thermodynamics introduce two other similarity parameters, known as the *Prandtl number* and the *Grashof number*. These parameters account for the ratio of momentum diffusivity to thermal diffusivity and the ratio of buoyancy to viscous force, respectively. In low-atmospheric flight at low speeds, the Prandtl number is usually equivalent for both full-scale and subscale conditions, given that the fluid in which they operate has the same ratio of specific heats. Although the Grashof number is usually not comparable, the effects it accounts for are negligible in most of the practical applications considered here [59].

Lastly, the external characteristics of the aircraft and its attitude relative to the flow also need to be considered, which leads to the similarity parameters (c) and (h) from Equation (3.4).

As a result, the general similarity requirements for such an experiment could be expressed as:

$$C_F,\ C_M = f\left(\overset{\text{(a)}}{\frac{\rho V l}{\mu}}, \overset{\text{(b)}}{\frac{V}{c}}, \overset{\text{(b*)}}{\frac{\bar{p}}{\rho V^2 l^2}}, \overset{\text{(c)}}{\delta}, \overset{\text{(h)}}{\alpha'}, \overset{\text{(j)}}{\frac{\Omega l}{V}}, \overset{\text{(l)}}{\frac{\omega l}{V}}, \overset{\text{(m)}}{\frac{V^2}{lg}}, \overset{\text{(n)}}{\frac{tV}{l}}, \overset{\text{(o)}}{\frac{\sigma}{\rho V^2 l}}\right) \tag{3.5}$$

where the terms that need further explanation are:

(b) For compressible flow: *Mach number*, as defined in Section 3.2

(b*) For incompressible flow: *Euler number* $= f\left(\frac{Fluid\ pressure\ force}{Fluid\ inertial\ force}\right) = \frac{\bar{p}}{\rho V^2 l^2}$

(m) *Froude number*: $Fr = f\left(\frac{Fluid\ inertial\ force}{Gravitational\ force}\right) = \frac{V^2}{lg}$

(o) *Webber number* $= f\left(\frac{Fluid\ surface-tension\ force}{Fluid\ inertial\ force}\right) = \frac{\sigma}{\rho V^2 l}$

The term (b) or Mach number relates to the pressure differential across shock waves and should only be used in compressible flow. It can be substituted by the term (b*) or Euler number in cases of incompressible flow, although this would only be necessary for problems in which the similarity of the pressure field is important, such as when the body forces are determined from measurements of pressure distribution. In other cases, this similarity parameter (b*) can normally be neglected [59].

Moreover, it should be observed that the term (m) or Froude number now accounts for the gravitational effect on the fluid and not on the vehicle. Considering that the effect of gravitation on the airflow is minimal, this parameter can also be disregarded in most cases [59].

According to these assumptions, the relevant similarity parameters for aerodynamic scaling can be reduced to:

$$C_F,\ C_M = f\underbrace{\underbrace{\left(\overset{\text{(a)}}{\frac{\rho V l}{\mu}}, \overset{\text{(b)}}{\frac{V}{c}}, \overset{\text{(c)}}{\delta}, \overset{\text{(h)}}{\alpha'},\right.}_{\substack{\text{static}\\\text{tests}}} \left.\overset{\text{(j)}}{\frac{\Omega l}{V}}, \overset{\text{(l)}}{\frac{\omega l}{V}}, \overset{\text{(n)}}{\frac{tV}{l}}\right)}_{\substack{\text{dynamic}\\\text{tests}}} \tag{3.6}$$

Despite these simplifications, satisfying all the aerodynamic scaling parameters at the same time is in most cases infeasible, as mentioned in wind-tunnel testing literature [2, 60, 59, 61]. This problem becomes even more significant in open test sections and free-flight testing, since flow properties such as chemical composition, pressure and temperature cannot be modified as in advanced wind-tunnel facilities. In most of the practical applications discussed here, the main obstacles to achieving flow similarity are those involving viscous and pressure forces, i.e. Reynolds number (a) and Mach number (b).

Fortunately, in many cases the impact of these two parameters can be studied independently, considering that Reynolds number effects are typically negligible outside the boundary-layer region near the body surface [60, 59, 61, 62]. Experimental studies such as [63] and [64] support this assumption by showing a clear distinction between the effect of Mach number and those caused by Reynolds number variations. This assumption is valid for subsonic and supersonic flow for Mach numbers less than approximately 5, a point at which the shock waves start interacting extensively with the boundary layer and hence Mach number effects couple to viscous effects [7].

3.4.2 Scale Effects

For certain experiments in subscale conditions, it could be infeasible, impractical or unnecessary to achieve complete flow similarity by satisfying all the scaling parameters. Dissimilarity in one or more of these parameters normally causes deviations from the full-scale results which are usually known as *scale effects*. The significance of these scale effects and the degree of uncertainty that they introduce varies greatly from case to case.

In fact, despite the inevitable exposure to undesirable scale effects, only a very small fraction of experimental aerodynamics testing is conducted at representative, full-scale Reynolds and Mach numbers, due to the high costs involved and the few operative ground facilities with the necessary capabilities [62]. It is therefore essential to understand and quantify the influence of scale effects in order to apply the necessary corrections. This is a complex task that often requires not only extensive knowledge and experience but also complementary data from other tests or methodologies [65].

In the context of vehicle aerodynamics and hydrodynamics, Barlow states that the understanding of scale effects consists mainly of the understanding of boundary layer properties and behaviour as they are affected by differences in the model and full-scale articles [60]. According to this author, even scale effects observed in flow wakes can, in most cases, be explained by changes in the boundary layer.

The role of Reynolds number

Flow aspects such as the boundary layer are very sensitive to variations in Reynolds number [62]. While it is clear that this parameter plays a significant role, scale effects of relevance for aerodynamics are not limited to a single Reynolds number problem. This issue has been extensively discussed in wind tunnel literature. For instance, according to Haines [61], scale effects that are often combined with Reynolds number effects can be classified into three categories:

- **"Scale effects"**: A term used by Haines to describe effects that are not dependent on Reynolds number, but are related to the scale model. These often include geometric similarity issues, such as model geometric fidelity and aeroelastic distortion.

- **Pseudo-Reynolds number effects**: Effects that at first may be wrongly identified as Reynolds number effects, but are ultimately dependent on other variables. Such effects could be introduced by an inadequate testing methodology, data processing errors and the influence of other variables that are not considered or known at the time of testing.

- **Reynolds number effects**: Effects that are directly or indirectly dependent on Reynolds number. Direct Reynolds number effects involve intrinsic boundary layer properties, such as laminar-turbulent transition, separation from the surface, shock wave interaction with the boundary layer and velocity inside it, and affect parameters like the viscous drag and the location of boundary layer separation. Indirect Reynolds number effects are those induced by the intrinsic characteristics of the boundary layer, such as effects on shock strength and location, and effects on the overall circulation and pressure distribution. These are reflected in parameters like lift, pitching moment, drag, stall characteristics and buffeting.

The interaction between all these effects is fairly complex and, in some cases, the role of Reynolds number cannot be totally clarified until the full-scale article is tested. The behaviour and magnitude of such scaling effects are often case-specific and generally unpredictable. In fact, experiments have occasionally shown counterintuitive results. In the investigation carried out by Banks et al. [66], wind tunnel data from large-scale low Reynolds number tests predicted the high-angle-of-attack flight characteristics of an F/A-18 fighter better than similar data from small-scale higher Reynolds number tests. In this case, the absolute geometric fidelity of the full-scale airframe used in the low Reynolds number test was more relevant for the forebody flow topology than the larger difference in Reynolds number.

As a consequence of the lack of general rules, extrapolation of results from lower Reynolds number data is largely based on the knowledge and experience of the aerodynamicist. Aerospace manufacturers often base Reynolds number corrections on empirical databases accumulated from years of experience with different programmes – extremely valuable information which usually remains company proprietary. This method produces reliable estimations for conventional or well-understood configurations, but introduces a considerable degree of uncertainty in cases where the configuration is not well understood or the flow is highly complex [2, 60, 62]. Nowadays, complementary analysis tools such as computational fluid dynamics (CFD) are also used to estimate scale effects in experimental data. According to Petterson et al.: "*Today, CFD methods are commonly used to predict flow features at Reynolds numbers higher than what the aircraft model is subject to in the wind tunnel, and at higher Reynolds number than the turbulence model has been calibrated to*" [67].

Because of their effects on the boundary layer, Reynolds number variations have a strong impact on the flow topology and forces produced across bodies for which there is no geometrically fixed separation, such as smooth and curved surfaces [60, 62]. Under these circumstances, extrapolating results obtained at one value of Reynolds number to a higher value could be misleading. According to Munro [62], even interpolation must be performed cautiously if the flow is especially Reynolds-number-sensitive since it might present rapid changes in topology; a phenomenon that is usually observed across the transitional region where many typical wind tunnel experiments are performed. A common technique to simulate flow conditions expected at a Reynolds number higher than the number achieved in the test is to artificially fix the laminar-turbulent transition and the separation at a predefined location by means of grit, strips and other flow-tripping devices [7, 60].

For flow around sharp corners, however, the separation is usually fixed at the edge and the flow often presents little or no dependence on Reynolds number. These kinds of sharp features are commonly found in modern combat aircraft with large flight envelopes and stealth capabilities. For instance, many contemporary fighters feature chined forebodies and highly swept lifting surfaces for controlled radar reflectivity, high-speed performance and high AOA excursions. The GFF configuration, shown in Figure 3.2, is a good example of these characteristics. The aerodynamics of such a configuration at high AOA are dominated by separated flow and vortex structures. Although the boundary layer region prior to separation is strongly dependent on Reynolds number, both the vortex sheet and the inviscid outer flow region remain relatively insensitive to Reynolds number variations [62]. Furthermore, the literature is in general agreement that, in sharp and highly swept surfaces, the separation location, trajectory and breakdown of the primary vortices are mainly determined by the geometry and the angles of attack and sideslip. Consequently, configurations with these characteristics are especially well suited for experiments with subscale models in which Reynolds number similarity cannot be maintained.

Even for more conventional configurations, it is still possible to study certain aerodynamic characteristics without a severe influence of scale effects caused by Reynolds number dissimilarity. For instance, according to Barlow, the rate of change of drag with lift, usually considered as the change in *span efficiency* or

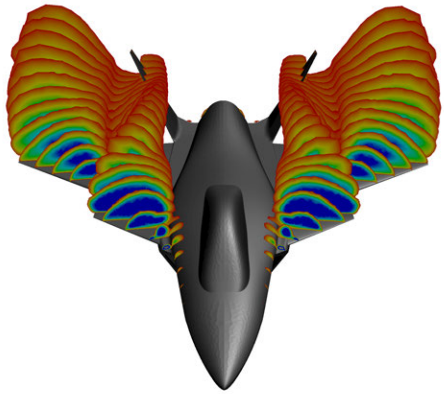

Figure 3.2 *Aerodynamic phenomena in which the flow transition and detachment are fixed by geometric features can be well-suited for experiments in subscale conditions with dissimilar Reynolds numbers. The image shows an example of such phenomena, in which profiles of detached flow on the sharp-cornered Generic Future Fighter (GFF) configuration have been obtained from CFD computations. Courtesy of Jörg Schminder, Linköping University.*

Oswald factor e, typically does not change with Reynolds number for straight wings [60]. This author explains that the slope of the nearly straight line resulting from a plot of C_L^2 versus the total drag coefficient C_D is practically independent of Reynolds number, although its position moves according to the scale effects on the parasite drag coefficient C_D. Accordingly, a subscale test with Reynolds number dissimilarity could still be used to estimate the full-scale e in straight wings by completing the following equation, as in [60]:

$$e = \frac{1}{(dC_D/dC_L^2)\pi AR} \tag{3.7}$$

The role of Mach number

There seems to be a clear agreement in the literature that the Mach number has a significant influence on the flow characteristics as soon as compressibility effects begin to be significant, and this may happen even far below the transonic regime. Wolowicz et al. [7] state that the differences in true and incompressible-flow dynamic pressure and temperature may be significant for Mach numbers in excess of 0.20, while other sources often extend this limit to Mach number 0.3. It should be noted that even in a flow with low free-stream Mach number, compressibility effects may be significant in local flow around certain geometries. For instance, the studies on the F/A-18 fighter configuration reviewed by Erickson et al. [68] revealed that the flow around some components such as the leading-edge extensions or *LEX* present Mach number effects at Mach numbers as low as $0.15 - 0.25$.

Mach number effects can be isolated from other scale effects for subsonic and supersonic flows until reaching a Mach number of approximately 5, the point at which the shock waves start interacting extensively with the boundary layer and hence Mach number effects couple to viscous effects [7].

In contrast to the cases in which a Reynolds number mismatch can be moderated by means of active boundary-layer control, there are no effective techniques to artificially compensate for Mach number dissimilarity. In fact, according to Rolston [69], the importance of matching the full-scale, free-flight Mach number during wind tunnel tests has historically never been in question. The need to achieve full Mach number similarity is, therefore, an important limitation for any kind of subscale testing in which compressible flow is to be studied.

3.4.3 Practical Limitations

Scale effects introduce important limitations for the design and execution of SFT experiments. Table 3.2 presents four different aircraft concepts that will be used here to visualise and discuss the main practical limitations associated with each scaling method. These concepts cover an extensive design space, and each of them corresponds to a subscale demonstrator manufactured at Linköping University.

Table 3.2 *Four different aircraft concepts used to visualise the impact of the scaling parameters under different circumstances. For each of these concepts, a subscale model has been developed at Linköping University.*

Picture	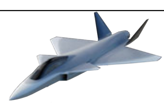		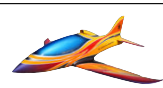	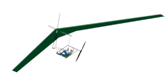
Identifier	(a)	(b)	(c)	(d)
Aircraft type	Generic Future Fighter (GFF)	Light business jet	Light-sport aircraft (LSA)	Human-powered aircraft (HPA)
Take-off mass	15400 kg	4000 kg	290 kg	100 kg
Wingspan	11 m	14 m	5 m	25 m
Cruise speed	300 $m\ s^{-1}$	160 $m\ s^{-1}$	50 $m\ s^{-1}$	8 $m\ s^{-1}$
Cruise altitude	9000 m	11000 m	3000 m	5 m
SFT scale factor	0.14	0.14	0.33	0.24
SFT Take-off mass	19.2 (42.3) * kg	11.0 kg	10.8 kg	1.4 kg
SFT Wingspan	1.5 m	1.9 m	1.7 m	6.0 m

As discussed earlier, one of the main challenges for aerodynamic scaling in SFT is the Reynolds number similarity: full-scale Reynolds number can rarely be achieved if the scale factor is far from the unity. Figure 3.3 shows this problem on the four aircraft types introduced in Table 3.2 by comparing the chord Reynolds number achieved with different scaled models and testing techniques with that expected during full-scale design conditions. Although a higher-than-test Reynolds number can, in some cases, be simulated by controlling the boundary layer behaviour, in most cases the scale effects derived from this dissimilarity should be taken into account. The magnitude of dissimilarity and the significance of the consequent Reynolds number effects differ from case to case. For example, the discrepancies related to Reynolds number effects on lifting surfaces between model and full-scale may be expected to be larger in case (c) than in case (a): despite being less than one order of magnitude apart in terms of chord Reynolds number, the vehicles in case (c) are within a regime where boundary-layer transition typically occurs and where significant changes in flow topology may be expected [70]. Additionally, the rounded geometry of (c) is likely more sensitive to these changes than the sharp-edged configuration (a).

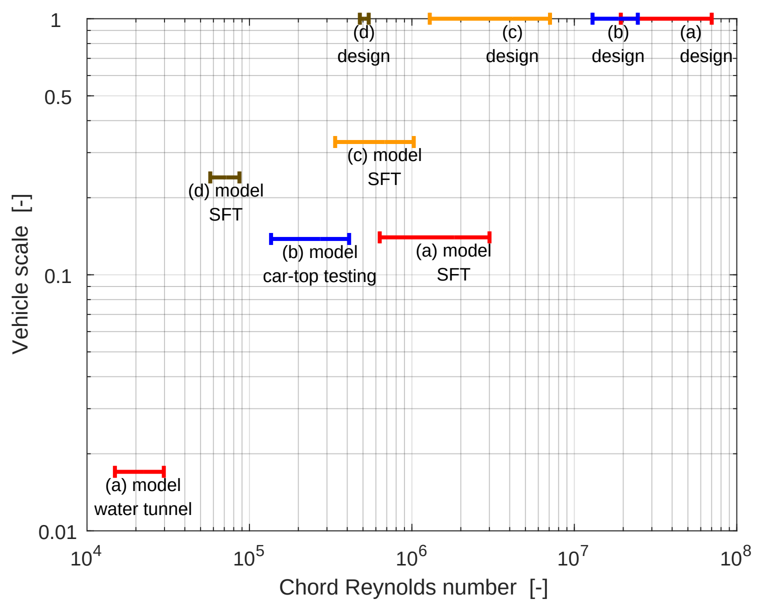

Figure 3.3 *Reynolds number obtained at the mean chord of the main wing for models of different scales using various testing techniques at sea level, compared to that expected on the full-scale vehicle during nominal operation. The four different cases correspond to the configurations described in Table 3.2.*

The other major challenge for aerodynamic scaling with subscale models in the open atmosphere is reproducing the compressibility effects by achieving Mach number similarity. As discussed earlier, this is essential for cases in which the full-scale phenomenon of interest involves compressible flow. In contrast to the Reynolds number, the maximum Mach number attainable during SFT is not directly related to the scale factor of the model. Instead, it is a consequence of the structural design of the model and its propulsion system, as well as the testing technique used and the maximum flight speed at which the model can be safely controlled. Figure 3.4 shows a practical example in which the Mach number achieved during testing of various subscale models is compared to the expected Mach number range of the full-scale vehicles. As can be seen in this figure, it is sometimes possible to neglect compressibility effects (green area) while in other cases it is only possible to study the low end of the full-scale flight envelope with the subscale model without introducing uncertainties due to compressibility effects (yellow area and beyond).

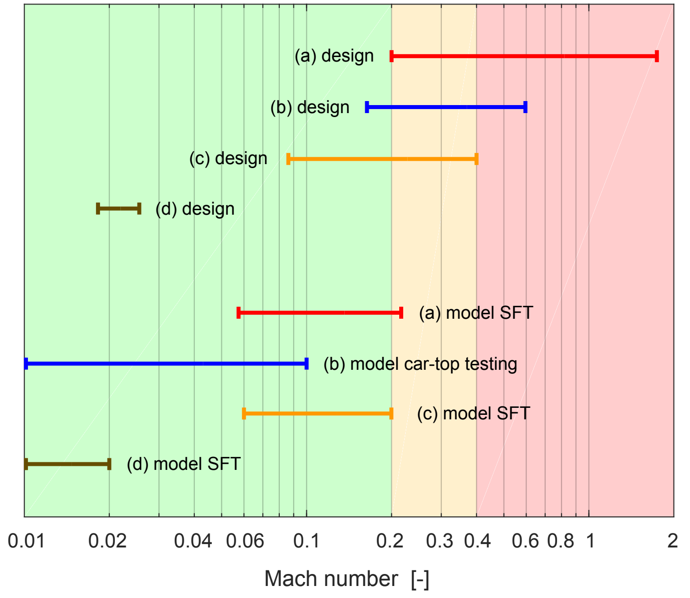

Figure 3.4 *Mach number at which various subscale models are tested in the open atmosphere, compared to the Mach number range where the full-scale vehicles would be operated. The four different cases correspond to the configurations described in Table 3.2, and the background colours represent incompressible (green), risk of compressibility (yellow) and compressible (red) flow regimes.*

Another aspect that needs to be taken into consideration is the geometrical distortion introduced by the additional systems and features needed to make the subscale model a functional flying vehicle. Examples of this distortion are external control-surface links, differences in the installed propulsion and intake ducts, access panels, antennas, differences in the landing gear arrangement, minor geometrical simplifications and other similar elements. In addition, the integration of external instruments such as probes, vanes and cameras may also be inconsistent with the full-scale geometry. Furthermore, the deformation of the airframe under load may also contribute to the dissimilarity; unless particular considerations are taken into account during design and manufacturing, the structural stiffness of the model would be generally different to the equivalent stiffness of the full-scale aircraft, a factor that may introduce additional geometrical distortion and, therefore, deviations in the measured aerodynamic parameters.

These and other concerns regarding aerodynamic scaling are summarised in Table 3.3. This table synthesises all the previous discussions and presents a list of the main practical issues and considerations of importance for aerodynamic scaling of subscale models in the open atmosphere.

Table 3.3 *Summary of the main concerns and issues regarding aerodynamic scaling for subscale free-flight models tested in the open atmosphere.*

	Issue	Discussed in
1	Aerodynamic scaling with free-flight models that are not dynamically scaled may be impractical. Since vehicle dynamics are dissimilar, attitude and motion must be externally enforced by actively controlling either the vehicle or the flow.	[7]
2	Reynolds number similarity is generally unattainable using models with a scale factor far from the unity. Related scale effects may be significant, and studies may need to be limited to phenomena that are insensitive to Reynolds number.	[2, 7, 60, 59, 62, 63, 68, 69]
3	For compressible flow, Mach number similarity may only be attainable for low-speed subsonic flow due to vehicle and operational constraints.	[7, 60, 59, 62, 63, 68, 69]
4	Model geometrical distortion: fidelity, actuation of control surfaces, propulsion system differences.	[2]
5	Model geometrical distortion: dissimilar aeroelastic deformation.	[2, 7]
6	Distortion introduced by the instrumentation: effects on the flow and on the measurements.	[2]

It can be concluded that one of the most important aspects regarding aerodynamic scaling is that it requires extensive understanding of the flow prior to designing the subscale experiment. As seen before, only a reduced number of flow problems can be explored with free-flight subscale models without accounting for undesired scale effects, and even in those cases, it may be difficult to achieve the right test conditions using non-dynamically scaled models. As a result, *pure* aerodynamic scaling is usually inappropriate for SFT, although it may be convenient for other methods such as car-top testing.

3.5 Dynamic Scaling

In many cases, the research focus is not only on the aerodynamic forces acting on the aircraft but also on the motion that they induce. While there are some well-established methods for estimating static characteristics of an aircraft, such as static aerodynamic coefficients, the determination of dynamic characteristics presents more difficulties. As shown in Figure 3.5, there are no analytical methods that provide medium or high-fidelity predictions of dynamic behaviour. While numerical methods such as CFD are making rapid progress in this area, wind-tunnel and flight testing remain essential for uncertainty reduction.

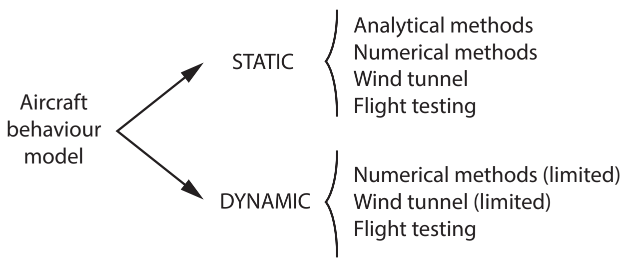

Figure 3.5 *Nature of different methods commonly used to investigate the static and dynamic behaviour of an aircraft at a medium/high fidelity level.*

Nevertheless, the study of dynamics in wind or water tunnels is generally difficult. The model support, the wall effects and the size of the test section severely limit the degrees of freedom and the types of motion that can be performed. Since real flight testing is generally not an option during the early stages of design, the uncertainty in dynamic behaviour has to be dealt with using alternative solutions. Historically, one of these solutions has been testing free-flight subscale models in the open atmosphere as well as inside sufficiently large wind tunnels [6, 7, 10], as introduced in Section 1.1. In this case, the vehicle is not held rigidly and it is free to develop its own motion. Consequently, the similarity principles have to be fulfilled not only for the aerodynamic forces but also for the vehicle motion.

3.5.1 Dynamic Scaling Parameters

While the similarity was limited only to the flow field in aerodynamic scaling, dynamic scaling also requires similarity for the vehicle motion.

According to the general similarity principles derived in Section 3.2, the similarity in flight dynamics is governed by the parameters given in Equation (3.4).

The parameters that refer to flow similarity are here needed to ensure similar aerodynamic forces, as in Equation (3.6). The additional parameters that account for all the aspects of the vehicle motion, (h,...,n), are also compulsory. The only simplification that can be made is to assume a rigid vehicle and hence leave aside those parameters that account for an elastic airframe, i.e. terms (f) and (g). By considering a rigid vehicle, any aeroelastic effects are either neglected or accounted for by other means. As a result, the relevant similarity parameters for dynamic scaling can be reduced to:

$$C_F,\ C_M = f\left(\overset{(a)}{\frac{\rho V l}{\mu}}, \overset{(b)}{\frac{V}{c}}, \overset{(c)}{\delta}, \overset{(d)}{\frac{m}{\rho l^3}}, \overset{(e)}{\frac{I}{\rho l^5}}, \overset{(h)}{\alpha'}, \overset{(i)}{\frac{al}{V^2}}, \overset{(j)}{\frac{\Omega l}{V}}, \overset{(k)}{\frac{\dot{\Omega} l^2}{V^2}}, \overset{(l)}{\frac{\omega l}{V}}, \overset{(m)}{\frac{V^2}{lg}}, \overset{(n)}{\frac{tV}{l}}\right) \tag{3.8}$$

where C_F and C_M are non-dimensional aerodynamic coefficients in the usual non-dimensional form, and all the other terms have been previously described in Section 3.2. It is noteworthy that the term (m), or Froude number, accounts here for the vehicle inertial forces and not for the fluid inertial forces as in Equation (3.5).

It may be observed that the terms (d) and (e) prescribe that the mass distribution of the full-scale and subscale vehicles must be similar in order to obtain equivalent inertial force and equivalent rigid-body motion. Hence, the moments of inertia of the subscale vehicle must be proportional to those of the full-scale counterpart; a condition that can substantially influence the structural design of the subscale airframe and the experiment limitations.

Another observation is that, while in aerodynamic scaling the focus is on recreating the flow field, in the study of rigid-body dynamics it is generally enough to ensure that the resultant aerodynamic forces and moments acting on the body are similar at every state. Although it is usually assumed that such a condition requires precise geometrical similarity, this is not true. Geometrical or flow-field modifications would not affect the results as long as all the aerodynamic forces and moments, as well as the mass properties of the body, are ultimately similar. This fact may be an advantage when it comes to reproducing certain forces, loads, or states that cannot be easily achieved at subscale conditions.

Perhaps the main observation to be made about Equation (3.8), however, is the following: the terms (a), (b) and (m) – i.e. the Reynolds, Mach and Froude numbers respectively – dictate contradictory requirements for the subscale model velocity. Even assuming a certain degree of Reynolds number dissimilarity, as seen in Section 3.4, the divergence of the Mach and Froude numbers remains problematic for SFT whenever flow compressibility is considered. Satisfying both similarity requirements at once would require an improbable change in the gravitational field. Once again, it is infeasible or impractical to fulfil all similarity parameters simultaneously: they need to be assessed and balanced during the design of the subscale experiment.

The disagreement between the similarity conditions prescribed by the terms (m) and (b) in Equation (3.8) generates two different subtypes of dynamic scaling strategies: one that pursues complete Froude number similarity at the expense of dissimilar fluid-compressibility effects, and another that pursues complete Mach number similarity at the expense of dissimilar proportions between inertial and gravitational effects. The first is commonly known as *Froude scaling*, while the latter is commonly known as *Mach scaling* [7]. Froude number similarity can be easily achieved by tailoring the mass properties of the subscale model, and Froude scaling is hence the natural choice for cases dealing with an incompressible flow or in which compressibility effects can be disregarded. On the contrary, Mach number similarity may be more difficult to meet for aircraft flying faster than the usual boundary for compressibility effects (see Section 3.4 and Figure 3.4), as the model velocity depends not only on its performance but also on any operating limitations.

3.5.2 Scale Effects

The exposure to undesired scale effects is, in this case, similar to that of the aerodynamic scaling method. Most of the discrepancies are introduced by the inability to achieve complete similarity for the aerodynamic forces and moments acting on the subscale vehicle.

To begin with, it is not usually possible to reach the required Reynolds number with a subscale model flying in natural atmospheric conditions: the large influence of the scale factor on this quantity (proportional to the characteristic length) cannot always be fully compensated for by altering the flight speed and the flight altitude. In most cases, a certain degree of Reynolds number dissimilarity has to be accepted and accounted for, as discussed in Section 3.4.

Furthermore, the divergence between the similarity conditions for Froude and Mach numbers and the consequent choice of scaling strategy will introduce additional scale effects. If the experiment is scaled following Froude number similarity, the Mach number of the model will be lower than it should be. Similarly, the Reynolds number of the model will be lower unless the full-scale vehicle is flying at high altitude. Figure 3.6 shows this trade-off for a Froude-scaled model flown at sea level.

A similar effect is found when the experiment is scaled following Mach number similarity. Although compressibility effects will be correct, the Froude number of the model will generally be higher than it should be, and its Reynolds number will be lower unless the full-scale vehicle is flying at high altitude. Figure 3.7 presents this alternative trade-off scenario.

The role of Froude number

The Froude number similarity applied to an aircraft accounts for an equivalent ratio between the inertial and gravitational effects during dynamic motion. Hence, a mismatch in this parameter will produce a dissimilar response during

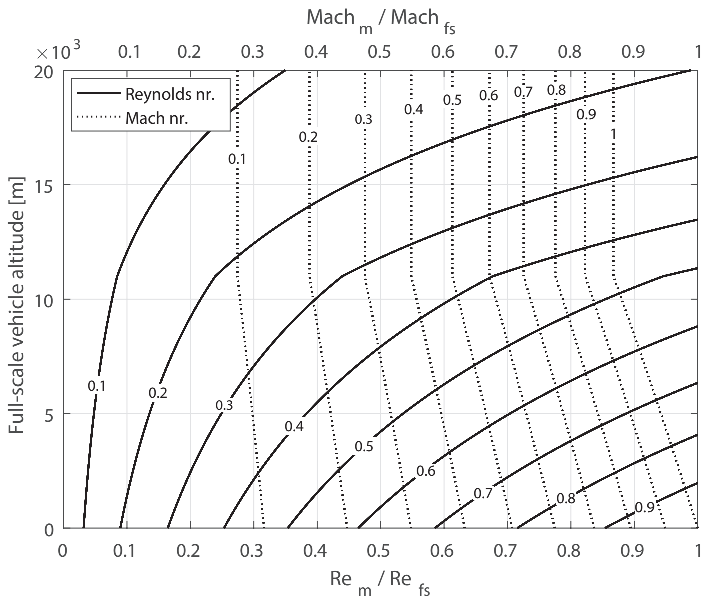

Figure 3.6 *Ratio of Reynolds number and ratio of Mach number for a subscale model tested at sea level with respect to those of a full-scale vehicle at different altitudes, according to dynamic scaling with Froude number similarity. Each line represents a different scale factor.*

flight manoeuvres, such as the resulting load factor in a banked turn at a given attitude, or the vehicle trajectory during a spin [7].

Nevertheless, the implications of Froude number similarity go beyond dynamic manoeuvring. Even at steady and level flight, where the load factor is equal to one, important characteristics such as the lift coefficient are also dependent on the ratio between inertial and gravitational effects. In the case of the lift coefficient, a discrepancy in Froude number will cause the model to find the equivalent equilibrium of forces at a different AOA than that of the full-scale aircraft.

3.5.3 Practical Limitations

Due to the need for similar aerodynamic forces and moments, dynamic scaling typically involves most of the practical issues mentioned earlier in Section 3.4. More specifically, issues 2, 3, 4, 5 and 6 in Table 3.3 apply in the same terms to typical dynamic scaling experiments. Figures 3.3 and 3.4 illustrate the first two of these issues using the cases presented in Table 3.2 as examples.

Unfortunately, the requirements for similarity in mass and inertial characteristics introduce additional problems for the practical execution of subscale

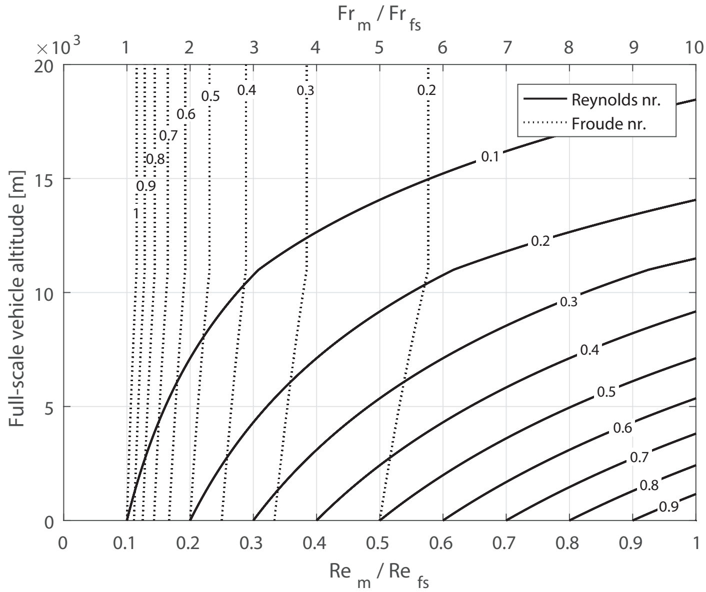

Figure 3.7 *Ratio of Reynolds number and ratio of Froude number for a subscale model tested at sea level with respect to those of a full-scale vehicle at different altitudes, according to dynamic scaling with Mach number similarity. Each line represents a different scale factor.*

experiments. The similarity of mass ratio and mass moments of inertia, terms (d) and (e) in Equation (3.8), often prescribe model weights that differ significantly from those usually found in similar non-dynamically scaled models. If the aircraft is assumed to be a rigid body, the moments and products of inertia can easily be matched by distributing individual masses along the airframe, although this technique is only applicable if the airframe is initially lighter than the target weight. In fact, achieving the right inertial characteristics becomes rather challenging if the prescribed weight is lower than that resulting from a typical model manufacturing process; special materials or manufacturing techniques may be necessary, and the inertia requirements may have a significant impact on the model design.

In some cases, the requirements for similarity in mass and inertial characteristics will make it directly impractical or infeasible to conduct a subscale experiment at certain scale factors. The different examples introduced in Table 3.2, plus two additional cases, are used in Figure 3.8 to illustrate this problem. In this figure, the background colours suggest the relative level of difficulty (and eventual cost) of performing SFT with instrumented, dynamically scaled models according to their take-off mass: low (green), medium (yellow) and high (red). For instance, the legal requirements for civil operation of this kind of vehicle in many European countries change significantly when the take-off mass exceeds 25 kg, and even more dramatically when it exceeds 150 kg. On the lower side, it becomes generally difficult to build and operate a functional model of less than 1 kg of take-off mass including the necessary instrumentation. Figure 3.8 shows two lines for each case: the solid lines represent similarity to the full-scale vehicle at sea level, while the dashed lines represent similarity to the full-scale vehicle when it flies at its design altitude. The GFF, indicated as (a), is a good example of the trade-off needed. In this case, the subscale model is usually operated below the required weight for dynamic similarity in order to avoid the legal requirements of a heavier vehicle category, and hence significantly lower the operating costs.

Another potential problem for the design of dynamically scaled experiments is the decrease in actuation and response times. According to the similarity parameters in Equation (3.8), the magnitude of time in the model should decrease as the scale factor is reduced. On the one hand, this affects the response time and makes the model motion quicker than that of the full-scale vehicle, as shown in Figure 3.9 (top) for the two types of dynamic scaling. Consequently, higher performance and faster sampling rates may be required from the instrumentation and the data acquisition system.

On the other hand, this effect also introduces higher demands on the control system: the speed at which the control surfaces are deflected should be increased in accordance with the time requirements. While the latency in the radio-control system is usually not a problem with modern equipment, the speed of proportional servo-actuators is more limited and could, in some cases, become a bottleneck. In extremely challenging cases in which proportional actuators with appropriate performance are not available, it could be necessary to utilise simpler, non-proportional (on-off) high-speed actuators, as tested by NASA in several small-scale models [6, 7]. Figure 3.9 (bottom) shows an example of how angular rates change according to the scale factor and type of dynamic scaling.

These practical limitations, together with other concerns discussed in previous sections, are summarised and presented in Table 3.4. Although this table contains by no means all the existing issues for dynamic scaling, it includes the most significant challenges for the design of subscale experiments using free-flight models in the open atmosphere.

As a consequence of all the above, it could be said that dynamic scaling builds on the similarity principles of aerodynamic scaling. Good knowledge of the phenomena of interest and the expected flow conditions is still essential, although this must be supplemented with a comprehensive evaluation of other variables related to the scaling of the vehicle itself. The feasibility of testing a dynamically scaled model at certain scale factors will, in most cases, be strongly influenced by the available resources for manufacturing and operation, as well as the characteristics of the available components and onboard systems, such as propulsion, control and data acquisition systems.

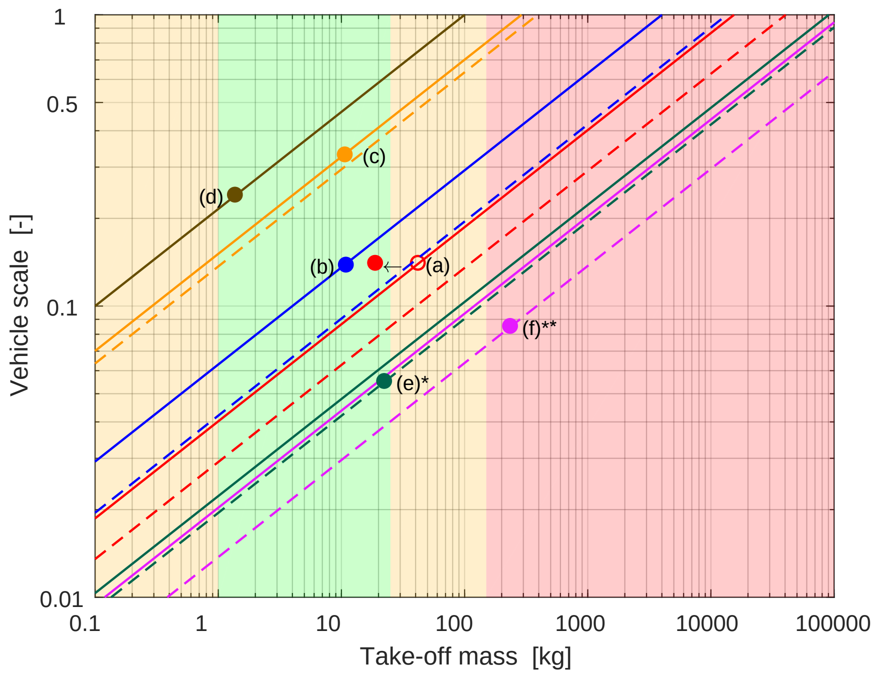

Figure 3.8 *Correlation between take-off mass and scale factor according to dynamic similarity for subscale testing at sea level. Background colours indicate different levels of cost according to the challenges of manufacturing and operating an instrumented model of the respective weight. For each of the cases, solid lines represent similarity to the full-scale vehicle at sea level while dashed lines represent similarity to the full-scale vehicle at its design altitude. In case (a), the subscale model is flown lighter than prescribed for cost and feasibility reasons. Besides the aircraft described in Table 3.2, two complementary examples have been added: *(e) corresponds to NASA's AirSTAR Generic Transport Model (GTM-T2) [20], and **(f) corresponds to NASA-Boeing's BWB demonstrator (X-48B) [17].*

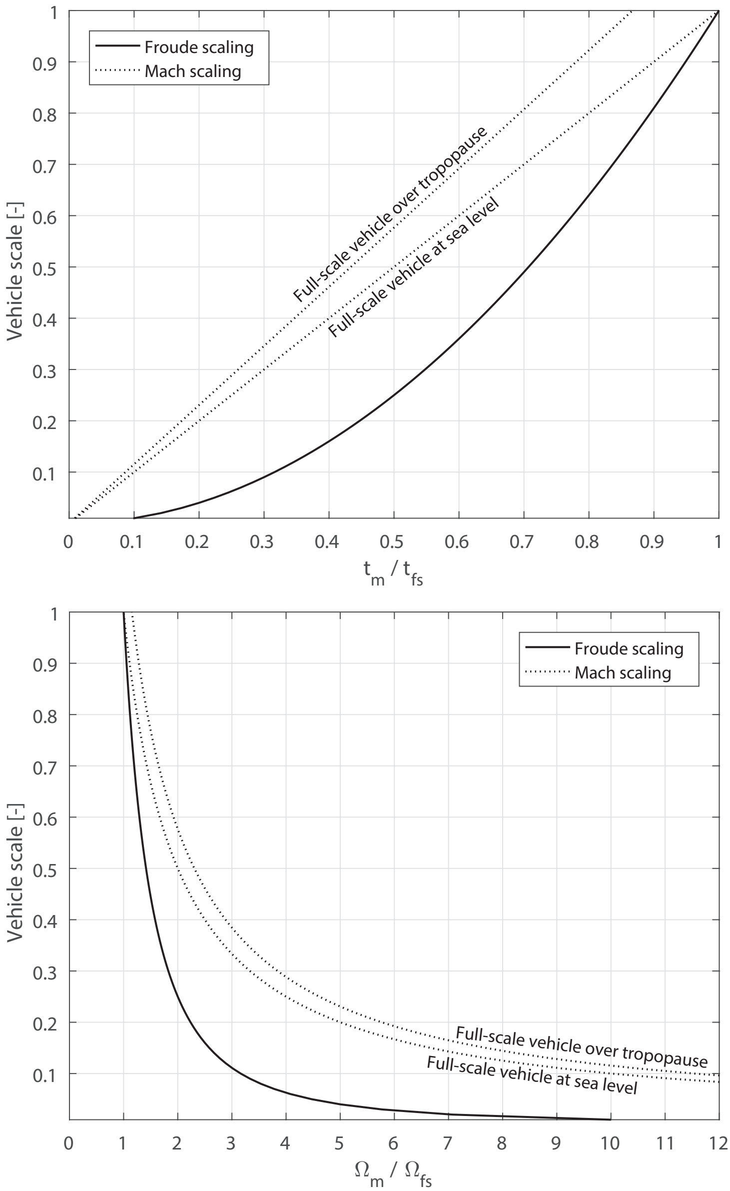

Figure 3.9 *Ratio of response time (top) and ratio of angular rates (bottom) for a subscale model tested at sea level with respect to those of the full-scale vehicle at any altitude (for dynamic scaling with Froude number similarity), and at two given altitudes (for dynamic scaling with Mach number similarity).*

Table 3.4 *Summary of the main concerns and issues regarding dynamic scaling for subscale free-flight models tested in the open atmosphere.*

	Issue	Discussed in
1	Similarity of aerodynamic forces and moments introduces issues 2, 3, 4, 5 and 6 from Table 3.3.	Section 3.4
2	Generally not possible to achieve Froude and Mach number similarity simultaneously. One of these two parameters has to be prioritised.	[6, 7]
3	Similarity of mass ratio and moments of inertia may require models that are either too light or too heavy to be produced and operated economically. Depending on the type of aircraft, only a reduced range of scales may be of practical use.	[6, 7, 71]
4	Mass and inertia characteristics might vary differently in subscale and full-scale vehicles during flight due to different fuel fractions and fuel system architecture.	
5	Deviations introduced by dissimilar dynamics in control and actuation systems. Especially at small scales, control-surface actuators might not operate as quickly as required.	[6]
6	The quick angular motion of models with small-scale factors may require data acquisition systems with high logging frequencies and can make manual piloting difficult or infeasible.	[6]

3.6 Aeroelastic Scaling

In other types of scaling we have systematically assumed that both the subscale and full-scale vehicles behave as a rigid body. This assumption is usually appropriate for studying static or pseudo-static characteristics of the aircraft, such as aerodynamic coefficients under certain conditions or performance at given points of the flight envelope. Moreover, steady states in which elastic airframe deformation is anticipated could also be studied in subscale conditions with rigid models that already incorporate the expected distortions. Nevertheless, neglecting the flexibility of the aircraft implies disregarding multiple dynamic phenomena that are increasingly relevant for aircraft conceptual design.

Although structural dynamics and flight dynamics were often studied separately in the past, the quest for performance optimisation in modern aircraft has led to increased use of light, more efficient, flexible structures in which these two disciplines are tightly coupled [72, 73]. The growing interest in studying and modelling these interactions during the early stages of aircraft design is also motivated by the development of optimum and adaptive flight control laws that take into account and utilise aeroelastic phenomena. Figure 3.10 is based on the *triangle of forces* conceived by Collar [72], and it graphically shows the interaction between the three main types of forces that define the aeroelasticity domain. Various phenomena are located on this triangle according to their relative dependence to the forces, although these couplings only correspond to a general definition and may be different for certain types of aircraft, conditions and modelling approach.

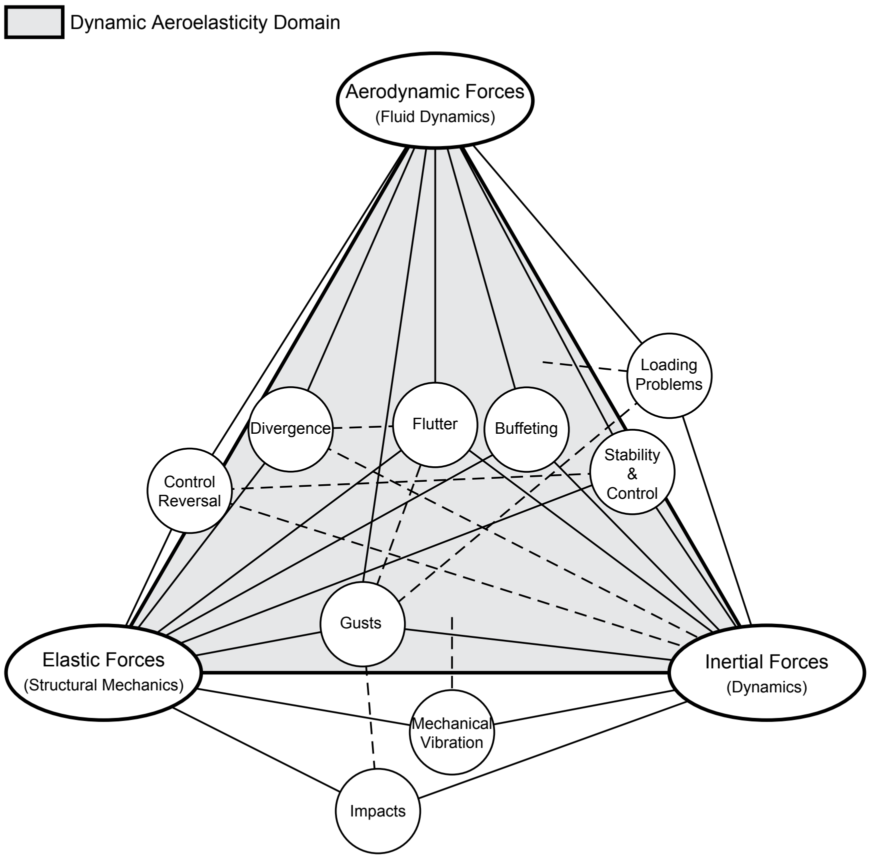

Figure 3.10 *The "triangle of forces", adapted from Collar [72], represents graphically the dynamic aeroelasticity domain and how different phenomena typically interact with its governing forces.*

The experimental validation of aeroelastic (mathematical or simulation) models and advanced control laws is a risky and generally expensive process, due to the potentially catastrophic damage that some of these phenomena could cause to the aircraft integrity. There is, therefore, a significant interest in finding alternative methods for evaluating these subjects as early as possible in the design process, and it is here that SFT can be an economical, low-risk alternative to full-scale flight and wind-tunnel testing. One of the best examples of this application is perhaps the *Drones for Aerodynamic and Structural Testing* (DAST) programme carried out by NASA from 1977 to 1983 [74, 75, 76]. In this programme, two *BQM-34 Firebee II target drones* were modified with supercritical aerofoils and new wing geometry, the *Aeroelastic Research Wing* (ARW). These vehicles were mainly used to evaluate active control systems and flutter suppression techniques, as well as for stability and structural investigations.

NASA's *AirSTAR Generic Transport Model* (GTM) has also been used for research on adaptive control and other advanced control laws [20, 77, 78, 79], even though this subscale model was not scaled according to aeroelastic similarity and is too stiff for the study of interactions between structural dynamics and control laws.

A recent example of an advanced subscale model specifically designed for the study of aeroelastic phenomena is the Lockheed Martin *X-56A* or *Multi-Utility Technology Testbed* (MUTT), a 15%-scaled version of the *SC006A Sensorcraft* configuration with interchangeable wings [80, 81, 82]. This remotely piloted model was mainly designed to investigate the development and suppression of the unstable coupling between the short-period mode and the first symmetric wing mode, a phenomenon known as body freedom flutter (BFF) which is commonly found in high aspect ratio wings [83]. This aeroelastic problem was also recently studied by Ouellette et al. using a much simpler remotely controlled model derived from a commercial off-the-shelf (COTS) model aircraft [73, 84].

A more recent take on active flutter control and aeroelastic tailoring is the European Flutter-free Flight Envelope Extension for Economical Performance Improvement (FLEXOP) research project [85, 86, 87, 88, 89, 90] and its continuation, *FLiPASED*.

3.6.1 Aeroelastic-Scaling Parameters

As hinted at in Figure 3.10, a subscale experiment that aims to investigate dynamic aeroelasticity will necessarily involve elastic, inertial and aerodynamic forces. Accordingly, similarity requirements for structural flexibility will add to those involved in dynamic scaling (Section 3.5), which already included those of aerodynamic scaling (Section 3.4).

Thus, for a general dynamic problem with a flexible aircraft, similar aerodynamic forces and moments can be obtained by satisfying all the similarity requirements initially included in Equation (3.4), which was obtained according to Wolowicz et al. [7]; i.e.:

$$C_F,\ C_M = f\left(\overset{(a)}{\frac{\rho V l}{\mu}}, \overset{(b)}{\frac{V}{c}}, \overset{(c)}{\delta}, \overset{(d)}{\frac{m}{\rho l^3}}, \overset{(e)}{\frac{I}{\rho l^5}}, \overset{(f)}{\frac{EI'}{\rho V^2 l^4}}, \overset{(g)}{\frac{GJ'}{\rho V^2 l^4}}, \overset{(h)}{\alpha'}, \overset{(i)}{\frac{al}{V^2}}, \overset{(j)}{\frac{\Omega l}{V}}, \overset{(k)}{\frac{\dot{\Omega} l^2}{V^2}}, \overset{(l)}{\frac{\omega l}{V}}, \overset{(m)}{\frac{V^2}{lg}}, \overset{(n)}{\frac{tV}{l}}\right) \tag{3.4}$$

This formulation includes the required elastic similarity between full-scale and subscale vehicles by means of the terms (f) and (g), which account for the aeroelastic bending and aeroelastic torsion, respectively. The other similarity parameters represent the same requirements as in dynamic scaling, although an important observation must be made: in this case, the requirements for similar mass moment of inertia characteristics imply similarity in the actual mass distribution. In Section 3.5 it was stated that, for a dynamically scaled rigid aircraft, similarity in mass moments and products of inertia could be met by adding the necessary masses on the airframe. However, aeroelastic scaling requires the actual distribution of these masses to be similar to that of the full-scale vehicle [7]. Even though this detail might not seem particularly important, it can add significant complexity to the design and manufacturing of the model.

Equation (3.4) is nevertheless a general formulation for complete similarity based on aerodynamic forces and moments that can rarely be fulfilled in practical applications. Specific aeroelastic problems usually demand applied formulations and partial similarity tailored to the phenomena of interest and the available testing possibilities. For instance, Ouellette et al. propose in [73] a more practical set of aeroelastic scaling laws applied to the study of couplings between the short-period mode and the wing structural dynamics, such as body freedom flutter (BFF). Among other simplifications, these authors argue that the sensitivity of the short-period mode to the Froude number is generally low, and the flight velocity can therefore be lower than that prescribed by typical Froude scaling. The reduced set of similarity requirements allowed for the development of a feasible subscale experiment, the results of which were reported in [84].

3.6.2 Scale Effects

Since there is no universal scaling methodology for aeroelastic problems it is impossible to discuss the particular effects that partial similarity would have on the experiment results. In general, the scale effects related to unfulfilled aerodynamic similarity, as discussed in Section 3.4, are still relevant here. In fact, dissimilarity in Reynolds number could be a major concern for the study of aeroelastic phenomena in which partially separated flow is involved [7].

Furthermore, the problem of divergence between Mach number similarity and Froude number similarity, as discussed in Section 3.5 and illustrated in Figures 3.6 and 3.7, takes on a more troubling dimension in aeroelastic scaling: when flow compressibility is a significant factor and Mach scaling is followed, the consequent dissimilarity in Froude number causes the model to fly at a different AOA than what the full-scale aircraft would. Due to the dissimilar attitude, the aeroelastic deformations are no longer equivalent to those of the full-scale aircraft [7]. Nevertheless, these effects are negligible for some aeroelastic problems such as the study of BFF mentioned above. In this case, the coupling between the short-period mode and the structural dynamics is much less sensitive to Froude number than to other factors like structural stiffness and the structural frequency [73].

3.6.3 Practical Limitations

Aeroelastic scaling generally combines most of the practical issues related to the aerodynamic and dynamic scaling methods. The similarity of aerodynamic forces and moments brings back issues 2, 3, 4 and 6 from Table 3.3. The first of these, i.e. the difficulty of achieving similarity in Reynolds number illustrated in Figure 3.3, might be of special importance for some aeroelastic interactions in which detached flow plays a significant role.

The similarity of inertial forces and motions also adds issues 2, 3, 4, 5 and 6 from Table 3.4. Regarding issue 2, and as mentioned previously, scarifying Froude number similarity for Mach number similarity in compressible-flow conditions will generally cause inconsistent aeroelastic deformations due to mismatched AOA, although this effect might be less significant for certain applications. As for issue 4, preserving the similarity in mass and inertial characteristics with different fuel systems on the full-scale and subscale vehicles becomes even more challenging in aeroelastic scaling since the mass distribution is also required to be similar.

Besides the issues accumulated from the previous scaling methods, aeroelastic scaling also presents some particular practical problems. Perhaps one of the most notable is the general difficulty of designing a subscale experiment in such a way that the aeroelastic phenomenon of interest is excited within the feasible flight envelope of the model. According to the similarity parameters in Equation (3.4), most of the models within the feasible region of Figure 3.8 would present a structural stiffness that is too high for experiencing observable aeroelastic interactions at the typical airspeeds achievable during SFT. The only exception would be the extremely flexible human-powered aircraft (HPA) or case (d). A usual solution to this problem is to reduce the structural stiffness of the model and hence sacrifice complete similarity with the full-scale vehicle. For instance, this was the solution adopted in the *X-56A* MUTT programme: the structural stiffness of the model was reduced to a level at which BFF could be experienced at lower airspeeds [80]. Another option is to design the whole subscale experiment starting from the available flight testing conditions and defining a hypothetical vehicle that would fit such conditions. This alternative was chosen in the FLEXOP project: the design of the test article was strictly bound to the mission design [86], and did not correspond to any particular full-scale aircraft. Nevertheless, strong accelerations and decelerations were still required to reach the desired flight conditions during the short legs of the remote flight test. These manoeuvres demanded high performance from the propulsion and braking systems, which were specifically optimised for this task instead of being scaled from full-scale characteristics [85].

Testing aeroelastic phenomena also places special requirements on the data acquisition system. Most inertial instruments and data fusion algorithms used in flight dynamics incorporate various types of filters that are generally tuned for the detection of rigid body motion and therefore inhibit the typical frequencies at which structural dynamics develop. Measuring structural dynamics generally requires specific sensors and filters that are able to register considerably higher frequencies. The integration of other types of sensors on the airframe, such as strain gauges, may also be necessary [84].

All these practical issues are summarised in Table 3.5. It should be noted that these are based only on general characteristics, and that certain aeroelastic problems may introduce significantly different concerns.

Table 3.5 *Summary of the main concerns and issues regarding aeroelastic scaling for subscale free-flight models tested in the open atmosphere.*

	Issue	Discussed in
1	Similarity of aerodynamic forces and moments introduces issues 2, 3, 4 and 6 from Table 3.3.	Section 3.4
2	Similarity of inertial forces introduces issues 2, 3, 4, 5 and 6 from Table 3.4.	Section 3.5
3	In addition to inertial characteristics, similarity in mass distribution is also required. This might be difficult to satisfy when the fuel system is considerably different.	[7, 80]
4	Dissimilarity in Froude number may cause inconsistent aeroelastic deformations due to mismatched AOA.	[7]
5	The structural stiffness prescribed by the similarity parameters might be too high for the excitation of aeroelastic phenomena at typical model flight speeds. Either structural stiffness is lowered or flight speed is increased.	[7, 73, 80, 86, 85]
6	Logging structural dynamics requires specific instruments and filters designed for sampling higher frequencies than those found in flight dynamics.	[84]

3.7 Demonstrative Scaling

Demonstrative scaling, or *demo-scaling*, is a term proposed here to encompass an increasingly common use of scaled models that does not follow the traditional interpretation of scaling laws. Demonstrative scaling can be defined as a scaling method in which the test article features a scaled form of a technology or capability that is yet to be proven in a relevant environment at a greater scale, while the test vehicle itself does not necessarily share a physical similarity with a full-scale vehicle. The similarity parameters, if applicable, depend on the nature of the feature or technology of interest. In most cases, an exact mathematical formulation of similarity is neither relevant nor necessary for a successful acquisition of information. This definition covers a wide variety of cases and applications, from basic functionality demonstration in a near-laboratory environment to sophisticated validation tests in the expected operational environment. Further, the mentioned attributes are shared by most of the research vehicles commonly known as *demonstrators*, but they do not correspond with near-production prototypes in which the features of interest are nearly in service.

In one way or another, technology demonstrators have always played an important role in the progress of the aerospace industry. For example, a glance at the historical evolution of American experimental aircraft – including the well-known *X-vehicles* [16, 91] as well as other projects like the Rockwell *HiMAT* [15] – reveals the critical effect that flight demonstration has on technology maturation. In the recent words of Eremenko [52]:

> "The goal of flight demonstrators is to provide a rapid maturation pull as well as a definitive measure of technology maturity far more convincing than the TRL.[1] And this is for those technologies that pose a particular integration or industrialisation risk, or where the effects of the flight environment cannot be adequately simulated on the ground."

A review of the historical progress of technology demonstrators also exposes an interesting trend. There seems to be a general tendency towards reducing the physical size of experimental vehicles in most cases where the nature of the technology and its integration allow this. Furthermore, unmanned demonstrators are preferred in many cases. This is not totally unexpected, considering that aircraft weight generally correlates well with complexity and cost, as Figure 3.11 shows.

More interestingly, however, this trend also reveals how recent disruptive innovations in the fields of electronics, computer science, manufacturing, power storage and communications have significantly altered the cost and capabilities

[1] The technology readiness level (TRL) is a well-known figure of merit for measuring and describing the maturity of technology. First proposed by NASA in the 1960's, it currently consists of nine different levels whose descriptions can be found in publications such as [92].

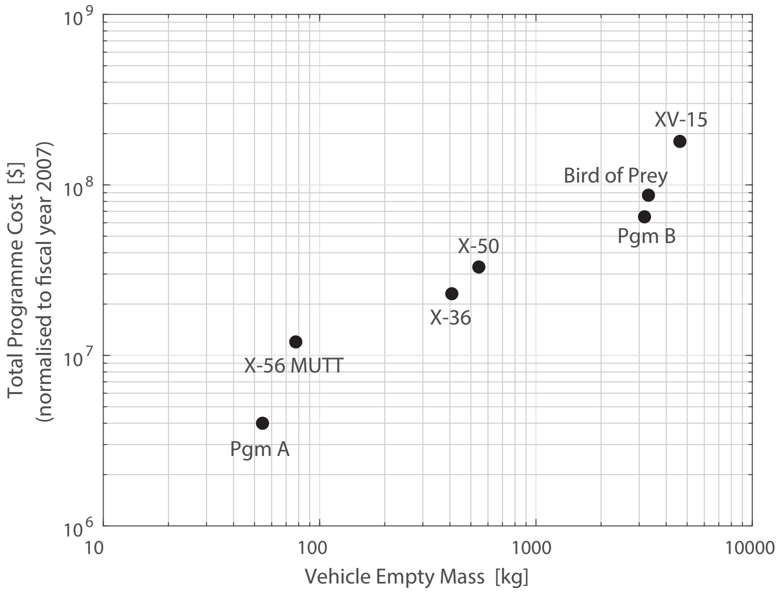

Figure 3.11 *Historical cost trend for a selection of American technology-demonstration vehicles, adapted from Beranek et al. [80].*

of small flying vehicles such as subscale models. Fairly sophisticated, unmanned test articles can now be built much more quickly and with considerably fewer resources; factors that also enable their use for experimentation with more immature technologies.

Recent examples of demonstrative scaling

A clear example of demonstrative scaling in this context can be found in the growing number of small companies and institutions that are currently testing radical vertical take-off and landing (VTOL) and electric aircraft concepts for urban mobility using relatively simple subscale models. Although it is difficult to quantify this phenomenon due to the lack of scientific publications covering these tests, an informed reader may have already noticed an explosion in the number of such projects during the last decade. Some of these are analysed in [93].

Established institutions like NASA are also increasingly relying on low-cost subscale platforms for experimentation with technologies at low TRL. An example is the *GL-10 Greased Lightning*, a tilt-wing subscale model with distributed electric propulsion. This low-cost platform has been used to experiment with distributed propulsion for VTOL and to investigate flight control and transition strategies [94, 95]. Another recent example is the *Prototype-Technology Eval-*

uation and Research Aircraft (PTERA). This research vehicle, developed for NASA by a small UAV manufacturer called Area-I, resembles a typical single-aisle transport at about 10% scale and is designed to be modular and easily reconfigurable. In a few years, this platform has already been used to evaluate technologies as diverse as flow-circulation control for short take-off and landing (STOL) [96] and morphing wings with folding wingtips [97].

A similar modular design was adopted for the European *Innovative Evaluation Platform* (IEP), also known as *Flexi-Bird* [22, 23, 98]. The geometry of this modular vehicle was also representative of a modern transport design, with slight variations in its configuration. It was intended to perform low-cost flight tests for investigating noise and environmental issues, flight dynamics and techniques for recovery from hazardous flight conditions.

Aurora Flight Sciences used a 20%-scale aircraft, the *VTOL X-Plane*, to demonstrate the feasibility of the future *XV-24A LightningStrike* VTOL vehicle with tilt-wing and hybrid-electric distributed propulsion [99].

In the BAE Systems research programme *FLAVIIR*, a light platform with a rather unconventional configuration was used to demonstrate fluidic thrust vectoring, circulation control devices and advanced flight control laws [19, 100]. Moreover, there are multiple examples of using similar subscale models as a low-cost test-bed for advanced flight control techniques, such as references [20, 77, 79, 101, 102, 103, 104]. In other cases, they have been used to evaluate novel system identification techniques and flight-test manoeuvres [105], or even the atmospheric influence on the flight performance of micro air vehicles [106].

In [26, 107, 108], subscale models are used to evaluate the characteristics of various unconventional configurations. In addition to NASA's experiments with the PTERA, research on unconventional and morphing structures has also been carried out in [109, 110, 111, 112].

Additionally, in [113, 114, 115], simple platforms were used to test and demonstrate the feasibility of flow and vehicle control by means of plasma actuators; a milestone that already entails a direct increase in the TRL.

In [33, 34], the vehicles demonstrated the maturity of flight guidance and automation technologies for unmanned aircraft system (UAS), while in [116, 117] small models were used to test various enabling vehicle technologies for future UAS traffic management systems.

Yanagihara et al. [14] demonstrated and validated autonomous flight technologies for future space transportation systems based on fixed-wing reentry vehicles.

Furthermore, Jung et al. proposed a methodology in [118] for conducting scaled sonic-boom flight tests using subscale models.

Three of the experimental platforms mentioned in the aeroelastic scaling section (3.6) could also be included in this section: the *X-56A* MUTT [80, 81, 82], the FLEXOP demonstrator [119, 86] and the modified COTS model by Ouellette et al. [84] leave aside complete similarities with full-scale vehicles in order to provide better capabilities for experimentation and demonstration within a feasible model flight envelope.

Impact of demonstrative scaling

The main strength of subscale technology demonstrators is the reduction of complexity, risk and hence cost over traditional research vehicles developed at full-scale. These characteristics, combined with shorter development and iteration times, make them suitable for early experimentation with immature technologies in a context of relatively low funding.

Low-cost demonstrators could be already useful for applied research at TRLs as low as two and three, although their most valuable capability is perhaps that they can be used to push the TRL across the first part of the technology development phase, approximately between TRL 4 and 6. This challenging phase, colloquially known as *the Valley of Death* [120], is usually characterised by a lack of sufficient resources to address the growing risk and cost, and the remaining uncertainties. Figure 3.12 aims to illustrate this situation and how low-cost subscale demonstrators could help to bridge the gap between the initial and final parts of the technology development phase.

Nevertheless, a question might arise from the lower levels of technology maturity: Is it always convenient to invest valuable resources in scaled flight demonstration? It is generally agreed that designing and performing practical experiments is a resource-consuming endeavour, and it has also been argued that virtual experiments often require fewer resources and are easier to reproduce and store [46]. It seems evident that there cannot be a categorical answer to this question. Different scenarios and technologies might require different or combined approaches. However, it may be interesting to also consider other by-products of experimental flight demonstration that are not exclusively of a technical nature: the positive effects on confidence and motivation.

An important side-effect of building flight demonstrators is the motivating effect on engineers and technologists, especially in the current scenario where large aerospace programmes are few and far between. Eremenko [52] recently acknowledged this effect on a large organisation such as *Airbus*, and also added another aspect: *"[A flying demonstrator] is a tool for attracting top talent, and an essential one for us [large and established companies] to compete with the start-ups, the Googles, and the Amazons of the world."*

Kress [3] highlighted similar motivational effects after an experimental campaign at *Grumman*, in which multiple R/C models were used to investigate and demonstrate conceptual V/STOL aircraft. Kress also mentioned the proficiency of these models in terms of revealing unforeseen design problems.

Positive effects of flight demonstration have also been reported in academic environments [35], where the authors found subscale models to be a motivating tool for transferring practical experience and confidence in solving applied engineering problems.

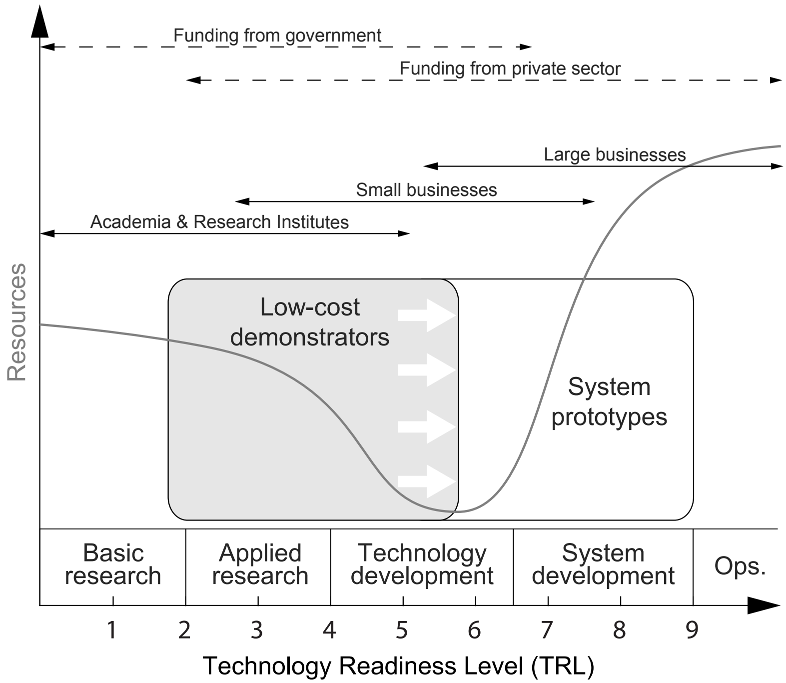

Figure 3.12 *Phases and factors involved the development of a new technology or system according to the TRL scale [92]; adapted from [121]. Low-cost subscale demonstrators could help to bridge the central gap, colloquially known as the Valley of Death [120].*

3.8 SFT Usage in Recent Projects

The extensive literature research presented in paper [V] aims to provide a picture of the common usage of SFT during the most recent years. Focusing on identifying projects with activity during the last decade, the selection criteria were defined as follows:

- Project or platform has produced at least one publication in English in a scientific journal or conference.
- Project or platform has shown signs of activity (publications or related research activities) during the last decade (2010–2020).
- Project or platform fits the definition of SFT given in section 3.1.

The methodology for review and classification of recent literature was based on the following steps:

1. Keyword- and keystring-based search using established search engines for scientific publications (SCOPUS, Google Scholar) with an extended timespan (1990–2020).
2. Filtering and removal of duplicates, resubmissions, drafts, and publications outside the field of interest.
3. First filtering of valid SFT projects based on information from title, abstract, main features and conclusions.
4. Tracing of citations in the already selected publications.
5. Expert consultation for additional references.
6. Second filtering of valid SFT projects according to the selection criteria detailed above.
7. Grouping of publications based on the project they relate to.
8. Analysis of each project's aim, methods and platforms.
9. Elaboration of a final list of SFT platforms according to its utilisation.

The resulting SFT platforms, along with the available information about the subscale model and the scaling method used, are listed in paper [V]. The following Figure 3.13 summarises the main purposes and research topics related to these platforms were used for, as well as their respective scaling method. As defined in the selection criteria, this figures only include those SFT platforms that have produced scientific publications. The actual number of relevant SFT projects or platforms is difficult to quantify due to the variety and unreliability of the communication channels used to disclose project information, but it is expected to be significantly higher. Clear examples of this are the numerous demonstrative SFT experiments on novel vertical lift vehicles being carried out by multiple start-up companies and SFT of unconventional configurations by other organisations that so far have only been communicated via press releases or the media. Furthermore, despite the explicit definition of SFT given in section 3.1, the border between UAV development and SFT is sometimes ambiguous. The inclusion or exclusion of certain projects from this review may therefore be subject to discussion.

The limited number of flow conditions can be explored with free-flying subscale models at low altitude without undesired scale effects and the convenience of new computational methods may explain why SFT seems currently unpopular for studying purely aerodynamic problems. The use of subscale flight testing to study both rigid- and flexible-body flight dynamics seems, however, more common. In these cases, aerodynamic (flow) similarity is typically relaxed or reduced to the replication of the most characteristic parameters. Further, the approach defined here as demonstrative scaling – the use of subscale models to evaluate a scaled version of a new technology or feature, partially or entirely disregarding vehicle similarity – is becoming increasingly common.

Figure 3.13 *Main research topics of SFT platforms that have been active or produced scientific publications in English during the last decade (2010–2020), along with their respective scaling methods. Note that each platform may have been used for multiple purposes.*

4 Development of Flight Test Instrumentation

Obtaining quantitative information from flight testing requires measuring and interpreting the aircraft behaviour during flight. External measurements are unfeasible in free-flight experiments in the open atmosphere and the measurement equipment needs to be carried on board. Registering accurately the motion of an aircraft in the air is a difficult task that involves a variety of sensing methods. In addition, some states cannot be measured directly and need to be estimated from the combination of indirect measurements of other properties. Acquiring flight data therefore requires the integration of different sensing and logging devices in a coordinated working system,

Figure 4.1 describes a typical process of modelling the flight characteristics of an aircraft from flight test data using a system identification approach. The shaded area indicates where the measurement of the aircraft's responses to test manoeuvres takes place and sets the context for this chapter, which summarises the development of a low-cost data acquisition solution SFT experiments. The information presented here relates to RQ2 and, besides later upgrades and additions to the system, it is mainly based on the developments presented in papers [I], [II] and in the licentiate thesis.

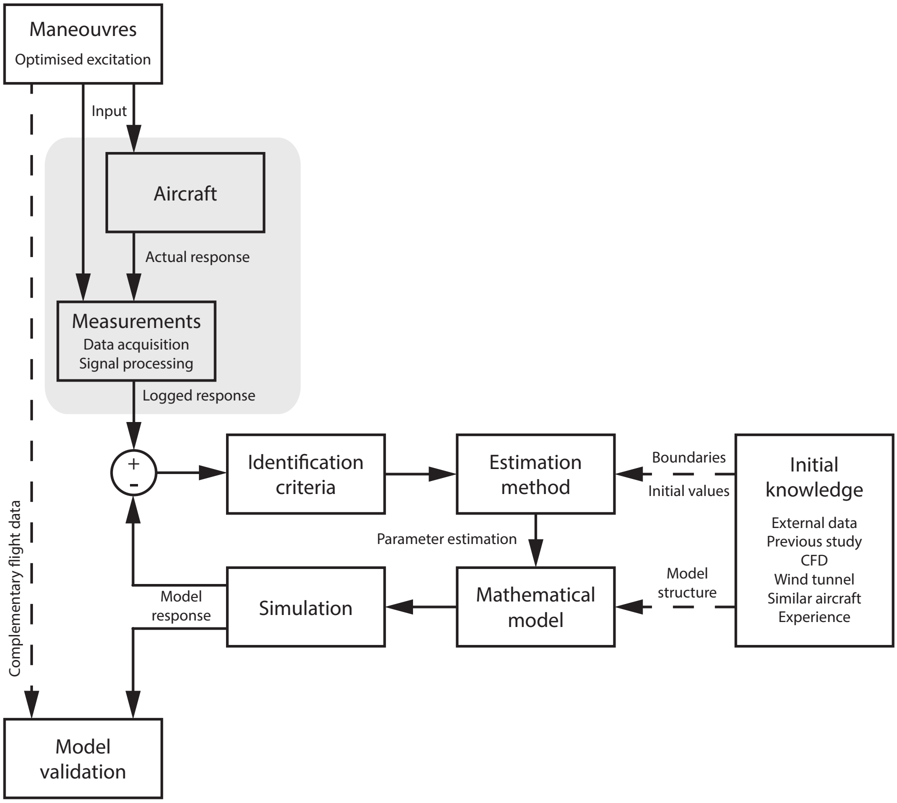

Figure 4.1 *Typical process of modelling an aircraft from real flight data using system identification, adapted from Hamel et al. [122]. This chapter focuses on the part corresponding to the measurements, highlighted in grey.*

4.1 Past and Current Data Acquisition Solutions

The flight-certified or aviation-grade instruments and data acquisition systems typically used in manned flight testing are, in most cases, not appropriate for subscale aircraft. The main reasons are often heavy weight, excessive size and cost, but can also include different needs in terms of resolution and sampling frequency. For example, while an altitude error of 5 metres and a sampling frequency of 25 Hz may be acceptable for flight testing the performance of a full-scale aircraft, it can be insufficient for a subscale aircraft with faster dynamics and operating between 0 and 120 metres above the ground.

Researchers have approached this issue with a variety of solutions, including both standalone data acquisition systems and integrated flight control systems (autopilots) with data logging capabilities. Dantsker et al. [123] present an extensive review of different solutions used for research purposes by different organisations. Until recently, COTS solutions for data acquisition were limited to few hobbyist-type systems such as the *Eagle Tree Systems Flight Data Recorder* [124] or higher-end, industrial UAV systems such as the *RCATS UAV* [125]. COTS autopilot systems for UAV, such as the *Cloud Cap Piccolo* series [126], have also been used for data logging in several projects. The gap between these two levels was filled with a variety of custom-made data acquisition solutions, most of which were based on the integration of custom and COTS sensors of different types but resulting in similar architectures [127, 128, 129, 130, 131, 132, 123]. A similar attempt to develop a data acquisition system for SFT was made at Linköping University in 2008 using a Diamond Systems PC board *Athena* with a Pentium-III-class processor running a streamlined Linux kernel as operating system [38]. Unfortunately, this system became slightly oversized for some of the platforms and it was affected by timing problems caused by the non-real-time operating system. The following attempt focused on minimising the hardware in order to reduce cost, size and power consumption. The new system, based on a 32-bit *Atmel* microcontroller, reached a fairly mature state by 2010, as described by Staack et al. in [40]. Since all the firmware in this system was programmed from scratch, its development was labour-intensive and its performance was limited in some aspects such as in the number of input/output (I/O) channels.

Over the last few years, in line with the expansion of the consumer and semi-professional UAV market, many open-source autopilot software projects have reached the community. In some cases, these projects also commercialise accompanying hardware with different capabilities and at different levels of integration. Paparazzi [133] and *PX4/Pixhawk* [134] are two well-known projects that are commonly used in research applications [135, 136, 137, 138, 139]. Open UAV-software development platforms such as *DRONEKIT* [140] and the *Dronecode Foundation* [141] also provide tools that facilitate a quick integration of data acquisition components and functions. The current availability of capable low-cost sensors and miniaturised processing boards, in combination with these software tools, enable the development of custom data acquisition solutions at very low costs, such as the system developed by Koeberle et al. [142] for educational purposes.

4.2 Development of a New System

In response to the need for a better performing solution for multiple SFT platforms at Linköping University, the work to develop and test a new data acquisition system started in 2014 and it is mentioned in papers [I] and [II]. Successive upgrades and modifications were incorporated later. The description shown here corresponds to the current configuration of the system at the time of writing this thesis.

The initial motivation behind this new system was to enable the study of flight performance and flight mechanical characteristics of small subscale models, while evaluating the capabilities of contemporary low-cost sensors and microcomputers. The following high-level requirements were set:

1. Use *low-cost* sensors and processors.
2. Use COTS components where possible.
3. Preferably use open-source hardware and software (enable maintenance and upgrade).
4. Modular structure, scalability high flexibility for reconfiguration.
5. Maximum mass of 500 g for main components (excluding platform-specific instruments).
6. Form factor suited for small fuselage cross-sections (12 cm).
7. Sampling rate of at least 50 Hz for the main state variables (later increased to 100 Hz).
8. Continuous power demand under 15 W.
9. Possibility of further development as a flight control system (FCS) (requirement dropped later in favour of a dedicated logger).

The term *low-cost* system can be defined here as a system with an acquisition cost below 1000 Euro or 10000 SEK for both hardware and software, but excluding the components of the main R/C link. In addition, no more than a person should be needed for system development and maintenance. The preference of low-cost components (1) was not only motivated by economic resources, but also by the aim of investigating the performance of the new low-cost sensors and processors that have been disrupting the market during the last decade along with the introduction of smart-phones and other portable devices; see Figure 2.4. At that time, studies such as [130] already indicated a promising performance of low-cost micro-electro-mechanical system (MEMS) sensors for data acquisition in small RPA.

The requirements for regarding low weight, small size and modular structure (4,5,6) originated from the intention of using this system in a wide variety of subscale platforms, ranging from jet-powered aircraft with a take-off mass (TOM) of 20 kg to small electric models under 1 kg of TOM.

The preference of a flexible system using open-source software and hardware (3), responds to the aim of further developing, modifying, and expanding easily such a system according to future changes in requirements or applications. In fact, the initial specification included the capability of functioning as a closed-loop FCS (9) as described in Paper [I]. While tested in small models, this capability was never used in the larger, jet-powered platforms due to the additional risk and the excessive development time required for meeting acceptable reliability and redundancy levels.

An important process inside a closed-loop FCS is to sense, integrate and evaluate the state of the aircraft by using a variety of sensors. Such a capability makes autopilot systems potentially good data acquisition systems. A initial survey of suitable solutions, focusing on open-source UAV autopilot systems that could meet at least part of the requirements, was carried out in 2014. Although a fully satisfactory solution was not found, two potential candidates were identified: *Paparazzi* autopilot project [133] and *PX4/Pixhawk* autopilot project [134]. A similar survey including commercial and custom-built hardware options was carried out at that time by Dantsker et al. [143]. While these authors decided to develop a new data acquisition system from scratch, it was preferred here to select an existing autopilot system as a base and to develop it further until meeting the desired specifications. The selected base system was a *Pixhawk* flight controller hardware [134] together with the *ArduPilot* open-source software in the version *Plane* [144].

4.2.1 System Architecture

The base system, a Pixhawk flight controller set, was expanded both with software modifications and new hardware devices in order to improve the logging performance and to include the measurement of additional states. Figure 4.2 shows a diagram of the current version of the data acquisition system, as integrated on the GFF demonstrator. The system consists of multiple distributed devices instead of a centralised unit. This facilitates not only its integration, but also to optimise the location of each component according to physical, functional, or electromagnetic conditions. Some of the main components are briefly described below.

Main Processing Board with Integrated Data Logger

The main processing board consists of a COTS Pixhawk core unit. Detailed characteristics of this device can be consulted in reference [134]. A main 32-bit processor, and additional safety processor, two analog-to-digital converter (ADC), several sensors, and a data logger with a Micro-SD memory card port are built into the main printed circuit board (PCB). The built-in sensors include:

- a barometric pressure sensor Measurement Specialities *MS5611*;
- an inertial measurement unit (IMU) composed by a STMicroelectronics *LSM303D* three-axis MEMS accelerometer and magnetometer, along with a STMicroelectronics *L3GD20* three-axis MEMS digital gyroscope;
- and a second IMU composed by a InvenSense *MPU-6000* six-axis MEMS motion tracking device.

These consumer-type MEMS sensors are inexpensive and are not certified for flight operations or technical measurements. Different types of noise can

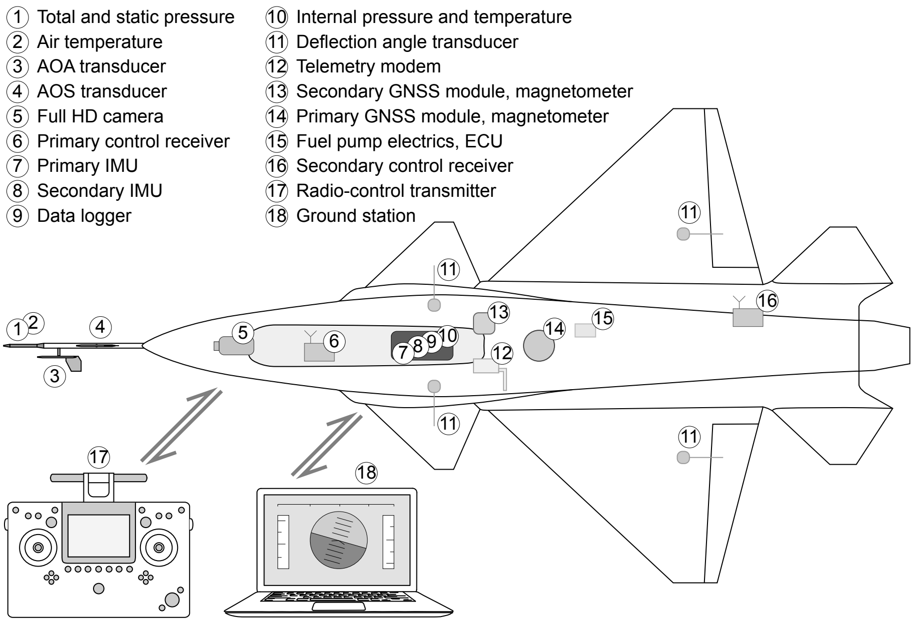

Figure 4.2 *Layout of the main devices and sensors that compose the current version of the data acquisition system installed in the GFF platform.*

compromise severely the attitude estimation. Nevertheless, even in the harsh environment found in small R/C aircraft, this type of sensors combined with appropriate filtering algorithms can offer a satisfactory performance during short periods of time [130, 143]. In the software used here, ArduPilot version Plane [144], approximate state estimations are obtained by filtering sensor data using an extended Kalman filter (EKF). This is an algorithm that linearises the system equations around the best state estimate available before applying the standard Kalman filter equations; see [145] for more information. One instance of this computation is run independently for each IMU, ensuring not only redundancy but a more reliable estimation.

Only minor physical modifications have been performed on the Pixhawk main processing board: one of the units has been modified with a tube that would allow the built-in barometric pressure sensor to take measurements via an external static pressure port, instead of measuring the ambient pressure inside the fuselage. This modification aims at reducing the noise in the pressure measurements caused by the internal jet turbine engine in some of the subscale aircraft; however, it has not been flight tested at the time of writing.

GNSS receivers and additional magnetometers

The system includes two different COTS non-augmented Global Navigation Satellite System (GNSS) receivers which also incorporate three-axis digital magnetometers built into their PCB. Electromagnetic noise caused by onboard equipment can disturb sensible sensors and receiver antennas, as measured by Dantsker et al. [129]. Since both GNSS antennas and magnetometers are highly sensitive to electromagnetic noise [130, 143], they are often grouped into the same module in order to be installed in a part of the airframe far from the main noise sources.

One of the receivers comprises a U-blox *M8N* module able to connect simultaneously with up to three of the main GNSS (GPS, Galileo, GLONASS, BeiDou); as well as two digital magnetometers: Honeywell *HMC5983*, and STMicroelectronics *LIS3MDL*. The other receiver comprises a U-blox GPS module *NEO7* and a single digital magnetometer Honeywell *HMC5883L*.

Both GNSS receivers usually operate at the same time. The ArduPilot software evaluates the accuracy of each one and selects or blends them as needed. Although not used here, GNSS augmentation would be an effective solution to improve the accuracy of the position estimations.

Air-data boom

Flow conditions such as angles of incidence, dynamic and static pressures are measured directly by using air-data booms designed and built in-house. These booms normally integrate a pitot-static probe and two flow-angle transducers, one for AOA and another for angle-of-sideslip (AOS).

These flow-angle transducers consist of mass-balanced vanes rotating on ball-bearings. The relative angles are measured using magnetic-induction rotary encoders extracted from inexpensive hobbyist-type R/C servos *HK28013DMG*. These encoders have a linear analogue output that is read via two of the available ADC ports on the main Pixhawk processing board. Posterior corrections are done in the software and include not only calibration curves but also account for the dynamic effects of the rigid-body movement of these vanes around the CG of the aircraft.

Figure 4.3 shows the air-data boom currently installed on the GFF, manufactured in carbon fibre with moving parts milled in aluminium. More information is available in [41]. Simplified, lighter versions of this boom design, featuring only an AOA transducer, have also been built for small subscale platforms weighing less than 0.9 kg of TOM; see Figure 4.4. In this case, the carbon fibre boom was completed with parts 3D-printed in plastic [146].

Control-surface position sensors

The original sensor-support capability of the Pixhawk hardware was extended by the addition of an Adafruit 16-Bit ADC *ADS1115*, which communicates

Figure 4.3 *Air-data nose-boom with two flow-angle transducers installed on the GFF platform.*

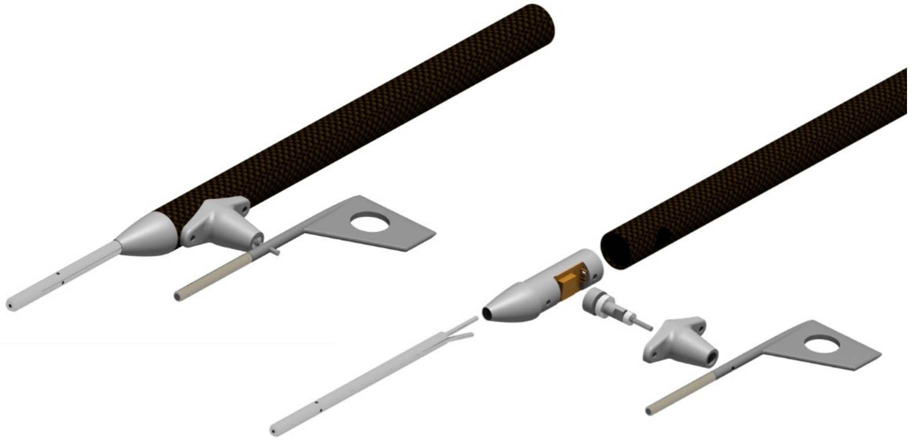

Figure 4.4 *CAD model of a small air-data boom comprising a pitot-static tube and a single flow-angle transducer. The sensor housing, the vane arm, and the vane were 3D-printed in plastic.*

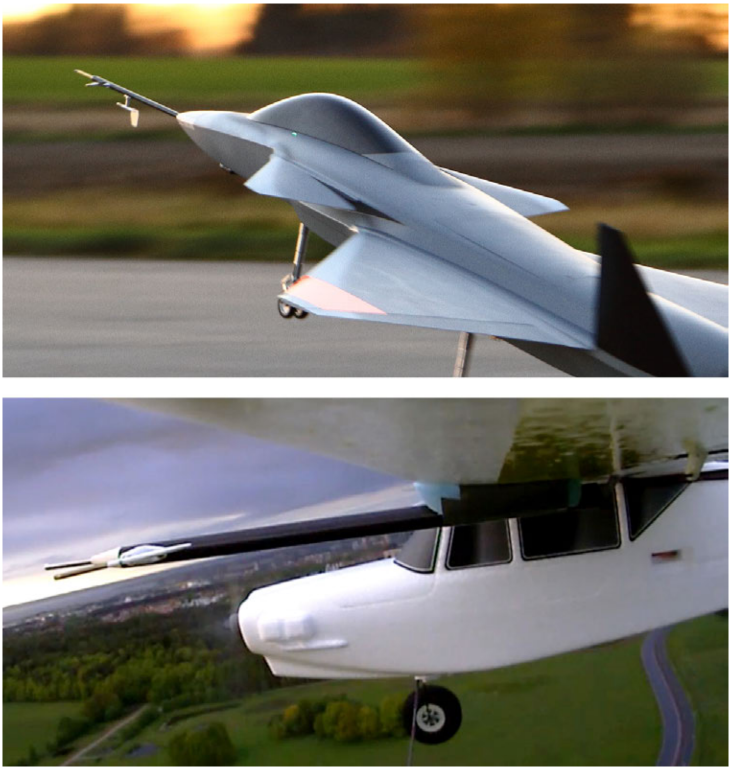

Figure 4.5 *Air-data booms during flight testing on the GFF (top) and a small test-bed aircraft (bottom).*

with the main processing board via *I2C* protocol. This enabled four additional analogue inputs that were used for the integration of four control surface position sensors on the GFF platform: one for each canard surface and one for each elevon, see Figure 4.2.

The real position of the control surfaces was previously estimated from the output signals sent to the servo-actuators and corrected with a calibrated model of the actuation mechanisms, as explained in paper [II]. However, measuring directly the real position of the actuators reduces the uncertainty, eliminates timing problems and simplifies the analysis of the flight data.

Voltage and current sensor

Power sensors typically measure the main and radio battery levels in hobbyist rigs. Here this set-up is only used in the smaller electric-powered test-bed aircraft. On the jet-powered platforms, it is used to monitor the fuel pump performance in order to estimate the fuel flow and fuel consumption.

Video camera and OSD

Light micro-cameras, with or without *On-Screen-Display* (OSD) of real-time flight data, are used to capture phenomena of interest such as the performance of the flow-angle transducers or the attitude of the aircraft in reference to the horizon. These cameras are attached externally and can be installed or removed depending on the experiment and the sensitivity for flow disturbances.

Figure 4.6 *Low-profile micro-camera installed under the nose of the GFF platform.*

Main control link

The R/C system used to operate the aircraft is generally not included in this data acquisition system, although its built-in telemetry system is used by the pilot to monitor critical flight-safety parameters such as the strength of the radio link or the voltage of the systems onboard. The R/C system used in most of these tests is a JetiModel *DC-24* [147] and operates in the 2.4 GHz band. The aircraft is equipped with a main dual-antenna receiver and a backup receiver working on the 900 MHz band.

Telemetry and ground station

The data acquisition system uses a separate COTS, low-cost, open-source telemetry system working on the 433 MHz band. This link is bidirectional and totally configurable. The unit on the ground is typically an ordinary laptop running the open-source software Mission Planner [148]. The limited bandwidth constraints the number the number of parameters and the sample rate that can be transmitted in real time to the ground station. Therefore, this link is mainly used to monitor the reading of certain sensors and the general health of the data acquisition system.

Thrust measurement system

An attempt to design and integrate a thrust-force measurement instrument for a jet engine was carried out in 2018. The chosen approach used strain gauges on specially designed engine mounts to measure only axial thrust and cancel any other inertial forces. The evaluation of different mount geometries and the design of the system is described in detail in [149]. The most promising configuration, shown in Figure 4.7, was built and integrated into the GFF's data acquisition system for evaluation. Unfortunately, ground tests showed that while the measurement equipment worked as expected, the thermal expansion and temperature gradients of the jet engine at different regimes introduced unexpected loads into the structure and contaminated the measurements. No further revisions of this system have yet been tested, and the thrust force in the GFF-system is currently estimated indirectly from engine and fuel-pump parameters.

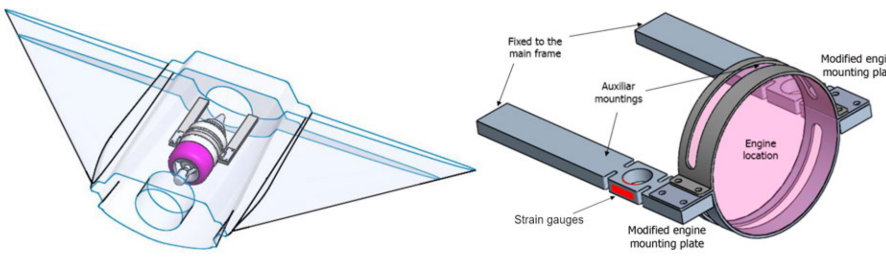

Figure 4.7 *A thrust-force measurement device developed for the GFF's jet engine, adapted from [149]. Later ground tests revealed unexpected thermal-expansion loads affecting the measurements and the system did not work as intended.*

4.3 Calibration

Different calibration techniques were used depending on the type of sensor and the platform in which it was installed. A detailed discussion of these procedures is not intended here, and only some particular observations will be mentioned.

In general, the calibration of the inertial instruments is effectively managed by the original ArduPilot software no modifications to these procedures were carried out. After some initial calibration of manufacturing and installation offsets, the software is able to recalibrate these sensors upon activation by using the gravity vector and data from other instruments. This process takes usually less than 60 seconds, and it is usually performed before every flight once the electronics have reached nominal working temperatures. Similarly, the calibration of the digital magnetometers is performed by the autopilot software before and even during the flight if new perturbations are detected. The EKF algorithm is also responsible for this process.

An accurate calibration of angle transducers such as control-surface position sensors and flow vanes was done following basic geometrical principles in the laboratory. Laser beams were used to increase the measuring distance and hence the precision.

The calibration of the airspeed transducer, the pitot-static probe, can be more challenging. For small and low-cost platforms it is usually sufficient with a manual calibration based on flight data obtained by flying circular patterns at a constant altitude, see Figure 4.8. Averaging the ground speed provided by the GNSS during circular flight cancels the effect of the wind and offers a good estimate of the real airspeed. The ArduPilot software has also a dedicated algorithm that can perform a similar in-flight calibration based on the estimations of the EKF.

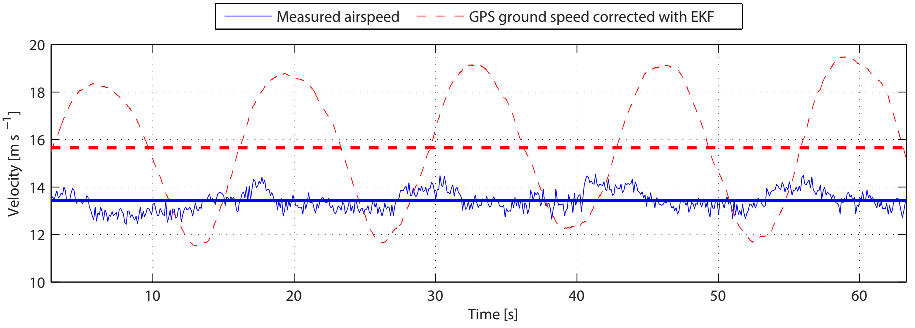

Figure 4.8 *Example of a manual calibration of the airspeed transducer using flight data from circular patterns. This approach can be useful for small subscale models flying at low AOA.*

Nevertheless, the large air-data boom installed on the GFF was also calibrated for airspeed and AOA variations at the wind tunnel of the Instituto Tecnológico de Aeronáutica (ITA) in Brazil. Figure 4.9 shows some of the data obtained in this experiment. A mathematical model for the airspeed-transducer behaviour was generated and implemented in the flight data analysis software.

Another interesting factor related to the calibration of some sensors is to obtain the right model for the dynamic rotation of the aircraft. High angular rates can introduce errors in the measurements of some sensors, such as accelerometers and flow-angle vanes. Assuming that the centre of rotation is the CG and that the aircraft is rigid, these dynamics can be mathematically formulated and accounted for. The main challenge usually lies in measuring

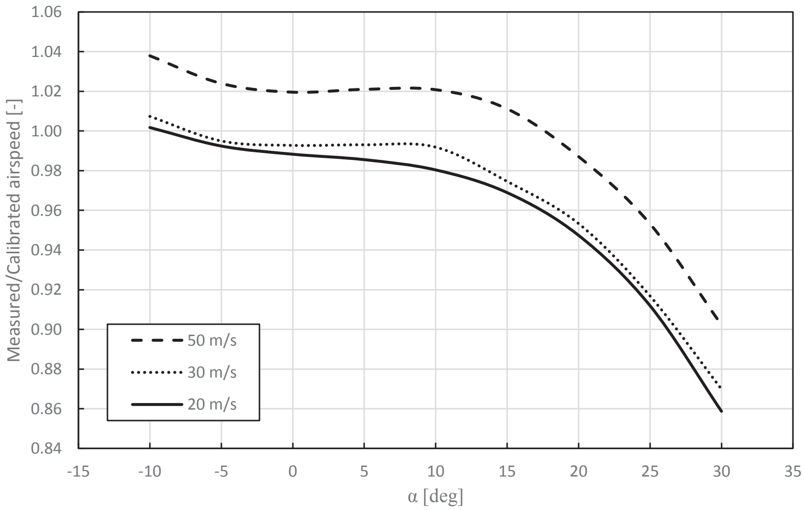

Figure 4.9 *Calibration of the airspeed transducer of the large air-data boom, performed at the wind tunnel of the Instituto Tecnológico de Aeronáutica (ITA) in Brazil. This figure shows the relative error of the pitot probe at different AOA and for various wind-tunnel airspeeds.*

the CG of the aircraft in three dimensions. A specific experiment was designed to determine its location with sufficient accuracy: the aircraft was hanged from a fixed structure so its CG could naturally align with the central vertical plane by the effect of gravity. A vertical laser beam was then used to identify and mark the section of the fuselage crossed by this vertical plane, as shown in Figure 4.10. By repeating the same operation at different hanging angles, it was possible to obtain different planes crossing the CG from different directions. These measurements were later transferred to a CAD model to compute the exact location of the CG. The entire experiment was repeated for different configurations, such as with the landing gear extended and retracted.

Although an accurate CAD model of the aircraft and its systems may offer a first approximation of the inertial properties of the aircraft, a direct experimental measurement is – considering the small size of the airframe – a practical way of reducing uncertainty. In this case, the aircraft moments of inertia were estimated using the swinging pendulum motion method, a traditional approach described in [150].

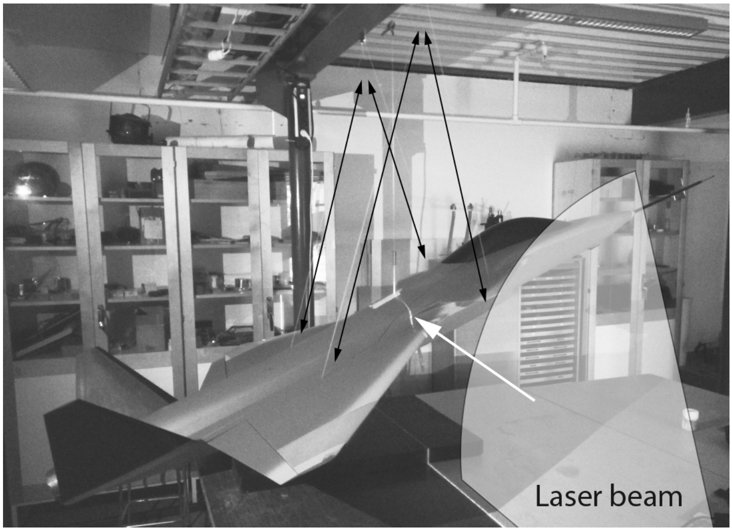

Figure 4.10 *Technique used for determining experimentally the position of the CG in three dimensions. The aircraft is hanging freely at different angles while a laser beam shows the vertical plane that crosses the CG.*

4.4 Logging Rates

The open-source autopilot software *ArduPilot* [144] was also modified in order to improve its sensor sampling and data logging capabilities at the expense of losing autopilot and auto-navigation performance; functions which are currently not used in the larger research platforms. The software modifications included the integration of the external ADC and its channels, as well as an increase of the sampling and logging rates for those sensors and parameters that are of most interest for flight dynamics.

The following Table 4.1 presents a summary of the principal parameters of interest for flight dynamics, along with the respective number of instances and logging rate available with the current version of the data acquisition system. Observe that some of these parameters are derived quantities and do not correspond directly to raw sensor measurements.

Table 4.1 *Summary of the main parameters logged by the current version of the data acquisition system, indicating the number of instances (parallel measurements), and respective logging rates.*

Parameter	**Instances**	**Rate [Hz]**
Attitude relative to the ground	2	100
Heading	2	100
Angular rates	2	100
Accelerations	2	100
AOA, AOS	1	100
Pilot inputs	1	100
Output signals to actuators	1	100
Control surface positions	1	100
Airspeed	1	25
Barometric altitude	2	25
Air temperature	2	25
Voltage, current	1	25
GNSS position and altitude	2	5
System health, error flags	1	2

5 Development of a Flight Test Method

The goal of flight tests is generally to acquire empirical data that can be used to develop and validate mathematical models, performance figures, or capabilities that were initially estimated and simulated during the design phase. The block diagram in Figure 5.1 presents again a typical outline of the entire process of modelling an aircraft from real flight data using system identification. This chapter corresponds to the very first part of the process, shaded in grey.

Flight testing full-scale manned aircraft is, in general, a risky and resource-intensive activity. Manufacturers strive to decrease the time spent in flight testing during development and certification. Hence, an important part of the current research in this field is therefore aimed at increasing the efficiency of the entire data acquisition, reduction, modelling cycle. Publications such as Morelli [151, 105] and Larsson et al. [152] are some examples of the efforts to improve the flight test techniques and the parameter estimation process.

SFT shares most of these characteristics but it also presents some particular challenges. Despite reducing and important part of the risk and infrastructure requirements associated with manned aircraft, operating and testing RPA in a safe and efficient manner is still a challenge for organizations with limited resources such as universities and small companies. This factor may be one of the main barriers preventing a more generalised use of SFT in research, education, and industrial applications. This chapter describes the work done towards finding a testing methodology that, while complying with the current regulatory framework, could improve the data quality for performance evaluation and system identification of fixed-wing RPA at a minimum economic cost. The content of this chapter is therefore related to RQ3, and it is mainly based on the developments presented in papers [III], [IV], [V] and in the licentiate thesis.

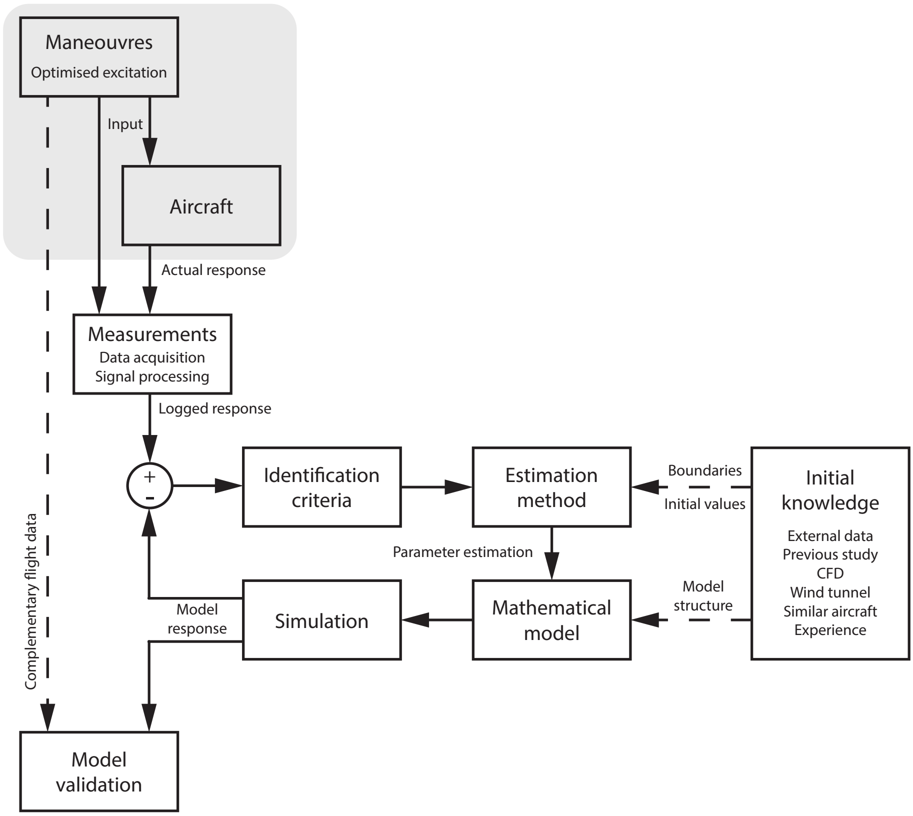

Figure 5.1 *Typical process of modelling an aircraft from real flight data using system identification, adapted from Hamel et al. [122]. This chapter focuses on the part corresponding to the aircraft flight and system excitation, shaded in grey.*

5.1 Different Approaches to RPA Operation

The simplest way of operating a subscale, unmanned aircraft is to control it in real time from the ground using a R/C system or a similar control station. The entire system is then commonly referred to as remotely piloted aircraft system (RPAS). Generally, the ability to perform autonomous flight or autonomous navigation does not present any relevant advantages for SFT activities aimed at modelling flight characteristics. On the contrary, such a feature would increase complexity, risk, and development cost. RPAS are often included in the broader category of UAS with regard to civil air regulations. Figure 5.2 tries to illustrate this classification.

In most countries, the current regulatory frameworks for the operation of

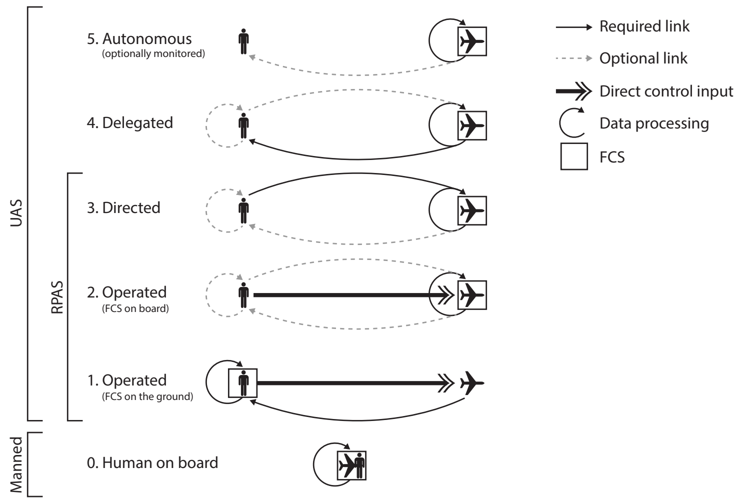

Figure 5.2 *Typical classification of aerial vehicles according to how they are controlled.*

civil UAS create a notable step between certified operations within visual line of sight (VLOS) and beyond visual line of sight (BVLOS) in terms of cost and requirements [153]. This issue is not caused by the cost of the extra technical equipment needed for extended visual line of sight (EVLOS) and BVLOS operations: inexpensive systems are already available in the market and they are sometimes used for hobby activities. Instead, the extra cost and complexity are caused by the difficulties and uncertainties derived from introducing this kind of unmanned vehicles in conventional controlled airspaces. A civil operator willing to obtain such permission is usually asked to either certify the system according to nearly full-scale standards or operate inside costly segregated airspaces [154, 155, 156]. Figure 5.3 exemplifies this situation by comparing various cost estimates for flight testing a civil RPA similar to those used for research at Linköping University; see Table 3.2. These cost estimates are not only direct operating costs but a sum of factors such as the estimated cost of qualified personnel, transportation, renting of appropriate facilities, cost of extra equipment for each type of operation and a very rough prediction of authorities approval costs. These costs were estimated based on the requirements from the Swedish civil air regulations that were in force during 2018 [157], previous experience in similar operations, expert consultation and commercial prices as of year 2018. The costs for 'Cat.4' are specially uncertain since specific requirements for BVLOS certification were not set. From the two different types of campaigns shown in this figure, nearly all the flight test campaigns carried out here are similar to the one labelled as "Campaign 1".

In practice, certification is usually prohibitive or directly not feasible for small

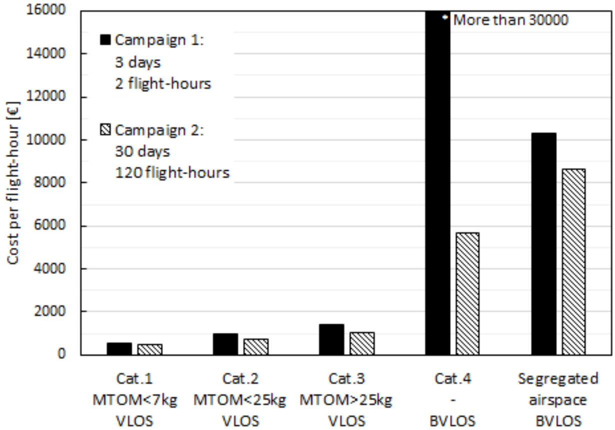

Figure 5.3 *Comparative of rough cost estimates for flight testing a subscale research platform similar to those at Linköping University, considering local regulation requirements as of year 2018.*

organisations. In addition, only a few civil organisations can make regular use of segregated airspaces to fly BVLOS operations. Instead, most organizations perform SFT in non-segregated airspace following VLOS or EVLOS rules as far as practical. While an exact classification cannot be formulated, most of the SFT experiments found in literature could be roughly divided into four different levels according to the type of operation and standards, see Table 5.1. The SFT experiments carried out at Linköping University can be included in levels 1 and 2 in this scale. Hence, the proposed techniques focus on improving flight testing only at such levels.

There is extensive literature covering flight-testing methods for both for conventional [162, 163] and relatively large unmanned vehicles [164, 165, 166], which could be related to SFT experiments of level 4 and some of level 3 in Table 5.1. Despite being more common, little has been published about specific methods for VLOS testing of relatively smaller RPA, i.e. experiments corresponding to levels 1 and 2, and even some at level 3. A good example of the testing conditions within VLOS is the FLEXOP project, where the limited airspace and the relatively large size of the demonstrator had an important impact on the design of the experiment and the vehicle itself [85, 86]. The procedure description given by Bunge et al. [136] illustrates a typical test of much smaller aircraft at level 1.

Most subscale platforms at Linköping University are tested at levels 1 and 2, with the GFF demonstrator being the most challenging case for SFT within VLOS at level 2. This case will therefore be used here to illustrate the proposed solutions to improving flight testing at both levels 1 and 2.

Table 5.1 *Rough 'de facto' classification of different approaches to SFT according to operation and safety levels.*

Level	Vehicle mass	Operation	Procedures, safety	Examples
4	$> 150\ kg$	BVLOS, segregated airspace, full redundancy	Professional, near full-scale	X-48B/C [158], X-56A [159]
3	$< 150\ kg$	BVLOS/EVLOS, segregated airspace, advanced redundancy	Professional, high-level	SAGITTA [160] , IEP [98]
2	$< 60\ kg$	VLOS, over airfield, limited redundancy	Professional, mid- to high-level	GFF [III], FLEXOP [86], MAGMA [161], AlbatrossONE [138]
1	$< 25\ kg$	VLOS, over airfield, limited/no redundancy	Relaxed, similar to leisure aeromodelling	Raven [38], Taylorcraft [136], ITA-BWB [IX]

5.2 Techniques for Flight Testing within VLOS

For operations within VLOS, the maximum allowed distance between the aircraft and the operator is determined by the specific definition in the local regulations, the most common presumption being 500 metres. The maximum allowed flight altitude is usually between 120 and 150 metres above ground level (AGL), although this is subject to local airspace rules or temporary clearances from the air traffic control services. The result is a cylindrical airspace of very limited dimensions, often affected by ground turbulence and obstacles on the surface. Figure 5.4 represents these conditions.

The short testing time, the need for constant manoeuvring and the imprecision of remotely executed excitation manoeuvres are some of the factors that complicate data acquisition. These challenges become even more evident when the test objects are heavy and complex aircraft models, such as dynamically scaled vehicles often used in research projects (see Section 3.5).

Figure 5.5 illustrates the reduced time available for manoeuvring inside a 500-metre test-window, the typical usable length of a straight trajectory in flight within VLOS. Experience has shown that test windows larger than 500 metres are difficult to achieve due to the need for appropriate safety margins, aircraft manoeuvrability and visibility constraints. This figure represents an optimistic estimation based on straight-and-level flight along the entire test window. In the real world, dynamic flying and weather conditions may further

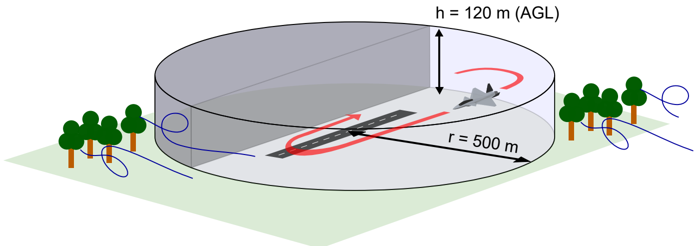

Figure 5.4 *Typical airspace available for flight testing within VLOS (levels 1 and 2 in Table 5.1): a challenging environment with severe exposure to ground turbulence.*

reduce the available time to execute each test manoeuvre.

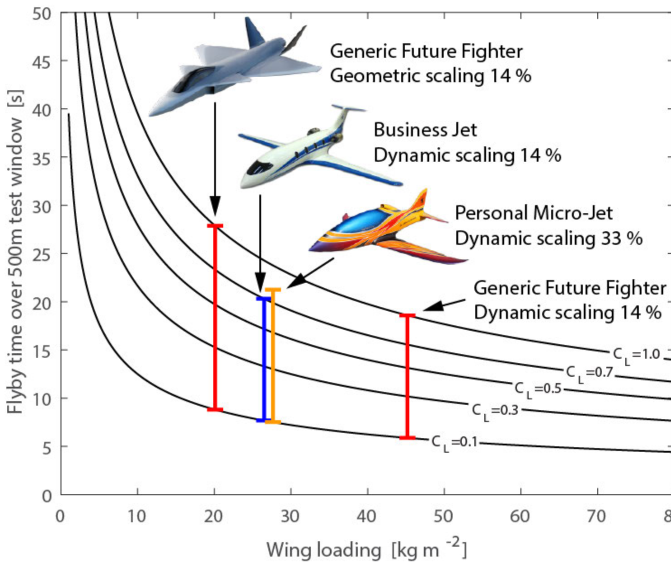

Figure 5.5 *Estimation of time available inside a 500-meter test window for different subscale aircraft, assuming straight-and-level flight. These models correspond to the cases (a), (b), and (c) from Table 3.2.*

5.2.1 Concept of Operations

Flight testing RPA within VLOS at levels 1 and 2 does not demand a complex infrastructure. The resources needed to support, operate and maintain these systems are in most cases only slightly more than those required by large R/C models operated by hobbyist for leisure activities. Further, VLOS operations do not require a large airspace and, depending on the characteristics of the test article, can be carried out in conventional model-flying fields. This not only increases the number of available locations but also lowers the operating cost in comparison to using general-aviation airfields.

For operation in civil airspace, the minimum roles and competences required may be directly specified by the competent aviation authorities in the corresponding UAS regulations. However, the roles needed for conducting efficient remote flight testing in practice may differ from the administrative roles formally required. The experience gathered during the flight-test campaigns carried out here led to the definition of three different roles that can be considered key to achieving satisfactory levels of safety and efficiency for VLOS tests at levels 1 and 2:

- test conductor, responsible for controlling the test execution, system health and data acquisition;
- pilot, flying the aircraft remotely from the ground control;
- test monitor, supervising the safety area, external factors and test performance.

As shown in figure 5.4, flight is constrained to a cylindrical volume of very limited dimensions. The approach followed here divides this airspace into three areas:

- a safety area, where only crew members are allowed;
- a nominal manoeuvring area;
- and a designated test window.

Figure 5.6 shows an example of this distribution during a typical flight test carried out with the GFF platform. In general, the orientation and placement of the different areas may depend on ground obstacles, visibility, sun position, eventual restrictions and wind direction.

Each circuit is divided into a test manoeuvre and a pattern flight or circuit. The test manoeuvre takes place inside a defined test window, while the pattern flight makes use of the available manoeuvring area inside the safety limits. Further, the desired manoeuvring inside the test window can be executed automatically using the application described in paper [III]. A representation of the proposed roles and this testing procedure is shown in Figure 5.7.

The detail to which the flight is planned and scripted in test cards is a good example of the differentiating characteristics of VLOS flight testing and how this approach aims at finding reasonable levels of flexibility and complexity. Instead of defining each consecutive movement of the aircraft during the circuit, the test cards focus on specifying the conditions at which the aircraft should

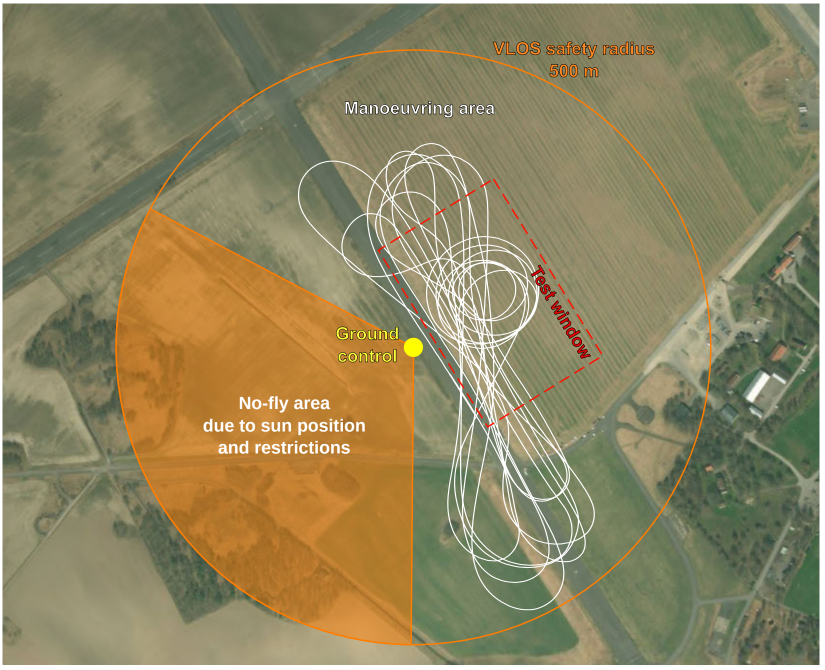

Figure 5.6 *Trajectory during a flight test of the GFF platform following the proposed distribution of the testing area.*

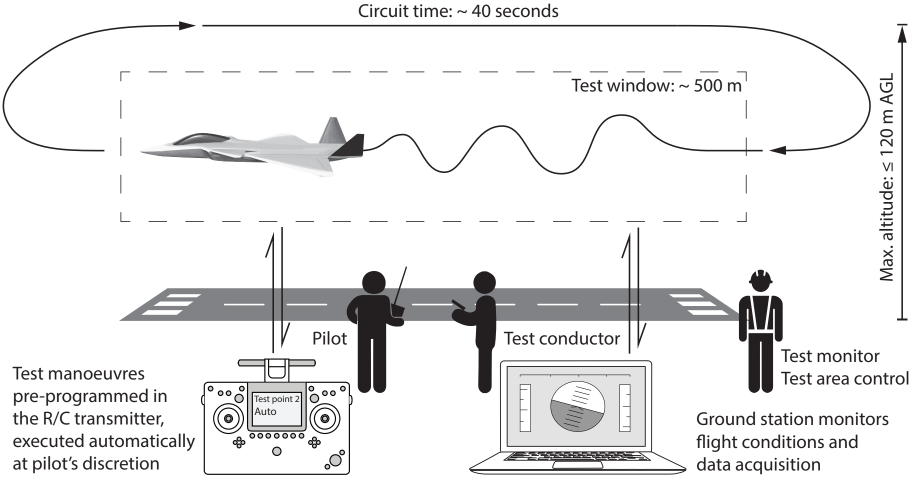

Figure 5.7 *Proposed roles and testing procedure for flight testing within VLOS at levels 1 and 2.*

enter the test window and the precise movements that should be done inside it, or the test point that should be selected if the manoeuvre is to be executed automatically. The pattern flight is then performed in a relatively free manner, but always within previously agreed parameters and speeds. Figure 5.8 follows the setup depicted in Figure 5.7 and illustrates these ideas by focusing on the test programme execution, involving both the test conductor and the pilot.

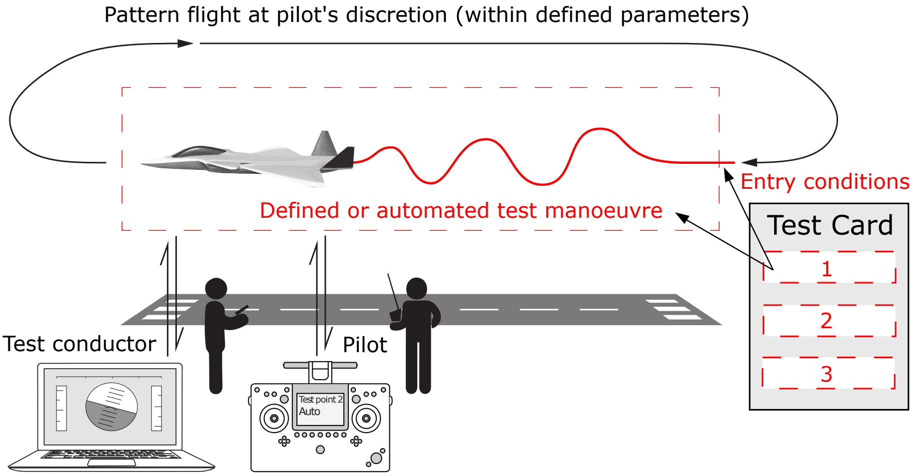

Figure 5.8 *A more practical approach to test-programme planning and execution: only entry conditions and manoeuvres inside the test window are scripted in detail.*

5.2.2 Automation of Manoeuvres

One of the most successful steps towards increasing VLOS testing capabilities with small platforms was achieved by developing a novel technique for commanding pre-programmed excitation manoeuvres without the need for a closed-loop flight controller or an on-line ground station. On the one hand, this benefits the smallest low-cost platforms by further simplifying their development. On the other hand, it may allow more complex platforms to perform automated flight test manoeuvres even before their flight control system is mature enough to fly autonomously, or in the case that this is not allowed by the regulations. In any case, this technique reduces effectively the workload of the pilot, who can focus on the challenging task of flying the aircraft through the narrow manoeuvring area at the required speed, altitude and attitude; see figures 5.6 and 5.7.

This technique is based on a custom-made application written in *Lua* language [167] that runs on the radio-control transmitter in parallel to its core software. The capability of interpreting Lua scripts was recently introduced by some R/C system manufacturers and it has been used mainly by hobbyists to visualize telemetry data in sophisticated ways or to customise user interfaces. This capability was used here to create a program able to actuate flight controls following complex pre-defined signals. The resulting application makes it also possible to easily configure an entire sequence of test points. The application can use an external library of customised input signals that can be updated or extended at any moment. Both analytically-described functions and discrete point-defined signals can be loaded. Once a test sequence has been configured, the script can also be used as electronic documentation for each flight test. Figures 5.9 and 5.10 illustrate some of these features.

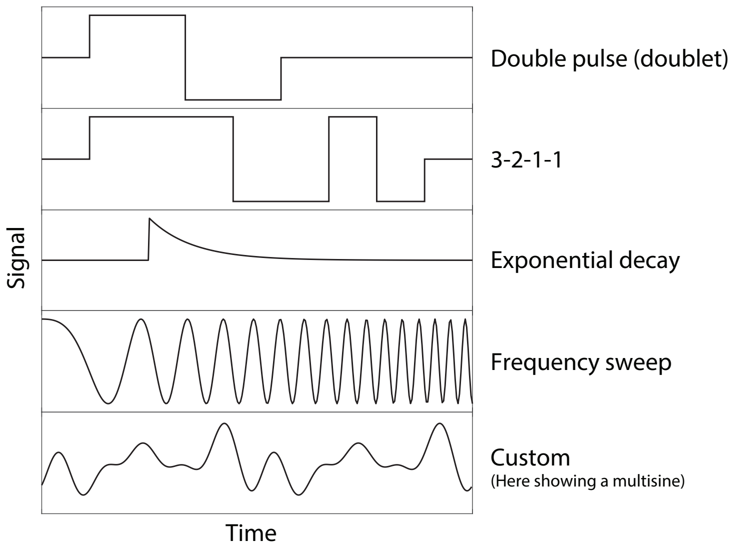

Figure 5.9 *Various types of input signals that can be generated with the flight test application.*

During flight, the operator selects the desired test point and triggers the manoeuvre by flipping and holding a switch. The corresponding signals are then executed on the intended control surfaces according to the specified timing and recurrence. Simultaneously, virtual flags are introduced into the logged data to mark the execution and to allow for automatic selection and post-processing of the desired flight segments. An information window, displayed on the transmitter's screen, shows the test point status and any incidences, see Figure 5.11. In addition, audible signals, messages, and flight parameters are played out through the transmitter's speakers to inform the pilot without losing visual contact with the aircraft. Several safety mechanisms have been introduced during the development of the application in order to avoid that any malfunction could compromise the flight safety. Ultimately, the pilot can

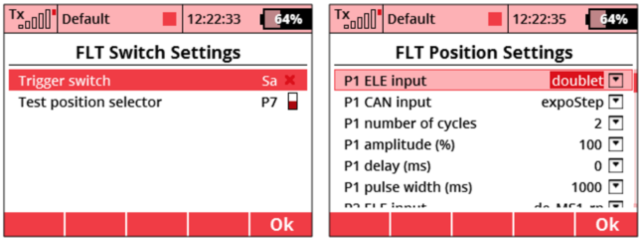

Figure 5.10 *Screenshots from the flight test application, here integrated into a transmitter Jeti Model DC-24: hardware setting menu (left), and configuration of test points (right).*

abort the process and regain manual control at any time by releasing the trigger switch. Due to the current hardware limitations, the signals can be transmitted up to a maximum frequency of 50 Hz. This rate is close to the typical refresh rate of radio-control systems and, so far, it has been sufficient for the intended applications, such as the study of the short-period modes of subscale models.

Figure 5.11 *Screenshots from the flight test application, here integrated into a transmitter Jeti Model DC-24: information window displayed to the operator during the execution of a test point.*

This tool has been released as open source in a public internet repository under the name of *LiU Flight Test App* and it has also been used by other academic organisations in similar SFT projects.

5.2.3 Manoeuvres for Performance Evaluation

During performance flight testing, manned aircraft are usually flown very accurately in still air and the large airspace available allows conducting stable test points [162, 163, 168]. As discussed earlier, this seldom possible when flight testing RPA within VLOS. The time to execute each test point is extremely limited (see Fig. 5.5) and steady trimmed flight is hardly achievable. The acquisition of performance data such as lift-to-drag polars using a traditional approach becomes therefore quite challenging. Short manoeuvres with a rich information content would be preferred over an extensive exploration of the flight envelope.

The advantages of using certain dynamic test techniques, i.e. involving dynamic manoeuvring instead of steady conditions, have been mentioned previously in the literature [168]. Although they are usually proposed for manned aircraft, dynamic test manoeuvres seem very well suited for performance testing of RPA under the constraints of VLOS. Among these, the following manoeuvres summarised in Table 5.2 have been used here to acquire performance data with the GFF demonstrator.

Table 5.2 *Various dynamic flight manoeuvres considered useful for aircraft performance evaluation within VLOS. Some of these have been inspired by manned-aircraft techniques described in [168].*

Manoeuvre	Condition	Expected results
Level deceleration or acceleration	Constant thrust, load factor close to 1g	Several polar points from low-positive to high AOA, low control deflections
Level deceleration to stall	Constant thrust, load factor close to 1g	Several polar points from high to maximum AOA, low control deflections
Vertical 'roller-coaster' (gentle push-over and pull-up)	Constant thrust, load factor from 0g to 2-3g	Several polar points from zero to mid AOA, large control deflections
Horizontal 'Bleed-off', closing banked turns	Constant thrust, constant altitude, load factor from 1g to near-maximum	Several polar points from positive to high AOA, large control deflections
Inverted deceleration or acceleration	Inverted flight, constant thrust, load factor close to -1g	Several polar points at negative AOA, low control deflections

The real portions of the flight envelope covered with these manoeuvres during a flight test with the GFF demonstrator are shown in Figure 5.12. As it can be seen here, the vertical 'roller-coasters' covered a wider area than initially expected, while the horizontal 'bleed-off' turns did not produce a high load factor.

The performance data obtained from these manoeuvres, in this case the lift coefficient of the entire aircraft, is shown in Figure 5.13. Thanks to the variety of manoeuvres, data could be acquired for different combinations of AOA and control-surfaces deflection, although in this particular test the elevons and the canard surfaces of the GFF demonstrator were actuated simultaneously.

5.2.4 Manoeuvres for Flight-Mechanical Characteristics

A similar problem affects the evaluation of flight-mechanical characteristics: there is a very short time to excite the desired flight-mechanical motion. Hence,

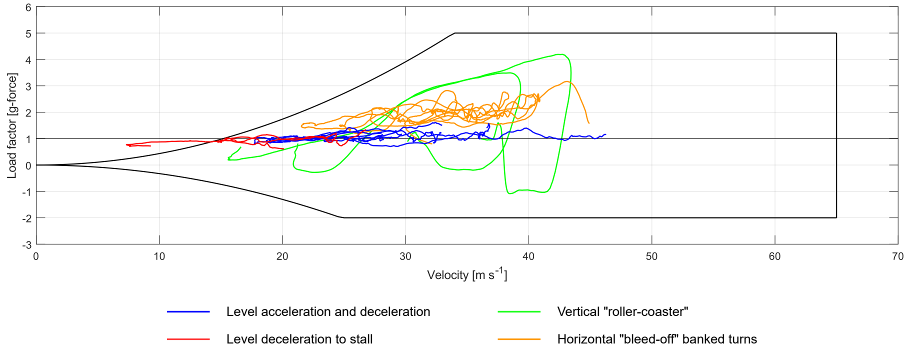

Figure 5.12 *Regions of the GFF flight envelope covered by some of the manoeuvres described in Table 5.2 during a performance flight test.*

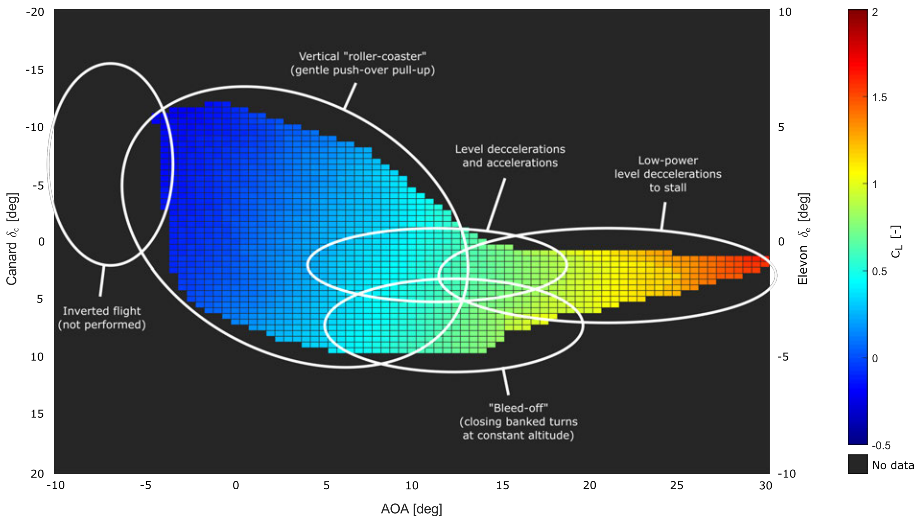

Figure 5.13 *Data successfully acquired (represented by coloured boxes) during the same manoeuvres visualised in Figure 5.12. The colour indicates the lift coefficient estimated from this data for each combination of AOA and control-surfaces deflection, in this case with a fixed coupling between canard and elevons on the GFF.*

it is necessary to find test manoeuvres and input signals that maximise the amount of information with a minimum exposure time.

An approach that could be well-suited for these conditions is the utilisation of simultaneous, uncorrelated inputs such as multisine signals [105, 151]. This approach is based on the fact that two or more sine signals are uncorrelated if they have different frequencies. This can be used to excite various control surfaces in parallel, shorten the excitation time that would be required with an excitation in series.

Figure 5.14 shows a comparison between an optimised multisine input and a conventional double pulse or *doublet* in a simulated excitation of the short-period motion of the GFF subscale demonstrator. While the multisine signal can be applied to both canard and elevons simultaneously, the double pulse needs to be applied separately to avoid a high regressor correlation, which more than doubles the manoeuvring time. It is clear that such an input signal cannot be performed manually by the pilot and it requires some degree of automation. The flight-test application for manoeuvre automation, presented earlier, is the key enabler that allows the use of such complex manoeuvres.

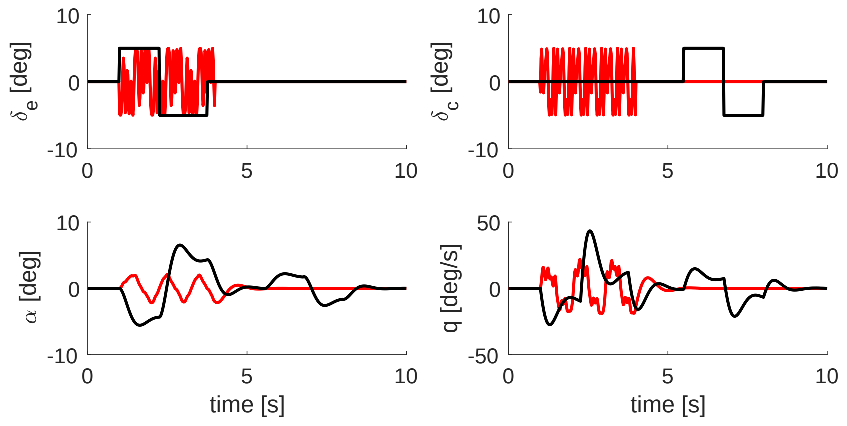

Figure 5.14 *Simulated excitation of the short-period motion of the GFF subscale demonstrator: simultaneous multisine inputs in red and separated double pulses or doublets in black.*

The results from flight tests with the GFF demonstrator presented in paper [IV] support the idea that the parameters estimated from the simultaneous multisine inputs are similar to those obtained with sequential ones, while the excitation time could be reduced by almost 50 %. Further, in these tests, both multisine approaches seemed to generate more accurate models than those from separated pulse inputs. Figure 5.15 shows an example of the validation of two of these models against flight data from an additional manoeuvre not used for identification. The efficiency of this approach could perhaps be further improved by incorporating an on-line monitoring method such as the one proposed in [152].

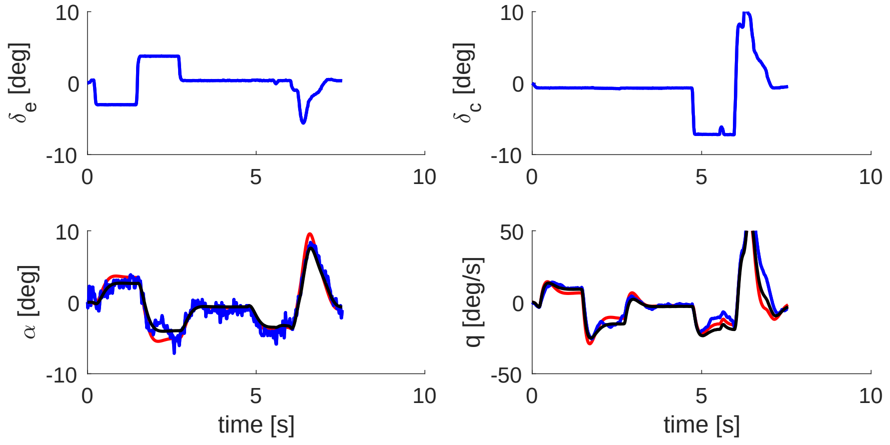

Figure 5.15 *Validation of the longitudinal models identified from flight data using an additional manoeuvre: model generated with multisine inputs in red, model generated with double pulse inputs in black, and real flight data in blue.*

6
Flight Data Analytics

Flight tests generate immense amounts of raw data and SFT is no exception: the data acquisition system described earlier logs more than 100 parameters at non-synchronised, variable rates ranging from 100 Hz to 1 Hz. A single ten-minute flight produces a considerable number of samples that need to be synthesised and interpreted to enable any rational analysis of the results. Being able to carry out at least a meaningful part of this analysis on site and between flights allows full advantage to be taken of the flexibility and agility offered by SFT at levels 1 and 2 (see Chapter 5).

This chapter focuses on flight data analysis tools and on the identification and evaluation of aircraft characteristics, a topic which corresponds to the shaded area of the familiar diagram in Figure 6.1. Rather than being based on a particular publication, the developments presented here are based on all attached papers as well as the licentiate thesis and a master's thesis project [169].

Synchronising and filtering signals, conditioning data, checking for consistency and estimating results are usual tasks performed in all sorts of flight testing, not only SFT. Organisations with flight-testing capabilities will normally have developed proprietary tools to cover these tasks both online (in real time) and offline, but in most cases these are focused on full-scale vehicles and manned flight-testing operations. Further, in order to be consistent with the *low-cost* approach, expensive commercial proprietary software licenses must be avoided. Software tools covering certain parts of the offline data analysis process have been released to the community for research (see NASA's *SIDPAC* for system identification [170]) and educational (see the collection of programmes offered in [171]) purposes. Further, NASA's open-source *Open Mission Control Technologies* (*OpenMCT*) visualisation framework is being increasingly used in SFT projects to manage, display and broadcast real-time telemetry data. Both

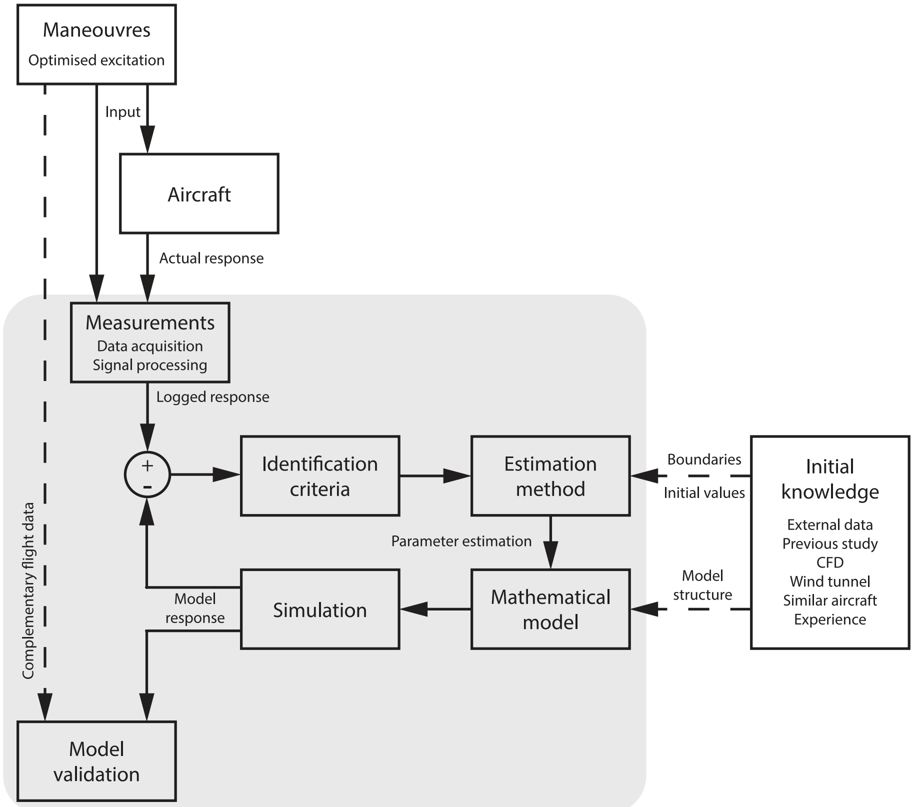

Figure 6.1 *Typical process of modelling an aircraft from real flight data using system identification, adapted from Hamel et al. [122]. This chapter focuses on general data analysis as well as identification and validation of characteristics, indicated by the grey area.*

commercial and open-source UAV ground-control software – such as *Mission Planner* [148] – are also beginning to offer some degree of data analysis capability. While most of these tools are perfectly applicable to SFT experiments, there is currently no freely available, integrated flight-test data analysis solution that is specifically tailored to SFT needs. Therefore, since the beginning of this project in 2015, a new set of tools has been developed from scratch using *MATLAB*, a familiar environment for both academia and industry with reasonable license costs and good maintenance.

6.1 Development of a Data Analysis Tool: The ALAN scripts

Aircraft Log Analysis (ALAN) is a family of scripts and functions written in a *MATLAB* environment to enable an agile SFT data processing at Linköping University. Its main tasks include synchronisation, verification, transformation, integration, visualisation and extraction of flight data in appropriate formats for the subsequent use in other analysis tools. It has also been expanded with its own data analysis capabilities such as parameter estimation and system identification submodules.

These scripts have been written to fit the specific characteristics and needs of the data acquisition system and the testing methods described earlier. Nevertheless, the structure of the program has been designed in such a way that makes it easily compatible with other systems and models, or any sources of flight data. Figure 6.2 describes the program flow. Some of the most relevant functions for processing SFT data will be briefly described below.

6.1.1 Platform Configuration

The compatibility between different aircraft models, different versions of the data acquisition system or different arrangements of sensors is maintained through the use of configuration files. These files contain the information needed to map and transfer the system-specific variables onto the standard variables and units in which the program works. In this way, the program and the flying platforms can also be developed independently. Instrument calibration data and synchronisation strategy is also defined at this stage.

6.1.2 Filtering and Plotting

Once the flight data has been imported and formatted, the program offers a choice between multiple tasks. These usually start with signal conditioning options, such as analysis of the spectral density and filtering. The program can display periodograms for the desired signals and then allow the user to choose which kind of filter to apply, see Figure 6.3. It is also possible to introduce a customised filter or to use other filters available in MATLAB.

Furthermore, the user is offered multiple plotting options. An automatic detection of take-off and landing manoeuvres is used to suggest a pre-selected range of time for visualisation, although the user may select any time segment of interest. The signals – filtered or raw – and their visualisation units can be selected dynamically to enable a quick comparison and understanding of the aircraft states. An example is shown later in Figure 6.12. The three-dimensional flight trajectory is plotted over a georeferenced satellite image where the average wind conditions, if available, are also presented. All these

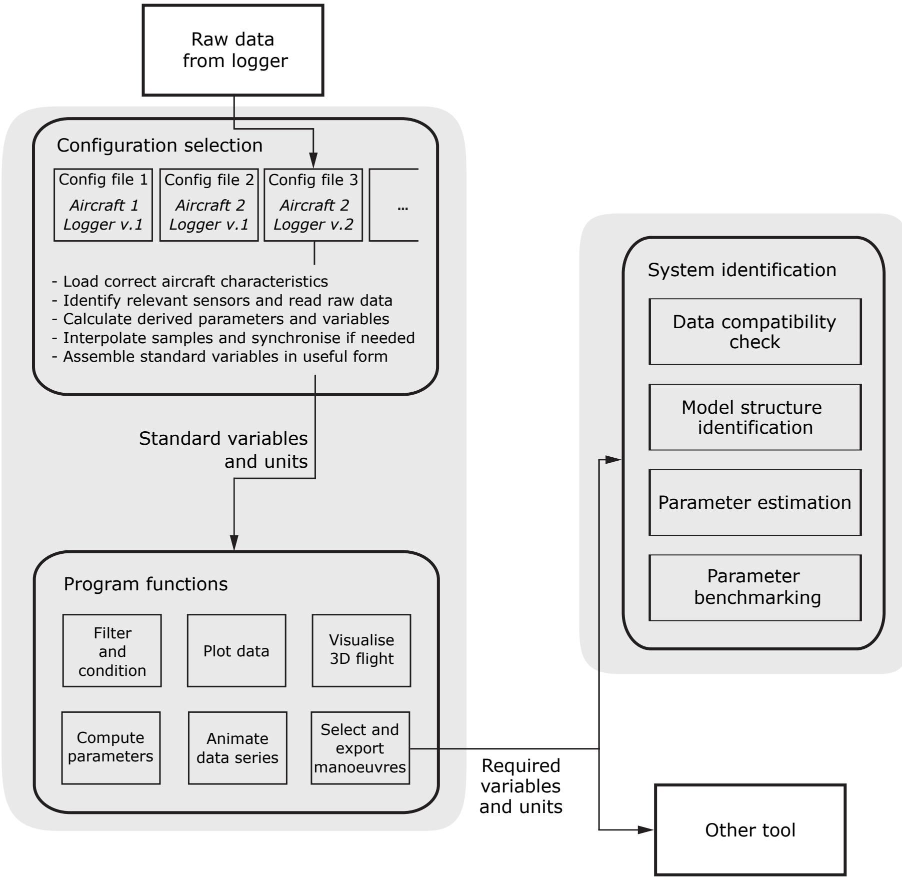

Figure 6.2 *Simplified program flow describing how flight test data is processed in ALAN, which currently covers the areas shaded in grey.*

plots can also be explored with the usual plot-visualisation tools available in the MATLAB interface.

6.1.3 Animated Flight Reconstruction

It is sometimes convenient to reconstruct and visualise certain parts of the flight dynamically. ALAN currently has two functions that allow for animated visualisation of the logged flights. The first, shown in Figure 6.5, is designed to give a general overview of the aircraft performance, flight conditions and pilot inputs.

The second, shown in Figure 6.6, features a 3D model of the aircraft with moving control surfaces. This 3D model reproduces the chosen segments of the

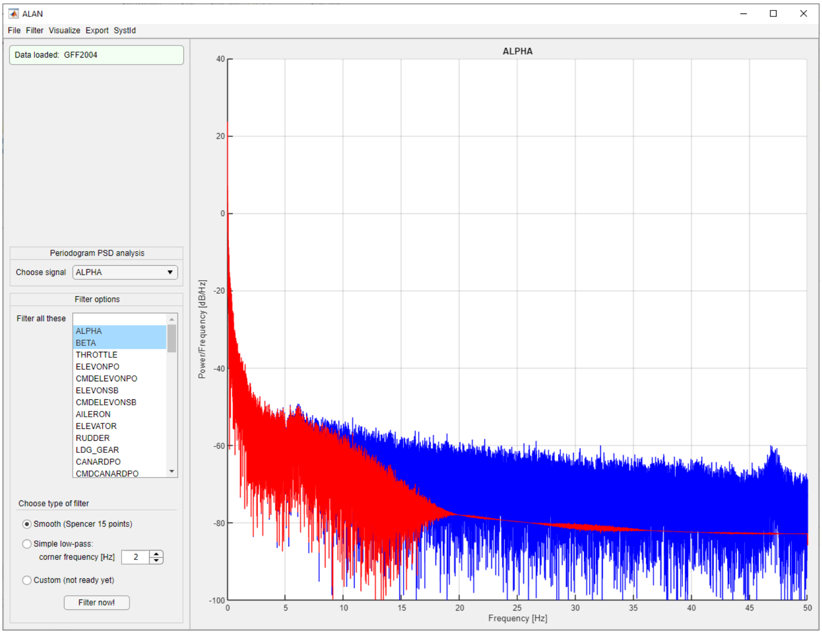

Figure 6.3 *Signal filtering interface in ALAN.*

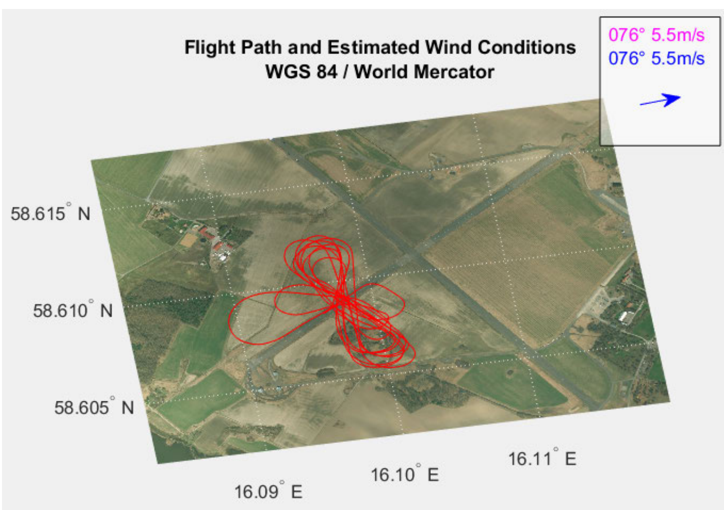

Figure 6.4 *A three-dimensional flight trajectory is presented over a georeferenced satellite image.*

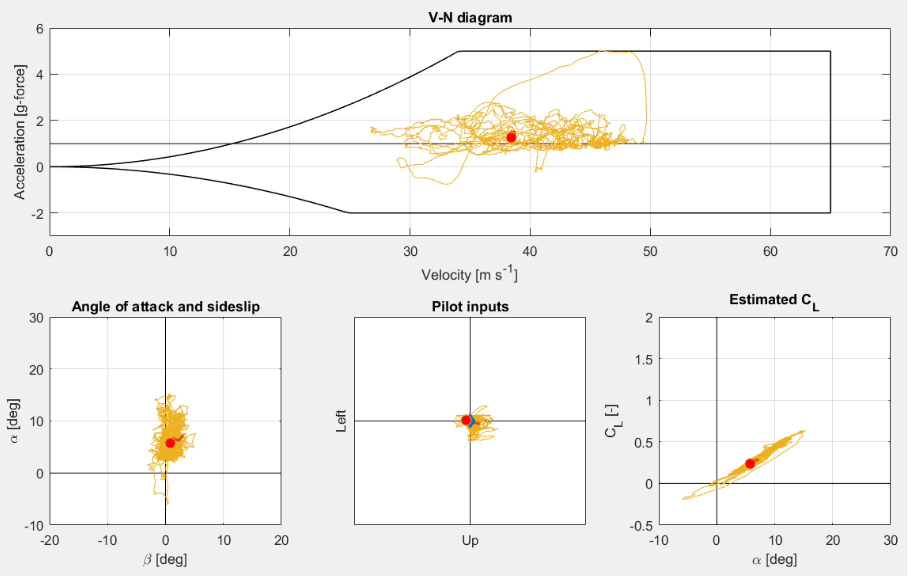

Figure 6.5 *Animated visualisation of flight parameters in ALAN.*

flight at the desired speed. The measured angles of incidence of the flow, or wind vector, are also visualised. Several options to customise the reproduction or capture a video sequence are also offered. This is an intuitive visualisation solution, useful for obtaining a general understanding of the events and for communicating findings.

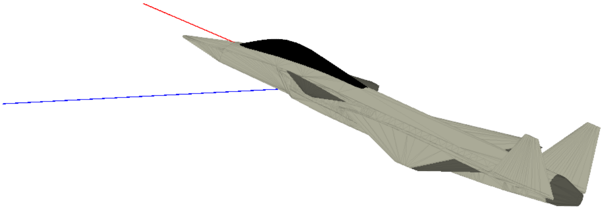

Figure 6.6 *Virtual reconstruction of the aircraft motion in ALAN. The 3D-model has moving control surfaces and displays the measured flow incidence vector.*

6.1.4 Simple Parameter Estimation

If the necessary aircraft states are available, basic performance parameters such as C_L or C_D can be approximated directly from the flight data using a conventional flight mechanics model. This function makes use of three-dimensional plots to visualise these parameters together with their main dependencies, as shown in Figure 6.7.

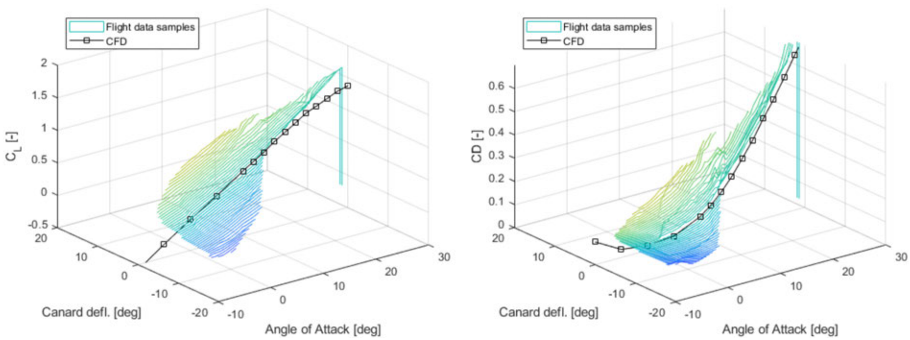

Figure 6.7 *Three-dimensional plots showing the lift (left) and drag (right) coefficients estimated directly from flight test data.*

6.1.5 Export of Manoeuvres

ALAN also offers an export function in which the desired manoeuvre or time segments can be selected interactively on the plot and packaged in multiple formats. Automatic selection, based on the time flags left by the Lua flight-test application described in Section 5.2.2, is also possible. Further, the user can refer to a text file in which the desired time segments are already specified; a useful option when multiple exports of the same segments are desired. Figure 6.8 shows the segment selection interface.

6.1.6 System Identification Module

As a complement to ALAN's core functions, an offline system identification module was developed through the academic projects [172] and [169]. This module and its main functions are represented on the right side of Figure 6.2. The data compatibility check function, also known as flight path reconstruction, is based on the method proposed by Jategaonkar [171]. Two time-domain parameter estimation methods are implemented – equation error and output error – and it is possible to choose between three optimization methods. An additional function for model structure identification, based on the orthogonalisation approach by Klein and Morelli [173], is also offered. The code imple-

Figure 6.8 *Interactive selection of manoeuvres for exporting to other tools.*

mentation and usage are explained and illustrated with examples by Arustei in [169].

Beyond typical stacked plots for comparing measured and simulated results over time, particular importance was attached to the intuitive and quick evaluation of results. Intuitive and graphical visualisation solutions, such as the estimated-parameter comparison shown in Figure 6.10, were therefore implemented.

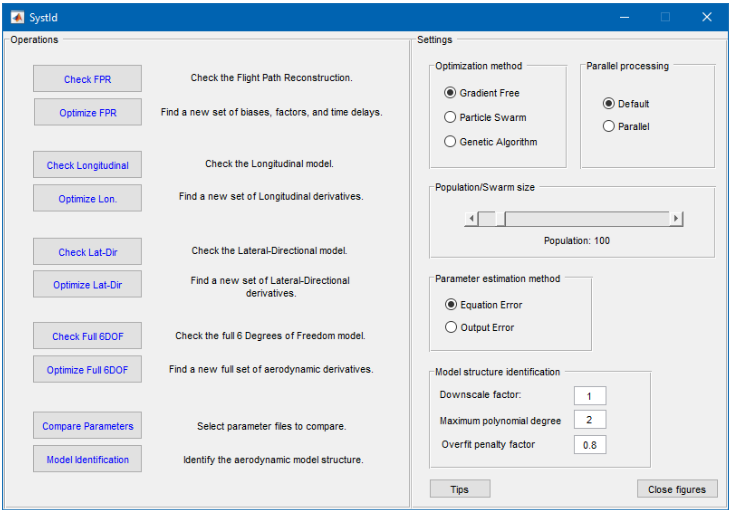

Figure 6.9 *User interface of the system identification module described in [169].*

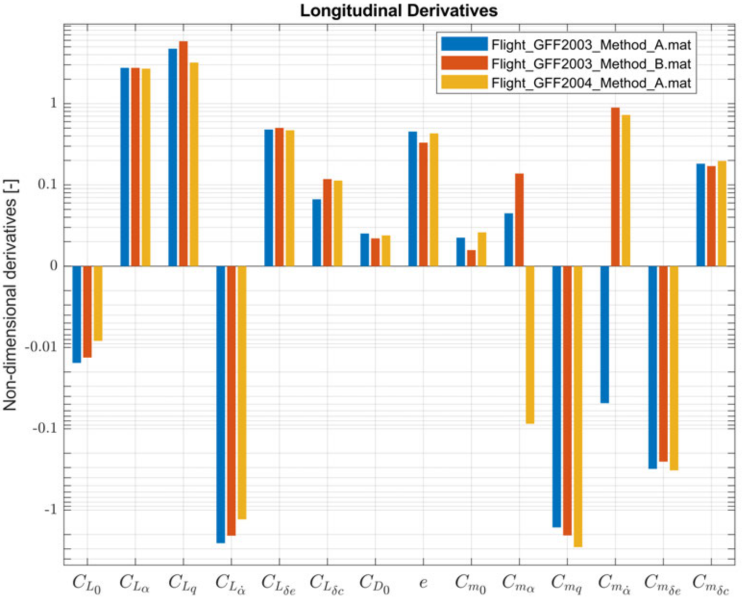

Figure 6.10 *Results from different methods can be easily compared graphically in the system identification module [169].*

6.2 Management of a Heterogeneous Database

Efficiently managing the immense amounts of data gathered during flight tests is not a trivial task. In fact, this challenge takes on a new dimension when the data sources are heterogeneous, such as in the case of experiments with different instrumentation – which may or may not measure the same variables – at different scales or under different testing conditions. The addition of data from other methods, such as wind tunnel or CFD, and other organisations, which may use different references, further complicates any consistent comparison of results.

The database management approach followed here was based on the principles of relational databases. While the *MATLAB* environment is not specifically prepared to support relational models, a similar functionality was achieved here by implementing a consistent database architecture based on nested structures. The results from each experiment, independently of the method, are added as a new database entry along with a variety of attributes defining the characteristics of the data. In addition, most dimensional quantities are non-dimensionalised according to model scale and experiment conditions.

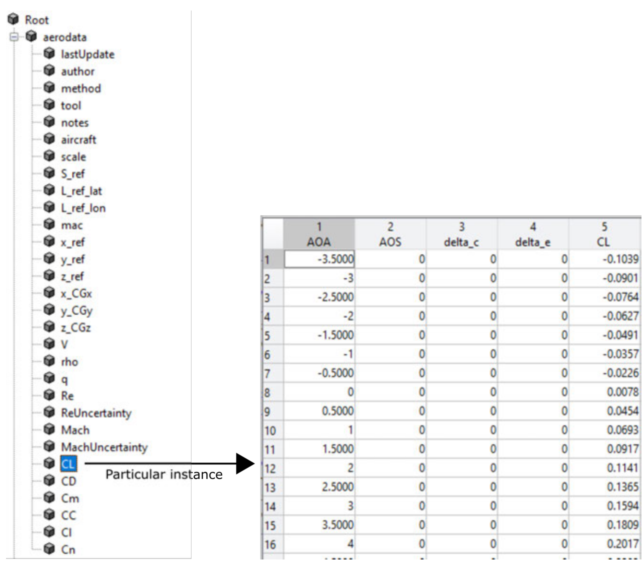

	1 AOA	2 AOS	3 delta_c	4 delta_e	5 CL
1	-3.5000	0	0	0	-0.1039
2	-3	0	0	0	-0.0901
3	-2.5000	0	0	0	-0.0764
4	-2	0	0	0	-0.0627
5	-1.5000	0	0	0	-0.0491
6	-1	0	0	0	-0.0357
7	-0.5000	0	0	0	-0.0226
8	0	0	0	0	0.0078
9	0.5000	0	0	0	0.0454
10	1	0	0	0	0.0693
11	1.5000	0	0	0	0.0917
12	2	0	0	0	0.1141
13	2.5000	0	0	0	0.1365
14	3	0	0	0	0.1594
15	3.5000	0	0	0	0.1809
16	4	0	0	0	0.2017

Figure 6.11 *Aerodynamic data is stored in a self-describing, nested structure that provides a functionality similar to that of a relational database.*

With all results stored in such a database, it is possible to easily browse and access any desired portions of information by using simple search queries, independently of the number or type of data sources. For example, one may request '*to visualise all C_m vs AOA curves using the same reference point,* *obtained from all available methods for vehicle scales under 50%, but limiting results to a minimum of Re* = 6e+5 *and zero AOS*', just by typing a single command. These functionalities complement those of the ALAN scripts and facilitate the processing of highly heterogeneous flight data, such as in the case of the multi-method study presented in paper [VI].

6.3 Use-Case Example: Investigating the Lift Characteristics of the GFF Demonstrator

A real investigation carried out with the GFF can illustrate how all these systems and software tools are used in practice. This example, part of the study presented in paper [VI], shows the estimation of the aircraft's lift characteristics from SFT data and its comparison to other estimation methods. The GFF demonstrator was equipped with the data acquisition system described in chapter 4. The flight was carried out within VLOS as shown in Figure 5.6 and most of the manoeuvres described in Table 5.2 were executed. Figures 5.12 and 5.13 show the outcome of these manoeuvres and the extent of the acquired information. The flight data was processed with ALAN, where the signals of interest were filtered, adjusted with a data compatibility check and examined – see Figure 6.12 – before selecting appropriate and informative segments to estimate the performance parameters.

Portions of data with near steady-state conditions were used as input for a simple approximation of the lift coefficient based on forces and accelerations, assuming a typical flight-mechanics model. The results revealed that the deflection of the canard surfaces had a significant impact on the total lift, as shown in Figure 6.13. Only results corresponding to near-zero (range -1 to 1 deg) control deflection were used for comparison with the other estimation methods shown in Figure 6.14: vortex lattice method (VLM), CFD and wind tunnel testing with a 3D-printed, 3.8%-scale model of the GFF.

Figure 6.15 show the results obtained with these tests along with two additional methods mentioned in paper [VI]: a theoretical estimation based on a single delta wing and a more sophisticated system identification method with neural networks carried out outside the ALAN scripts. All methods present a good agreement for the linear region around zero AOA. While little data is available in the negative region, the results reduced from flight testing using the simple identification method suggest that the subscale model may produce less negative lift than could be expected from the CFD and VLM estimations. The various landing-gear openings and access ports – all located in the underside of the model – might contribute to this effect. This method also seems to diverge from most of the other predictions in the nonlinear region at AOAs higher than 15 degrees, where it indicates a continuous increase of lift. Not enough flight data was gathered in this region to ascertain if this effect was recurrent or just a particular anomaly. Possible explanations include the influence of dynamic

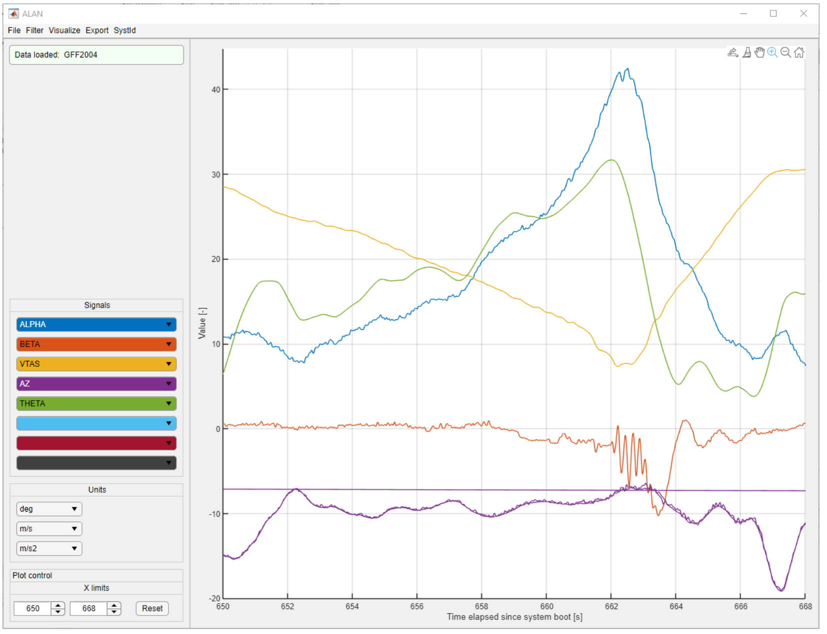

Figure 6.12 *ALAN's plotting interface showing various signals during a deep stall.*

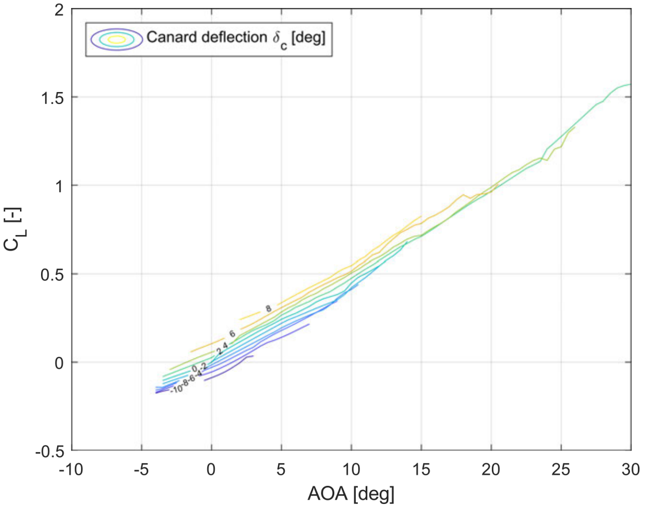

Figure 6.13 *Lift coefficient of the GFF demonstrator for different canard deflection angles, as estimated from near steady-state segments of flight-test data.*

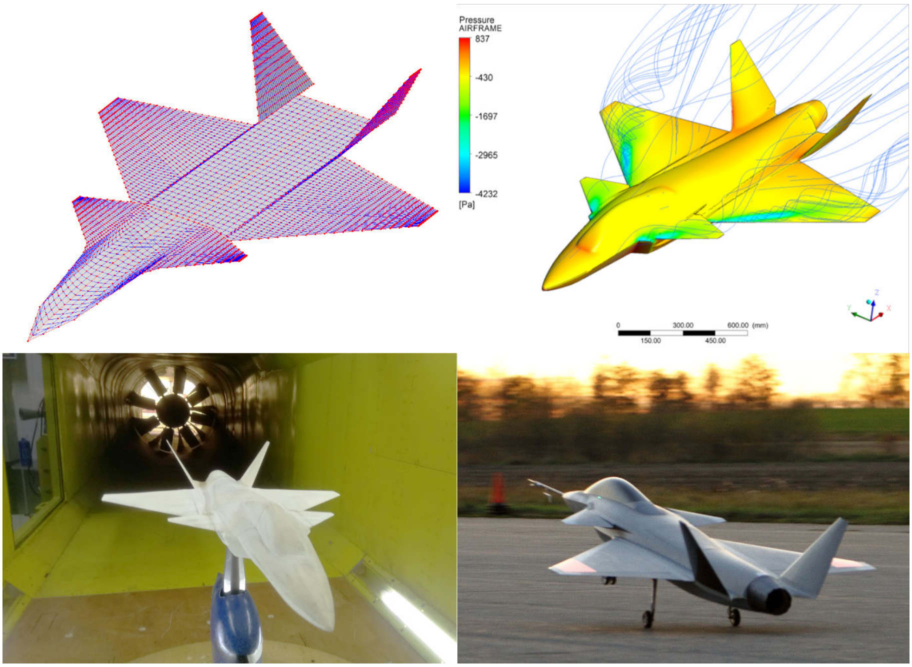

Figure 6.14 *Four estimation methods used for the study of the lift characteristics: VLM (top left), CFD (top right, courtesy of Paulo Greco and Fernando Catalano at USP in Brazil), wind tunnel (bottom left, courtesy of Leonardo Nepomuceno at ITA in Brazil), and SFT.*

effects (steady-state assumption not valid), the uncertainty introduced by the engine-thrust model (thrust was not directly measured), or the limitations of the nose-boom airspeed transducer at such high AOA (see Figure 4.9).

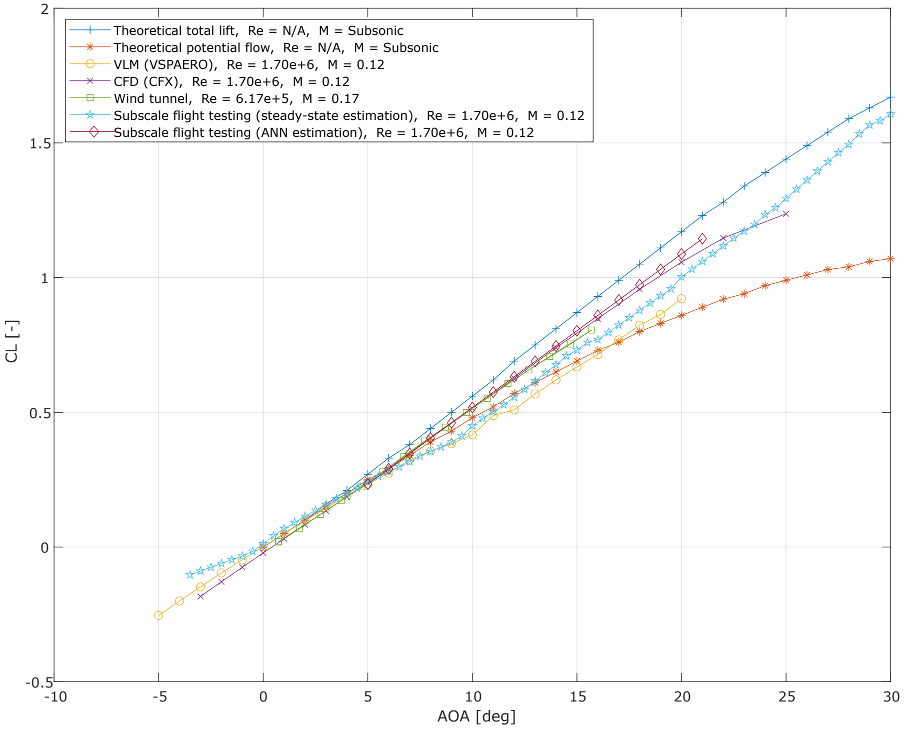

Figure 6.15 *Comparison between the lift-curve results obtained by different methods.*

7 Discussion

In comparison to traditional, relatively costly SFT programmes such as those carried out by NASA [6], this thesis has studied the implementation of SFT in contexts where both human and economic resources are significantly limited. Cost figures are rarely published and are difficult to estimate without knowing the details of each program. Hence, a balanced comparison between these different approaches cannot be made. Nevertheless, the main cost drivers of SFT can be linked to the platform requirements, the systems characteristics and the conditions in which the experiment takes place. These areas correspond approximately to the three different domains that this thesis covers: the theoretical principles of SFT and its potential applications, the technology needed to generate and interpret information, and the practical execution of experiments.

The analysis presented in chapter 3 approaches the similarity principles from a flight-mechanical perspective [7]. In this context, four main scaling methodologies are identified: aerodynamic, dynamic, aeroelastic and the newly proposed *demonstrative* scaling. The theoretical similarity requirements are correlated to practical constraints and main cost drivers using examples from projects by Linköping University and other organisations. It is shown that, unless relaxing certain similarity requirements, the number of aerodynamic, dynamic and aeroelastic problems that can be reproduced with SFT at low cost is relatively limited. Nevertheless, it is feasible to study some relevant dynamic and aeroelastic problems at low speeds – such as loss of control and body-freedom flutter – that are otherwise costly or impractical to reproduce by other means or tools. Applying SFT to a wider range of aerodynamic and dynamic problems requires a careful study and management of the effects of incomplete similarity [174, 175, 176]. In this case, a good knowledge of the issue of interest is required beforehand, a paradox illustrated in Figure 7.1.

Besides the study of airframe characteristics through similarity, low-cost SFT offers even better opportunities for technology demonstration and acceleration. The novel techniques demonstrated with the GFF in papers [III] and [IV] may

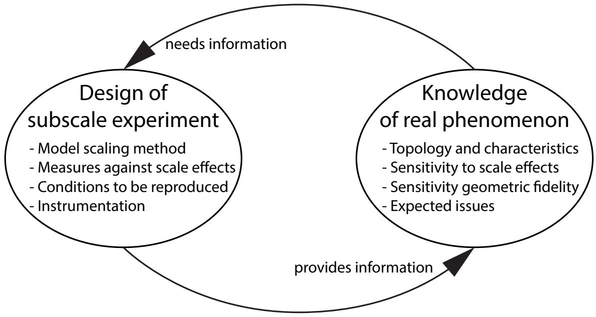

Figure 7.1 *Tailoring a subscale experiment to achieve a high degree of similarity can become a "catch 22" situation: a deep understanding of the expected phenomenon is a fundamental prerequisite to design an appropriate subscale experiment, which in return will reveal more information about such a phenomenon.*

serve as an example. Furthermore, experimentation with demonstrative models can also be valued from a more conceptual and didactic perspective. New aircraft development programmes are nowadays infrequent, follow cycles of several decades and engineers rarely experience first-flights during their careers. SFT allows a more continuous contact with the routines of fielding a new system and can, therefore, provide additional benefits in terms of experience, morale and confidence [3, 35, 52]. In addition, the potential of SFT to reveal unforeseen design problems – that could remain undetected in the virtual or analytical domains – is acknowledged in the literature [3, 6] and is supported by the practical experiences described in this thesis.

The work described in chapters 4 and 5 can be seen as a practical approach to determining the minimum technological complexity needed to enable meaningful experiments. With a strong focus on low-cost solutions and short-time implementations, both a data acquisition system and an effective testing methodology have been developed and validated. Furthermore, chapter 6 shows that software tools capable of analysing and interpreting data from subscale experiments can also be developed within a low-cost environment. Conclusions should, however, be drawn carefully. It must be acknowledged that the experiments comprised a limited number of platforms and conditions. Further, the proposed testing methods are strongly influenced by the existing regulations at the time this work was carried out. Different testing purposes, official regulations or particular risk factors may impose additional requirements on equipment and methods. Therefore, these results should only be considered representative for similar applications and conditions.

The experiments carried out here were primarily aimed at verifying the feasibility and the functionality of systems and methods at a high level, not at producing high-fidelity data. Although the multi-method investigation described

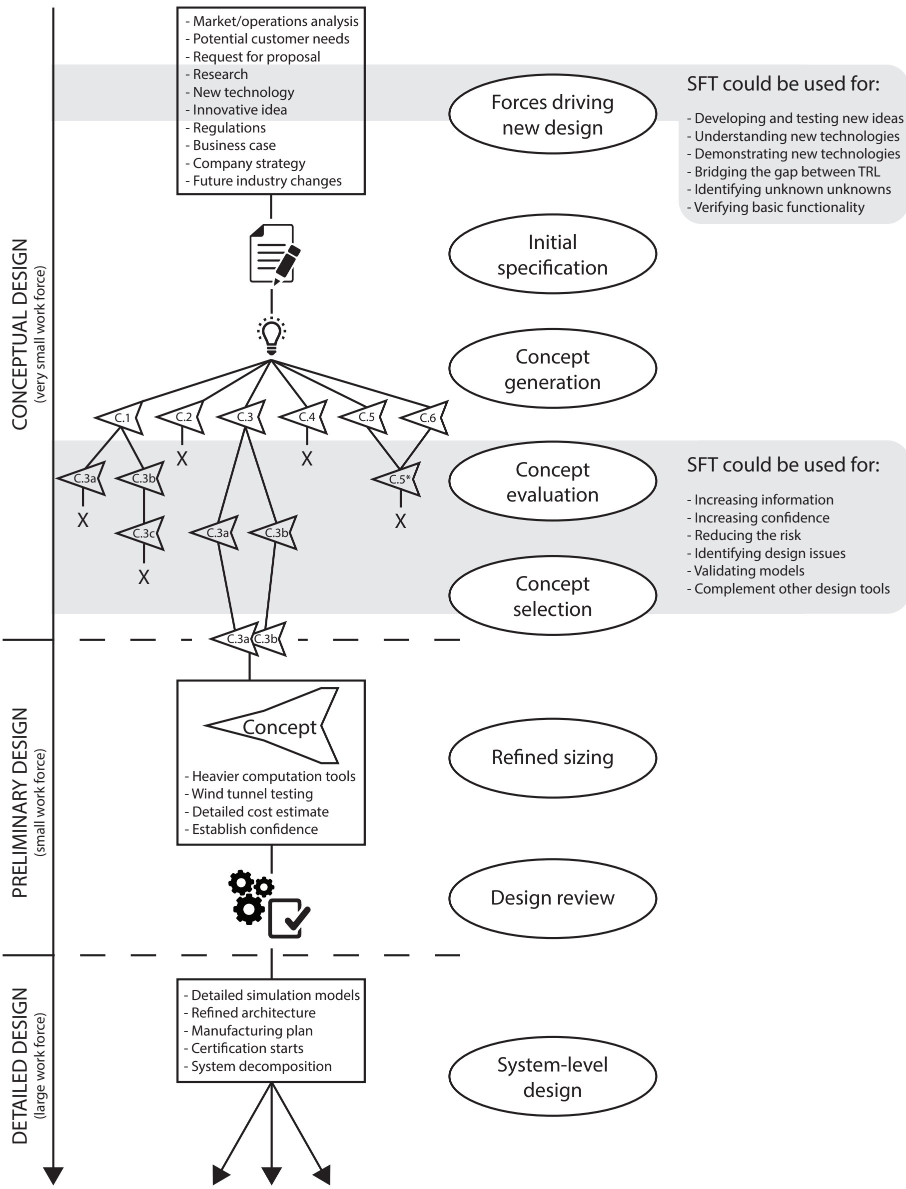

Figure 7.2 *An interpretation of the initial design stages during a typical aircraft development process. The shadowed areas indicate where and how SFT could be an added value.*

in paper [VI] suggests that the polar data obtained through SFT is of similar quality to that of first-cut numerical estimations, the lack of relevant wind-tunnel or full-scale data did not allow any further evaluation of other static or dynamic characteristics. The extrapolation of results to a larger scale could not be assessed either, since no full-scale vehicles exist.

In any case, low-cost SFT should be considered a design exploration tool and not a precise estimation tool. In an industrial context, the benefits of this method are therefore limited to the initial, conceptual design phase of the aircraft development process. Figure 7.2 represents such a process and indicates the two main roles that SFT could play in this context: contributing to the development and demonstration of new technologies, and complementing conventional estimation tools and generating confidence during the concept evaluation process. At this stage, the uncertainties surrounding the proposed design are potentially more significant than those related to the subscale experiment measurements. Without a reliable reference for validation, obtaining accurate quantitative measurements may be considered of secondary importance. In fact, according to experts in the field of experimental design methods such as Barlow [60], much design work is already considered successful if improvements are achieved, i.e. regardless of whether the methods used provide absolute accuracy in terms of predicting all performance quantities of interest.

8 Conclusions

This dissertation presents both theoretical and practical work carried out in order to contribute to knowledge on the use of the SFT method for aeronautical research and development. The obtained results support the idea that it is possible to utilise low-cost, time-efficient solutions to conduct meaningful research through SFT even at small organisations with very limited economic and human resources. According to these findings, the four research questions formulated in Section 1.2 can be answered as follows:

RQ1: What are the main opportunities, challenges and limitations for the cost-efficient use of SFT within contemporary aircraft research and development?

The practical use of SFT for the accurate replication of full-scale flight behaviour is limited by unavoidable physical constraints derived from the similarity principles. Only few flight conditions can be explored economically with free-flight subscale models at low altitude without accounting for undesired scale effects. While the usefulness of this method to study purely aerodynamic problems is hence quite limited, it still has a good potential for the preliminary study of relevant flight-dynamics problems that otherwise require costly or unfeasible wind-tunnel tests or numerical simulations. Accepting and managing the effects of incomplete similarity is key to maximising this potential.

Low-cost SFT should be considered a design exploration tool rather than a precise estimation tool. Its use is hence appropriate for technology development and during the conceptual design phase. In fact, the use of SFT as a low-cost technology-testing platform – partially or entirely disregarding the physical similarity of the vehicle to evaluate a representative version of its technology – is probably one of its most interesting applications within contemporary aircraft development.

Besides the constraints of establishing a useful similarity relationship, the severe airspace and operational constraints, the detrimental effects of wind gusts and turbulence at low-level flight and the lack of appropriate instrumentation and data analysis frameworks for small vehicles are the main identified challenges for the realisation of cost-efficient SFT experiments.

RQ2: To what extent can low-cost platforms, equipment and instrumentation fulfil flight testing requirements and be used to gather useful information?

The recent proliferation of mass-produced COTS and open-source components for the consumer UAV market has facilitated the development of economical data acquisition solutions. The data acquisition system developed here, integrating both custom-made and commercially sourced components with an open-source UAV autopilot, is a good example of a low-cost implementation. The results obtained with this system suggest that this type of low-cost avionics may bridge the gap between amateur and flight-certified professional systems by providing sufficient performance for the general study of rigid-body flight characteristics. However, any generalisation of this result should be done cautiously since the minimum requirements for test hardware and software are generally determined by the specific characteristics of each experiment.

RQ3: Which flight-testing techniques and infrastructure are suitable for a small organisation in order to safely perform SFT at low cost?

For small organisations, imitating many of the flight test techniques normally used in conventional flight testing of large UAS or manned vehicles is not efficient and, in many cases, unfeasible. The SFT campaigns carried out here with relatively small vehicles show that – considering the current local regulations for UAS – operating within VLOS requires considerably fewer resources and infrastructure. A methodology for VLOS flight testing involving only three people and less than one square kilometre of test area has been implemented here with successful results in terms of productivity and safety. By demonstrating a simple approach to manoeuvre automation and the execution of short excitation manoeuvres, this work also shows how the severe airspace constraints can, to some extent, be compensated with specifically developed, techniques to improve testing capabilities and data acquisition efficiency.

RQ4: What is a suitable approach to the analysis and interpretation of flight data gathered during SFT experiments?

As a consequence of the cost-efficient approach to SFT followed here, flights are short and easily influenced by external factors but also numerous and relatively flexible. The data analytics tools developed here have therefore been optimised for agility and for enabling direct, comprehensible feedback directly on the field using ordinary computers. Although online analysis and feedback could be useful, the short flight duration and the relatively low cost of flight repetitions reduce its advantages with respect to rapid offline tools such as the ones presented here.

The data obtained in most of these campaigns suggest that the effects of wind gusts and turbulence – with similar dynamic frequencies than those of small subscale platforms – plays a more significant role in data quality than the sensor noise or the limitations of low-cost instrumentation. Besides appropriate signal conditioning, using robust system identification methods can, therefore, be considered a key factor for the successful estimation of flight characteristics. Here, a specifically modified method in the frequency domain has shown better performance than other time-domain methods for data gathered during turbulent conditions.

Furthermore, the experience and feedback gathered during this work indicate that the importance of understandable and intuitive visualisation of both raw and processed data should not be overlooked. The addition of advanced visualisation solutions to the analysis software has played a valuable role in the transfer of information, team coordination and the execution of efficient test campaigns.

8.1 Future Work

Despite the efforts summarised here, some of the SFT method's previously discussed issues remain partially unresolved. Other aspects or potential applications of SFT are currently insufficiently explored, or lack a contemporary analysis. The following topics, listed in no particular order, could be of great interest for future research, :

- **Implications of partial similarity and scaling inaccuracies on the measurability, fidelity and extrapolability of flight characteristics:** Beyond basic aerodynamic considerations such as Reynolds number or compressibility deviations, the effects of not fulfilling other similarity parameters is still a controversial topic, especially if the purpose of the SFT experiment is to estimate the flight or handling characteristics of a full-scale vehicle. While this topic has been widely discussed in the wind-tunnel literature, little open information is available for free-flight models. Recent publications [174, 175, 176, 177] show the current interest and ongoing efforts to identify and quantify these effects using both theoretical and practical approaches.

- **Benefits of early subscale experimentation in the maturation of new technology using a demonstrative scaling approach:** While the growing interest in using demonstrative subscale platforms to increase the technology readiness level (TRL) of new technologies may indicate that the method has a positive effect in the development process, no scientific studies have tried to interpret or quantify these benefits in comparison to other development strategies.

- **Suitability of SFT for the evaluation of handling qualities with a human pilot in the loop:** The usefulness of SFT for experimenting with automatic flight control laws is, at this point, indisputable. However, its suitability for obtaining human-pilot ratings of handling qualities is unclear. Earlier experiences from NASA [6] suggest that SFT may not be appropriate for this purpose while Mandal et al. [178] suggest wide variations in pilot behaviour. Specific studies taking into account modern control and information augmentation systems would be desirable.

- **In-depth study of specific flight-testing methods and measurement techniques for subscale models:** Experience shows that the type of operation, the testing environment, the procedures and even the measurement solutions are critical factors defining both the capabilities and the quality of results of SFT. For instance, certain basic parameters such as drag are still challenging to measure in free-flight models. This thesis are presents some contributions aimed to improve low-cost flight testing of small platforms, but further understanding and developments within these topics are not only possible but key to enabling efficient and useful SFT experiments.

- **Improved data analysis and system identification methods for data gathered with SFT:** Traditional techniques do not always perform well against turbulence contamination, poor signal synchronisation or high noise ratios from low-cost instrumentation. In addition, basic data acquisition systems may not measure certain parameters such as flow angles. The further development of identification methods able to cope with these issues is therefore fundamental for SFT, especially with small vehicles. The use of artificial intelligence, machine learning and big data techniques could be potentially interesting for this application.

9

Review of Papers

Paper I

Design and Testing of a Low-Cost Flight Control and Data Acquisition System for Unstable Subscale Aircraft (2016)

This paper presents a low-cost solution for providing small, R/C models with control augmentation and data acquisition capabilities. First, the performance of inexpensive, hobbyist-type COTS equipment is evaluated using different test-beds. A complete system architecture, comprised of both COTS and custom-made components, is proposed. The system is then modelled and its capabilities are incrementally explored using simulation and real flight tests. Although it is outside the main focus of this paper, a first generation of data processing and visualisation codes is also developed at this point. It is noteworthy that, during the following years, the importance of data acquisition capabilities was prioritised over control augmentation functions for larger, jet-powered platforms. The system proposed here evolved into a more capable data acquisition system without the need for a dedicated data logger, in contrast to what was initially proposed in this paper.

Paper II

Subscale Flight Testing of a Generic Fighter Aircraft (2016)

This paper provides an overview of the experimentation conducted using the GFF demonstrator up until 2016. Besides commenting on the characteristics of this aircraft, the paper also describes how the data acquisition system – initially developed in paper [I] – is integrated into this particular platform. The flight-testing methods and procedures used at that time are also described, as are some of the difficulties encountered. When comparing papers [II] and [III], the reader will note that some of the testing methods and the capabilities of the data acquisition system were subsequently improved. Two examples are the method for automating test manoeuvres and the improved logging frequency in most channels, including a direct sampling of the control surface deflections. Lastly, this paper also describes some improvements regarding data processing and visualisation tools.

Paper III

Methods for efficient flight testing and modelling of remotely piloted aircraft within visual line-of-sight (2018)

This paper begins by briefly introducing the current regulatory context for the operation of RPAS, and justifies the choice of flight testing within VLOS based on its major cost advantages. Due to the severe limitations in airspace and flight time, a special testing methodology is needed. Various methods and procedures, as refined during previous flight-testing campaigns, are suggested. Among these, the paper presents a novel method for commanding automatically pre-programmed excitation manoeuvres without the need for a closed-loop flight controller or an online ground station. This enables the study of complex, highly efficient excitation signals such as multisines. Furthermore, the paper presents an experiment in which a multisine input is used to identify the longitudinal dynamics of the aircraft in less exposure time than that of a conventional manoeuvre.

Paper IV

A method for improved flight testing of remotely piloted aircraft using multisine inputs (2020)

With the same context as paper [III], this paper delves into the development and testing of efficient, multisine excitation signals and the improvement of an existing frequency-domain method by using an instrumental variable (IV) approach to better handle turbulence and measurement noise. Simulations are compared to flight data obtained with the GFF demonstrator using the semi-automated flight-test technique introduced in [III]. The results show that the combination of multisine input signals and the enhanced frequency-domain method is an effective way of improving flight testing of remotely piloted aircraft in confined airspace.

Paper V

A review of current research in subscale flight testing and analysis of its main practical challenges (2021)

This paper presents an overall picture of how the SFT method has been used in scientific publications during recent years. It also analyses the most common scaling methodologies and synthesises its main practical issues and limitations. This extensive review provides a broader context to most of the methods and solutions developed throughout this thesis, describes how these are implemented in practice and how they compare to those adopted by other organisations.

Paper VI

Estimation of lift characteristics of a subscale fighter using low-cost experimental methods (2021)

This paper presents a case study. Focusing on a relatively simple property, the lift curve, this study exemplifies how basic aerodynamic characteristics of a complex stealth configuration can be studied experimentally using low-cost equipment, rapid prototyping methods and SFT. Lift-curve estimates are obtained from a wind-tunnel test of a 3D-printed, 3.8%-scale model of the GFF and from flight testing the 14%-scale demonstrator using both a simple and a more advanced identification technique based on neural networks. These results are compared to a CFD study, a panel-method computation and a theoretical approach based on radical geometry simplifications.

Bibliography

[1] John D. Anderson. *Introduction to Flight*. Fifth. 2005. ISBN: 0072825693.

[2] Dennis M. Bushnell. "Scaling: Wind Tunnel to Flight". In: *Annual Review of Fluid Mechanics* 38.1 (2006), pp. 111–128. DOI: 10.1146/annurev.fluid.38.050304.092208.

[3] Robert W. Kress. "Use of Radio Controlled Models in the Conceptual Development of V/STOL Aircraft". In: *SAE Technical Paper 781050* (1978). DOI: 10.4271/781050.

[4] Karl T. Ulrich and Steven D. Eppinger. *Product design and development*. Sixth. New York, NY, USA: Mc Graw Hill Education, 2015. ISBN: 9780078029066.

[5] Peter Hallberg. "Low-Cost Demonstrators". PhD thesis. Licentiate thesis. Linköping University, 2012.

[6] Joseph R. Chambers. *Modeling Flight: The Role of Dynamically Scaled Free-Flight Models in Support of NASA's Aerospace Programs*. First. Washington, DC, USA: NASA, 2009. ISBN: 9780160846335.

[7] Chester H. Wolowicz, James S. Bowman, and William P. Gilbert. *Similitude Requirements and Scaling Relationships as Applied to Model Testing*. Technical Paper 1435. NASA, Aug. 1979.

[8] Mark A. Croom, David J. Fratello, Raymond D. Whipple, Matthew J. O'Rourke, and Todd W. Trilling. "Dynamic model testing of the X-31 configuration for high-angle-of-attack flight dynamics research". In: *Flight Simulation and Technologies, Guidance, Navigation, and Control and Co-located Conferences*. Monterey, CA, USA: AIAA, 1993. DOI: 10.2514/6.1993-3674.

[9] C. Michael Fremaux. *Spin-Tunnel Investigation of a 1/28-Scale Model of the NASA F-18 High Alpha Vehicle (HARV) With and Without Vertical Tails*. Tech. rep. Hampton, VA, USA: NASA, 1997.

[10] Joseph R. Chambers. *Cave of the Winds : the remarkable history of the Langley full-scale wind tunnel*. Washington, DC, USA: NASA, 2014. ISBN: 9781626830165.

[11] Jay M. Brandon, Frank L. Jordan, Robert a Stuever, and Catherine W. Buttrill. *Application of Wind Tunnel Free-Flight Technique for Wake Vortex Encounters*. Technical Paper November. NASA, Nov. 1997, p. 74.

[12] Vladislav Klein and Keith D. Noderer. "Aerodynamic parameters of the X-31 drop model estimated from flight-data at high angles of attack". In: *Guidance, Navigation and Control Conference*. Hilton Head Island, SC, USA: AIAA, 1992, pp. 174–181. DOI: 10.2514/6.1992-4357.

[13] Mark A. Croom, Holly Kenney, Daniel Murri, and Kenneth Lawson. “Research on the F/A-18E/F using a 22%-dynamically-scaled drop model”. In: *Atmospheric Flight Mechanics Conference*. Denver, CO, USA: AIAA, 2000, pp. 117–131. DOI: 10.2514/6.2000-3913.

[14] Masaaki Yanagihara and Takao Munenaga. “High Speed Flight Demonstration Project”. In: *24th Congress of the International Council of the Aeronautical Sciences*. Yokohama, Japan, 2004.

[15] Dwain A. Deets, V. Michael DeAngelis, and David P. Lux. *HiMAT Flight Program: Test Results and Program Assessment Overview*. Technical Memorandum 86725. NASA, 1986.

[16] Laurence A. Walker. *Flight Testing the X-36 - The Test Pilot’s Perspective*. Contractor Report 198058. NASA, 1997.

[17] Tim Risch, Gary Cosentino, Chris Regan, Michael Kisska, and Norman Princen. “X-48B Flight Test Progress Overview”. In: *47th AIAA Aerospace Sciences Meeting including The New Horizons Forum and Aerospace Exposition*. Reston, Virigina, USA: AIAA, 2009. ISBN: 978-1-60086-973-0. DOI: 10.2514/6.2009-934.

[18] Ali Yarf-Abbasi and John P. Fielding. “Design Integration of the Eclipse and Demon Demonstrator UAVs”. In: *7th AIAA Aviation Technology, Integration and Operations Conference (ATIO)*. Belfast, UK: AIAA, 2007. ISBN: 978-1-62410-014-7. DOI: 10.2514/6.2007-7725.

[19] Ali Yarf-Abbasi, A. Clarke, C. P. Lawson, and John P. Fielding. “Design and Development of the Eclipse and Demon Demonstrator UAVs”. In: *26th Congress of the International Council of the Aeronautical Sciences*. Anchorage, AK, USA, 2008.

[20] Thomas L. Jordan and Roger M. Bailey. “NASA Langley’s AirSTAR Testbed: A Subscale Flight Test Capability for Flight Dynamics and Control System Experiments”. In: *AIAA Guidance, Navigation and Control Conference and Exhibit*. Honolulu, HI, USA: AIAA, 2008. ISBN: 9781563479458. DOI: 10.2514/6.2008-6660.

[21] Bruce Owens, David Cox, and Eugene Morelli. “Development of a Low-Cost Sub-Scale Aircraft for Flight Research: The FASER Project”. In: *25th AIAA Aerodynamic Measurement Technology and Ground Testing Conference*. San Fracisco, CA, USA: American Institute of Aeronautics and Astronautics, 2006. ISBN: 978-1-62410-029-1. DOI: 10.2514/6.2006-3306.

[22] P. Schmollgruber, J. L. Gobert, P. E. Gall, Z. Goraj, H. W. Jentink, A. Näs, and R. Voit-Nitchmann. “An innovative evaluation platform for new aircraft concepts”. In: *The Aeronautical Journal* 114.1157 (2010), pp. 451–456. DOI: 10.1017/S0001924000003936.

[23] Peter Schmollgruber, Henk W. Jentink, and Marthijn Tuinstra. “IEP: a Multidisciplinary Flying Testbed for New Aircraft Concepts”. In: *27th Congress of the International Council of the Aeronautical Sciences*. Nice, France, 2010.

[24] Brad A. Seanor. “Flight testing of a remotely piloted vehicle for aircraft parameter estimation purposes”. PhD thesis. West Virginia University, 2002.

[25] D. Jung, E. J. Levy, D. Zhou, R. Fink, J. Moshe, A. Earl, and P. Tsiotras. “Design and Development of a Low-Cost Test-Bed for Undergraduate Education in UAVs”. In: *44th IEEE Conference on Decision and Control, and the European Control Conference*. Seville, Spain, 2005, pp. 2739–2744.

[26] Martin Trittler, Walter Fichter, Rudolf Voit-Nitschmann, Robert Schmoldt, and Klaus Kittmann. “Preliminary System Identification of the Blended Wing Body Flight Demonstrator VELA 2 from Flight Data”. In: *AIAA Atmospheric Flight Mechanics Conference and Exhibit*. Honolulu, HI, USA, 2008. DOI: 10.2514/6.2008-6896.

[27] Austin M Murch, Yew Chai Paw, Rohit Pandita, Zhefeng Li, and Gary J Balas. "A low cost small UAV flight research facility". In: *Advances in Aerospace Guidance, Navigation and Control* (2011), pp. 29–40.

[28] Ony Arifianto. "A Low-cost Unmanned Aerial Vehicle Research Platform: Development, Modeling, and Advanced Control Implementation". Ph.D. thesis. Virginia Tech, 2013.

[29] Or D. Dantsker, Miles J. Johnson, Michael S. Selig, and Timothy W. Bretl. "Development of the UIUC Aero Testbed: A Large-Scale Unmanned Electric Aerobatic Aircraft for Aerodynamics Research". In: *31st AIAA Applied Aerodynamics Conference*. San Diego, CA, USA: AIAA, 2013. DOI: 10.2514/6.2013-2807.

[30] Adam M. Ragheb, Or D. Dantsker, and Michael S. Selig. "Stall/spin flight testing with a subscale aerobatic aircraft". In: *31st AIAA Applied Aerodynamics Conference*. San Diego, CA, USA: AIAA, 2013. DOI: 10.2514/6.2013-2806.

[31] Robert F. Dorr, René Francillon, and Jay Miller. "Saab J35 Draken". In: *Aerofax Minigraph 12* (1987).

[32] K. E. Henriksson. *Spin testing the Viggen aircraft*. Tech. rep. Society of Experimental Test Pilots, 1974.

[33] Simone Duranti and Viktor Malmfors. "Flight Testing of Saab UAV SHARC Technology Demonstrator". In: *SETP/SFTE European Symposium*. London, UK: Royal Aeronautical Society, 2004.

[34] Simone Duranti and Viktor Malmfors. "Flight Test of the Autonomous Take Off and Landing Functions of the SHARC Technology Demonstrator". In: *Systems Concepts and Integration Panel Symposium*. Warsaw, Poland: RTO-MP-SCI-162, 2005.

[35] Christopher Jouannet, Patrick Berry, and Petter Krus. "Aircraft Design Education at Linköpings University". In: *Proceedings of the Institution of Mechanical Engineers, Part G: Journal of Aerospace Engineering*. Vol. 221. 2007, pp. 217–224. DOI: 10.1243/09544100JAERO131.

[36] Christopher Jouannet, David Lundström, Kristian Amadori, and Patrick Berry. "Design and Flight Testing of an ECO-Sport Aircraft". In: *48th AIAA Aerospace Sciences Meeting Including the New Horizons Forum and Aerospace Exposition*. American Institute of Aeronautics and Astronautics, 2010. DOI: 10.2514/6.2010-1206.

[37] Christopher Jouannet, David Lundström, Kristian Amadori, and Patrick Berry. "Design of a Very Light Jet and a Dynamically Scaled Demonstrator". In: *46th AIAA Aerospace Sciences Meeting and Exhibit*. Reno, NV, USA, 2008.

[38] David Lundström and Kristian Amadori. "Raven - a Subscale Radio Controlled Business Jet Demonstrator". In: *26th Congress of the International Council of the Aeronautical Sciences*. Anchorage, AK, USA: ICAS, 2008.

[39] Kristian Amadori, David Lundström, and Petter Krus. "Evaluation of Automatically Designed Micro Air Vehicles and Flight Testing". In: *48th AIAA Aerospace Sciences Meeting Including the New Horizons Forum and Aerospace Exposition*. Orlando, FL, USA, 2010.

[40] Ingo Staack and David Lundström. "Subscale Flight Testing at Linköping University". In: *27th Congress of the International Council of the Aeronautical Sciences*. Nice, France, 2010.

[41] David Lundström. "Aircraft Design Automation and Subscale Testing: With Special Reference to Micro Air Vehicles". Doctoral Thesis. Linköping, Sweden: Linköping University, 2012. ISBN: 9789175197883. URL: http://www.diva-portal.org/smash/record.jsf?pid=diva2:561097.

[42] Kristian Amadori, Christopher Jouannet, and Patrick Berry. "Development of a subscale flight testing platform for a generic future fighter". In: *27th Congress of the International Council of the Aeronautical Sciences*. Nice, France, 2010. ISBN: 9781617820496.

[43] Christopher Jouannet, Patrick Berry, Tomas Melin, Kristian Amadori, David Lundström, and Ingo Staack. "Subscale flight testing used in conceptual design". In: *Aircraft Engineering and Aerospace Technology* 84.3 (2012), pp. 192–199. DOI: `10.1108/00022661211222058`.

[44] Robert Nola and Howard Sankey. "The hypothetico-deductive method". In: *Theories of Scientific Method: an introduction*. London, UK: Routledge, 2007. Chap. 7.

[45] Steven A. Brandt, Randall J. Stilles, John J. Bertin, and Ray Whitford. *Introduction to Aeronautics: A Design Perspective*. Second. Vol. 2. Reston, VA, USA: AIAA Education Series, 2004. ISBN: 1563477017.

[46] Martin Hochwallner. "On Motion Control of Linear Incremental Hydraulic Actuators". Doctoral dissertation. Linköping University, 2017.

[47] Lloyd R. Jenkinson, Paul Simpkin, and Darren Rhodes. *Civil jet aircraft design*. First. London, UK: Arnold, 1999. ISBN: 034074152X.

[48] Jaroslaw Sobieski. *Multidisciplinary systems optimization by linear decomposition*. Tech. rep. Hampton, VA, USA: NASA Langley Research Center, 1984.

[49] Egbert Torenbeek. *Synthesis of subsonic airplane design*. Rotterdam, The Netherlands: Delft University Press, 1976. ISBN: 9029825057.

[50] Daniel P. Raymer. *Aircraft design: A conceptual approach*. Second. Washington, DC, USA: AIAA Education Series, 1992. ISBN: 0930403517.

[51] Ingo Staack. "Aircraft systems conceptual design: An object-oriented approach from <element> to <aircraft>". Doctoral dissertation. Linköping University, 2016. DOI: `10.3384/diss.diva-132614`.

[52] Paul Eremenko. *Innovation in the age of the third aerospace revolution*. Denver, CO, USA, 2017.

[53] McKinsey Global Institute. *The Internet of Things: Mapping the value beyond the hype*. Tech. rep. June. McKinsey & Company, 2015.

[54] Wikipedia. *Mobile operating system: Market share*. 2018. URL: `http://en.wikipedia.org/wiki/Mobile_operating_system` (visited on 07/17/2018).

[55] SESAR Joint Undertaking. *European Drones Outlook Study*. Tech. rep. November. Eurocontrol, European Union, 2016. DOI: `10.2829/219851`. URL: `https://www.sesarju.eu/sites/default/files/documents/reports/European_Drones_Outlook_Study_2016.pdf`.

[56] Petter Krus. "Simulation based optimisation for system design". In: *14th International Conference on Engineering Design*. Stockholm, Sweden: ICED, 2003.

[57] E. Buckingham. "On physically similar systems; Illustrations of the use of dimensional equations". In: *Physical Review* 4.4 (1914), pp. 345–376. DOI: `10.1103/PhysRev.4.345`. arXiv: `arXiv:1011.1669v3`.

[58] S. J. Kline. *Similitude and Approximation Theory*. McGraw-Hill, 1965.

[59] Thomas G. Gainer and Sherwood Hoffman. *Summary of Transformation Equations and Equations of Motion Used in Free-Flight and Wind-Tunnel Data Reduction and Analysis*. Tech. rep. NASA, 1972.

[60] Jewel B. Barlow, William H. Rae, and Alan Pope. *Low-Speed Wind Tunnel Testing*. Third. New York, NY, USA: John Wiley & Sons, 1999, p. 713. ISBN: 0471557749.

[61] A. B. Haines. *Scale Effects on Aircraft and Weapon Aerodynamics*. Tech. rep. AGARD, 1994.

[62] Cameron D. Munro, Christopher Jouannet, and Petter Krus. "Implications of scale effect for the prediction of high angle of attack aerodynamics". In: *Progress in Aerospace Sciences* 41.3-4 (2005), pp. 301–322. DOI: 10.1016/j.paerosci.2005.05.001.

[63] Charles L. Ladson. *Effects of independent variation of Mach and Reynolds numbers on the low-speed aerodynamic characteristics of the NACA 0012 airfoil section.* Tech. rep. NASA, 1988.

[64] George W. Jones, Joseph J. Cincotta, and Robert W. Walker. *Aerodynamic forces on a stationary and oscillating circular cylinder at high reynolds numbers.* Tech. rep. Washington, DC, USA: NASA, 1969.

[65] Karl Pettersson and Arthur Rizzi. "Aerodynamic scaling to free flight conditions: Past and present". In: *Progress in Aerospace Sciences* 44.4 (2008), pp. 295–313. DOI: 10.1016/j.paerosci.2008.03.002.

[66] Daniel W. Banks, David F. Fisher, Robert M. Hall, Gary E. Erickson, Daniel G. Murri, Sue B. Grafton, and William G. Sewall. *The F/A-18 High-Angle-of-Attack Ground-to-Flight Correlation: Lessons Learned.* Tech. rep. NASA, 1997.

[67] Karl Pettersson and Arthur Rizzi. "Comparing Different CFD Methods Accuracy in Computing Local Boundary Layer Properties". In: *Engineering Applications of Computational Fluid Mechanics* 3.1 (2009), pp. 98–108. DOI: 10.1080/19942060.2009.11015257.

[68] Gary E. Erickson, Robert M. Hall, Daniel W. Banks, John H. Del Frate, John A. Schreiner, Robert J. Hanley, and Craig T. Pulley. "Experimental investigation of the F/A-18 vortex flows at subsonic through transonic speeds". In: *7th Applied Aerodynamics Conference.* Seattle, WA, USA: AIAA, 1989. DOI: 10.2514/6.1989-2222.

[69] Stephen Rolston. "High Reynolds number tools and techniques for civil aircraft design - An overview of the European 'HiReTT' project". In: *19th AIAA Applied Aerodynamics Conference.* Anaheim, CA, USA: American Institute of Aeronautics and Astronautics, 2001. DOI: 10.2514/6.2001-2411.

[70] John J. Bertin and Russell M. Cummings. *Aerodynamics for Engineers.* Sixth. Harlow, England: Pearson Education, 2001, p. 275. ISBN: 0132355213.

[71] Thomas L. Jordan, Mark A. Hutchinson, Vernon E. Watkins, William M. Langford, Christopher M. Cagle, and Michael J. Logan. *National Aeronautics and Space Administration Langley Research Center's Design Criteria for Small Unmanned Aerial Vehicle Development.* Tech. rep. NATO, 2007.

[72] Arthur R. Collar. "The Expanding Domain of Aeroelasticity". In: *Journal of the Royal Aeronautical Society* 50 (1946), pp. 613–636. DOI: 10.1017/S0368393100120358.

[73] Jeffrey A. Ouellette, Mayuresh J. Patil, and Rakesh K. Kapania. "Scaling Laws for Flight Control Development and Testing in the Presence of Aeroservoelastic Interactions". In: *AIAA Atmospheric Flight Mechanics Conference.* Minneapolis, MN, USA: AIAA, 2012.

[74] Harold N. Murrow. "Status and future plans of the Drones for Aerodynamic and Structural Testing (DAST) program". In: *Advanced aerodynamics and active controls. Selected NASA research.* (1981), pp. 21–36.

[75] Robert M. Bennett and Irving Abel. *Application of a flight test and data analysis technique to flutter of a drone aircraft.* Tech. rep. NASA-TM-83136, 1981.

[76] Glenn B. Gilyard and John W. Edwards. *Real-time flutter analysis of an active flutter-suppression system on a remotely piloted research aircraft.* Tech. rep. NASA-TM-84901, 1983.

[77] Irene Gregory, Chengyu Cao, Enric Xargay, Naira Hovakimyan, and Xiaotian Zou. “L1 Adaptive Control Design for NASA AirSTAR Flight Test Vehicle”. In: *AIAA Guidance, Navigation, and Control Conference*. Chicago, IL„ USA: AIAA, 2009. ISBN: 978-1-60086-978-5. DOI: 10.2514/6.2009-5738.

[78] Enric Xargay, Naira Hovakimyan, Vladimir Dobrokhodov, Isaac Kaminer, Irene M. Gregory, and Chengyu Cao. “L1 Adaptive Flight Control System : Flight Evaluation and Technology Transition”. In: *AIAA Infotech@Aerospace 2010*. Atlanta, GA, USA: merican Institute of Aeronautics and Astronautics, 2010. ISBN: 978-1-60086-963-1. DOI: 10.2514/6.2010-3365.

[79] Irene Gregory, Ross Gadient, and Eugene Lavretsky. “Flight Test of Composite Model Reference Adaptive Control (CMRAC) Augmentation Using NASA AirSTAR Infrastructure”. In: *AIAA Guidance, Navigation, and Control Conference*. 2011, pp. 1–30. ISBN: 978-1-60086-952-5. DOI: 10.2514/6.2011-6452.

[80] Jeff Beranek, Lee Nicolai, Mike Buonanno, Edward Burnett, Christopher Atkinson, Brian Holm-Hansen, and Pete Flick. “Conceptual Design of a Multi-Utility Aeroelastic Demonstrator”. In: *13th AIAA/ISSMO Multidisciplinary Analysis Optimization Conference*. Fort Worth, TX, USA: American Institute of Aeronautics and Astronautics, 2010. ISBN: 9781600869549. DOI: 10.2514/6.2010-9350.

[81] Wesley W. Li and Chan-gi Pak. “Aeroelastic Optimization Study Based on the X-56A Model”. In: *AIAA Atmospheric Flight Mechanics Conference*. Atlanta, GA, USA: AIAA, 2014. ISBN: 978-1-62410-294-3. DOI: 10.2514/6.2014-2052.

[82] Jessica Jones and Carlos E. Cesnik. “Nonlinear Aeroelastic Analysis of the X-56 Multi-Utility Aeroelastic Demonstrator”. In: *15th Dynamics Specialists Conference*. San Diego, CA, USA: AIAA, 2016. ISBN: 978-1-62410-398-8. DOI: 10.2514/6.2016-1799.

[83] Michael H. Love, P. Scott Zink, Paul A. Wieselmann, and Harold Youngren. “Body Freedom Flutter of High Aspect Ratio Flying Wings”. In: *46th AIAA/ASME/ASCE/AHS/ASC Structures, Structural Dynamics and Materials Conference*. Austin, TX, USA: AIAA, 2005. ISBN: 978-1-62410-065-9. DOI: 10.2514/6.2005-1947.

[84] Jeffrey A. Ouellette, Mayuresh J. Patil, and Craig Woolsey. “Flight testing of a subscale aeroservoelastic aircraft”. In: *AIAA Atmospheric Flight Mechanics Conference*. National Harbor, MD, USA: AIAA, 2014. DOI: 10.2514/6.2014-0032.

[85] Franz-Michael Sendner, Philipp Stahl, Christian Rößler, and Mirko Hornung. “Designing an UAV Propulsion System for Dedicated Acceleration and Deceleration Requirements”. In: *17th AIAA Aviation Technology, Integration, and Operations Conference*. Denver, CO, USA: AIAA, 2017. ISBN: 978-1-62410-508-1. DOI: 10.2514/6.2017-4105.

[86] Philipp Stahl, Franz-Michael Sendner, Christian Rößler, Mirko Hornung, and Andreas Hermanutz. “Mission and Aircraft Design of FLEXOP Unmanned Flying Demonstrator to Test Flutter Suppression within Visual Line of Sight”. In: *17th AIAA Aviation Technology, Integration, and Operations Conference*. Denver, CO, USA: AIAA, 2017. ISBN: 978-1-62410-508-1. DOI: 10.2514/6.2017-3766.

[87] Christian Roessler et al. “Aircraft Design and Testing of FLEXOP Unmanned Flying Demonstrator to Test Load Alleviation and Flutter Suppression of High Aspect Ratio Flexible Wings”. In: *AIAA Scitech 2019 Forum*. American Institute of Aeronautics and Astronautics, 2019. DOI: 10.2514/6.2019-1813.

[88] Christian Roessler et al. “Results of an Aeroelastically Tailored Wing on the FLEXOP Demonstrator Aircraft”. In: *AIAA Scitech 2020 Forum*. American Institute of Aeronautics and Astronautics, 2020. DOI: 10.2514/6.2020-1969.

[89] Jurij Sodja et al. “Ground Testing of the FLEXOP Demonstrator Aircraft”. In: *AIAA Scitech 2020 Forum*. American Institute of Aeronautics and Astronautics, 2020. DOI: 10.2514/6.2020-1968.

[90] Béla Takarics et al. "Active Flutter Mitigation Testing on the FLEXOP Demonstrator Aircraft". In: *AIAA Scitech 2020 Forum*. American Institute of Aeronautics and Astronautics, 2020. DOI: 10.2514/6.2020-1970.

[91] Dennis R. Jenkins, Tony Landis, and Jay Miller. "American X-Vehicles: An Inventory, X-1 to X-50". In: *NASA Monographs in Aerospace History* 31.SP-2003-4531 (2003). URL: http://history.nasa.gov/monograph31.pdf.

[92] NASA. *NASA Systems Engineering Handbook*. Washington, DC, USA, 2017. URL: https://www.nasa.gov/connect/ebooks/nasa-systems-engineering-handbook.

[93] AHS/NARI Transformative Vertical Flight Working Group-2. *Commercial Intra-City On-Deman Electric-VTOL: Status of Technology*. Tech. rep. Prepublication copy, 2018. URL: https://vtol.org/files/dmfile/TVF.WG2.YR2017draft.pdf.

[94] William J. Fredericks, Robert G. McSwain, Brian F. Beaton, David W. Klassman, and Colin R. Theodore. *Greased Lightning (GL-10) Flight Testing Campaign*. Tech. rep. NASA TM-2017-219643, 2017.

[95] Robert G. Mcswain, Louis J. Glaab, and Colin R. Theodore. *Greased Lightning (GL-10) Performance Flight Research - Flight Data Report*. Tech. rep. NASA TM-2017-219794, 2017.

[96] Bruce Cogan, Nicholas Alley, Craig Hange, Nhan Nguyen, and Brian Spivey. *Flight validation of cruise efficient, low noise, extreme short takeoff and landing (CESTOL) and circulation control (CC) for drag reduction enabling technologies (presentation)*. 2014.

[97] Patricia Ortiz and Nicholas Alley. *Spanwise Adaptive Wing - PTERA Flight Test (oral presentation)*. Atlanta, GA, USA, 2018.

[98] Zdobyslaw Goraj, Klaus Kitmann, Rudolf Voit-Nitschmann, and Marcin Szender. "Design and integration of flexi bird - a low cost sub-scale research aircraft for safety and environmental issues". In: *27th Congress of the International Council of the Aeronautical Sciences*. Nice, France, 2010.

[99] Aurora Flight Sciences. *LightningStrike: Innovation for Runway Independence. XV-24A LightningStrike Brochure*. 2018. URL: https://www.aurora.aero/wp-content/uploads/2016/07/LightningStrike_brochure.pdf (visited on 08/20/2018).

[100] J. P. Fielding, C. P. Lawson, R. Pires, and G. Monterzino. "Development of the Demon Technology Demonstrator UAV". In: *27th Congress of the International Council of the Aeronautical Sciences*. Nice, France, 2010.

[101] Mark A. Motter, Michael J. Logan, Michael L. French, and Nelson M. Guerreiro. "Simulation to Flight Test for a UAV Controls Testbed". In: *25th AIAA Aerodynamic Measurement Technology and Ground Testing Conference*. San Fracisco, CA, USA: AIAA, 2006. ISBN: 1563478110. DOI: 10.2514/6.2006-3305.

[102] Mark A. Motter and James W. High. "Remotely Piloted Vehicles for Experimental Flight Control Testing". In: *AUVSI's Unmanned Systems North America 2009*. 2009.

[103] Kevin Cunningham, David Cox, Daniel Murri, and Stephen Riddick. "A Piloted Evaluation of Damage Accommodating Flight Control Using a Remotely Piloted Vehicle". In: *AIAA Guidance, Navigation, and Control Conference*. 2011. ISBN: 978-1-60086-952-5. DOI: 10.2514/6.2011-6451.

[104] Jason Gross, Yu Gu, Brad Seanor, Srikanth Gururajan, and Marcello Napolitano. "Advanced Research Integrated Avionics (ARIA) System for Fault-Tolerant Flight Research". In: *AIAA Guidance, Navigation, and Control Conference*. Chicago, IL, USA, 2009, pp. 1–13. ISBN: 978-1-60086-978-5. DOI: 10.2514/6.2009-5659.

[105] Eugene A. Morelli. "Flight Test Maneuvers for Efficient Aerodynamic Modeling". In: *Journal of Aircraft* 49.6 (2012), pp. 1857–1867. DOI: 10.2514/1.C031699.

[106] David Lundström and Petter Krus. “Testing of Atmospheric Turbulence Effects on the Performance of Micro Air Vehicles Testing of Atmospheric Turbulence Effects on the Performance of Micro Air Vehicles”. In: *International Journal of Micro Air Vehicles* 4.2 (2012), pp. 133–149. DOI: 10.1260/1756-8293.4.2.133.

[107] Zdobyslaw Goraj, Miroslaw Rodzewicz, Wojciech Grendysa, and Marek Jonas. “Design and Configuration Layouts of an Advanced Long Endurance Uav- Lessons Learnt After Flight Testing”. In: *28th Congress of the International Council of the Aeronautical Sciences*. Brisbane, Australia, 2012.

[108] Cezary Galiński, Wieńczysław Stalewski, Mateusz Lis, and Jaroslaw Hajduk. “Overview of the Inverted Joined Wing Scaled Demonstrator Programme”. In: *30th Congress of the International Council of the Aeronautical Sciences*. Daejeon, South Korea: ICAS, 2016.

[109] Ronald M. Barrett. “Adaptive aerostructures: the first decade of flight on uninhabited aerial vehicles”. In: *Smart Structures and Materials*. Vol. 5388. 2004, pp. 190–201. DOI: 10.1117/12.536681.

[110] Jamey D. Jacob, Andrew Simpson, and Suzanne Smith. “Design and Flight Testing of Inflatable Wings with Wing Warping”. In: *SAE World Aerospace Congress* (2005). DOI: 10.4271/2005-01-3392. URL: http://papers.sae.org/2005-01-3392/.

[111] Ben Loh, Pradeep Gaddam, Jamey D. Jacob, Suzanne Smith, and Laila Asheghian. “Stowed Unmanned Air Vehicle Engineering (SUAVE): Deployable wing and testing”. In: *53rd AIAA/ASME/ASCE/AHS/ASC Structures, Structural Dynamics and Materials Conference*. Honolulu, HI, USA, 2012.

[112] S. A. Meguid, Yu Su, and Yue Wang. “Complete morphing wing design using flexible-rib system”. In: *International Journal of Mechanics and Materials in Design* 13 (2017), pp. 159–171. DOI: 10.1007/s10999-015-9323-0.

[113] Sven Grundmann, Michael Frey, and Cameron Tropea. “Unmanned Aerial Vehicle (UAV) with Plasma Actuators for Separation Control”. In: *47th AIAA Aerospace Sciences Meeting including The New Horizons Forum and Aerospace Exposition*. Orlando, FL, USA: AIAA, 2009. ISBN: 978-1-60086-973-0. DOI: 10.2514/6.2009-698.

[114] Ved Chirayath and Juan J. Alonso. *Plasma Actuated Unmanned Aerial Vehicle - The First Plasma Controlled Flight in History*. Stanford, CA, USA, 2012.

[115] Wilm Friedrichs. “Unmanned Aerial Vehicle for Flow Control Experiments with Dielectric Barrier Discharge Plasma Actuators”. Doctoral dissertation. Technische Universität, Darmstadt, 2014.

[116] Louis J. Glaab, Chester V. Dolph, Steven D. Young, Neil C. Coffey, and Donald E. Harper. *Small Unmanned Aerial System (UAS) Flight Testing of Enabling Vehicle Technologies for the UAS Traffic Management Project*. Tech. rep. TM-2018-219816. NASA, 2018.

[117] Christine M. Belcastro, David H. Klyde, Michael J. Logan, Richard L. Newman, and John V. Foster. “Experimental Flight Testing for Assessing the Safety of Unmanned Aircraft System Safety-Critical Operations”. In: *17th AIAA Aviation Technology, Integration, and Operations Conference*. Denver, CO, USA: AIAA, 2017. ISBN: 978-1-62410-508-1. DOI: 10.2514/6.2017-3274.

[118] Timothy P. Jung, Ryan P. Starkey, and Brian Argrow. “Methodology for Conducting Scaled Sonic-Boom Flight Tests Using Unmanned Aircraft Systems”. In: *Journal of Aircraft* 49.5 (2012), pp. 1234–1244. DOI: 10.2514/1.C031449.

[119] Vladyslav Rozov, Andreas Hermanutz, Christian Breitsamter, and Mirko Hornung. “Aeroelastic Analysis of a Flutter Demonstrator With a Very Flexible High-Aspect-Ratio Swept Wing”. In: *International Forum on Aeroelasticity and Structural Dynamics IFASD*. Como, Italy, 2017. ISBN: 9788897576280.

[120] National Research Council of the National Academies. *Accelerating Technology Transition: Bridging the Valley of Death for Materials and Processes in Defense Systems*. Washington, DC, USA: The National Academies Press, 2004. ISBN: 0309093171.

[121] Jan L. M. Hensen, Roel C. G. M. Loonen, Maria Archontiki, and Michalis Kanellis. "Using building simulation for moving innovations across the Valley of Death". In: *REHVA Journal* 52.3 (2015), pp. 58–62.

[122] Peter G. Hamel and Ravindra V. Jategaonkar. "Evolution of flight vehicle system identification". In: *Journal of Aircraft* 33.1 (1996), pp. 9–28. DOI: 10.2514/3.46898.

[123] O. D. Dantsker and R. Mancuso. "Flight data acquisition platform development, integration, and operation on small-to medium-sized unmanned aircraft". In: *AIAA Scitech 2019 Forum*. 2019. DOI: 10.2514/6.2019-1262.

[124] Eagle Tree Systems. *Eagle Tree eLogger v3 and v4*. (accessed on 01-03-2018). URL: http://www.eagletreesystems.com.

[125] RCATS Systems. *RCATS UAV data systems*. (accessed on 18-12-2020). URL: https://www.rcatsystems.com/uav.php.

[126] Collins Aerospace. *Cloud Cap Technology Piccolo autopilot systems*. Available online: http://www.cloudcaptech.com/products/auto-pilots. (accessed on 20-01-2021).

[127] Sean A. Laughter. "Expanding Airstar capability for flight research in an existing avionics design". In: *2012 IEEE/AIAA 31st Digital Avionics Systems Conference (DASC)*. Williamsburg, VA, USA, 2012, pp. 8C1–1–8C1–9. ISBN: 978-1-4673-1700-9. DOI: 10.1109/DASC.2012.6382438.

[128] T. Larrabee, H. Chao, T. Mandal, S. Gururajan, Y. Gu, and M. Napolitano. "Design, simulation, and flight test validation of a UAV ground control station for aviation safety research and pilot modeling". In: *AIAA Guidance, Navigation, and Control (GNC) Conference*. 2013.

[129] Or D. Dantsker, Renato Mancuso, Michael S. Selig, and Marco Caccamo. "High-Frequency Sensor Data Acquisition System (SDAC) for Flight Control and Aerodynamic Data Collection". In: *32nd AIAA Applied Aerodynamics Conference*. Atlanta, GA, USA: AIAA, 2014.

[130] Christoph Göttlicher and F. Holzapfel. "Flight Path Reconstruction for an Unmanned Aerial Vehicle Using Low-Cost Sensors". In: *30th Congress of the International Council of the Aeronautical Sciences*. Daejeon, South Korea: ICAS, 2016.

[131] A. Zeitler, S. Hiergeist, and A. Schwierz. "COTS components for a large scale UAS demonstrator datalink system". In: *AIAA/IEEE Digital Avionics Systems Conference - Proceedings*. Vol. 2017-September. 2017. DOI: 10.1109/DASC.2017.8102017.

[132] H.-H. Lu, J. Harris, V. G. Goecks, E. Bowden, and J. Valasek. "Flight test instrumentation system for small UAS system identification". In: *2017 International Conference on Unmanned Aircraft Systems, ICUAS 2017*. 2017, pp. 1696–1705. DOI: 10.1109/ICUAS.2017.7991399.

[133] École Nationale de l'Aviation Civile and Paparazzi develpers community. *Paparazzi project, open-source autopilot system*. Available online: http://wiki.paparazziuav.org/. (accessed on 01-03-2018). URL: http://wiki.paparazziuav.org/ (visited on 03/01/2018).

[134] Lorenz Meier, ETH Zürich, and 3D Robotics, Inc. *PX4/Pixhawk open-hardware autopilot project*. Available online: http://pixhawk.org/. (accessed on 01-03-2018). URL: http://pixhawk.org/ (visited on 03/01/2018).

[135] Gautier Hattenberger, Murat Bronz, and Michel Gorraz. "Using the Paparazzi UAV System for Scientific Research". In: *International Micro Air Vehicle Conference and Competition IMAV 2014*. Delft, Netherlands, 2014, pp. 247–252.

[136] Roberto Bunge, Felipe Munera Savino, and Ilan Kroo. "Stall/Spin Flight Test Techniques with COTS Model Aircraft and Flight Data Systems". In: *AIAA Flight Testing Conference*. American Institute of Aeronautics and Astronautics, 2015. DOI: 10.2514/6.2015-3225.

[137] F. Arthurs, J. Valasek, and M. D. Zeiger. "Precision onboard small sensor system for unmanned air vehicle testing and control". In: *2016 AIAA Guidance, Navigation, and Control Conference*. 2016. DOI: 10.2514/6.2016-1138.

[138] T. Wilson, J. Kirk, J. Hobday, and A. Castrichini. "Small scale flying demonstration of semi aeroelastic hinged wing tips". In: *International Forum on Aeroelasticity and Structural Dynamics*. IFASD 2019, 2019.

[139] Christopher Courtin, R. John Hansman, and Mark Drela. "Flight Test Results of a Subscale Super-STOL Aircraft". In: *AIAA Scitech 2020 Forum*. American Institute of Aeronautics and Astronautics, 2020. DOI: 10.2514/6.2020-0977.

[140] Dronekit development community. *DRONEKIT: Developer tools for drones*. Available online: http://dronekit.io/. (accessed on 10-12-2020).

[141] Dronecode Project, Inc. *Dronecode Foundation Projects*. Available online: https://www.dronecode.org/projects/. (accessed on 13-01-2021).

[142] Sebastian J. Koeberle, Moritz Rumpf, Bastian Scheufele, and Mirko Hornung. "Design of a Low-Cost RPAS Data Acquisition System for Education". In: *AIAA Aviation 2019 Forum*. American Institute of Aeronautics and Astronautics, 2019. DOI: 10.2514/6.2019-3658.

[143] Or D. Dantsker, Andrew V. Louis, Renato Mancuso, Marco Caccamo, and Michael S. Selig. "SDAC-UAS : A Sensor Data Acquisition Unmanned Aerial System for Flight State Monitoring and Aerodynamic Data Collection". In: *AIAA Infotech @ 53rd AIAA Aerospace Sciences Meeting*. Kissimmee, FL, USA: AIAA, 2015.

[144] ArduPilot Dev Team. *ArduPilot open-source autopilot suite: Plane*. (accessed on 01-04-2017). URL: http://ardupilot.org/plane/.

[145] Dan Simon. *Optimal State Estimation: Kalman, H Infinity, and Nonlinear Approaches*. Hoboken, NJ, USA: Wiley Interscience, 2006, p. 552.

[146] Alejandro Sobron. "Design and Testing of a Flight Control System for Unstable Subscale Aircraft". Master's Thesis. Linköping University, 2015. URL: http://www.diva-portal.se/smash/get/diva2:859608/FULLTEXT01.pdf.

[147] JetiModel. *DC-24 Computerized Radio Control System*. 2017. URL: http://www.jetimodel.com/en/katalog/Transmitters/@produkt/DC-24/ (visited on 06/18/2017).

[148] Michael Oborne and Dronecode Project Inc. *Mission Planner open-source ground station software*. (accessed on 10-01-2021). URL: http://ardupilot.org/planner/.

[149] Anna Martinez. "Design and manufacturing of a thrust measurement system for a micro jet engine: Enabling in-flight drag estimation for subscale aircraft testing". MA thesis. Linköping University, 2018. URL: http://urn.kb.se/resolve?urn=urn:nbn:se:liu:diva-149288.

[150] Marvel P. Miller. *An accurate method of measuring the moments of inertia of airplanes*. Tech. rep. NACA-TN-351. NACA, 1930.

[151] Eugene A. Morelli. "Efficient Global Aerodynamic Modeling from Flight Data". In: *50th Aerospace Sciences Meeting, AIAA*. Nashville, TN, USA: AIAA, 2012. DOI: 10.2514/6.2012-1050.

[152] Roger Larsson and Martin Enqvist. "Sequential Aerodynamic Model Parameter Identification". In: *IFAC Proceedings Volumes* 45.16 (July 2012), pp. 1413–1418. DOI: 10.3182/20120711-3-BE-2027.00293.

[153] Claudia Stöcker, Rohan Bennett, Francesco Nex, Markus Gerke, and Jaap Zevenbergen. "Review of the current state of UAV regulations". In: *Remote Sensing* 9.5 (2017), pp. 33–35. DOI: 10.3390/rs9050459.

[154] L. A. Ingham, T. Jones, and A. Maneschijn. "Considerations for flight testing of UAVs in South African airspace". In: *Aeronautical Journal* 110.1114 (2006), pp. 803–811. DOI: 10.1017/S0001924000001676.

[155] ICAO. *Doc 10019, Manual on Remotely Piloted Aircraft Systems (RPAS)*. First. Montréal, Canada: International Civil Aviation Organization, 2015. ISBN: 9789292497187.

[156] Eurocontrol. *RPAS ATM CONOPS*. Fourth. 2017. URL: http://www.eurocontrol.int/sites/default/files/publication/files/rpas-atm-cocept-of-operations-2017.pdf.

[157] Transportstyrelsen (Swedish Transport Agency). *Transportstyrelsens föreskrifter om obemannade luftfartyg TSFS 2017:110 (in Swedish)*. 2017.

[158] Michael Kisska. "Flight Testing the X-48C: Advancing the BWB Concept". In: *AIAA Southern California Aerospace Systems and Technology Conference*. 2013.

[159] Jared A. Grauer and Matthew Boucher. "System Identification of Flexible Aircraft: Lessons Learned from the X-56A Phase 1 Flight Tests". In: *AIAA Scitech 2020 Forum*. American Institute of Aeronautics and Astronautics, 2020. DOI: 10.2514/6.2020-1017.

[160] Martin E. Kügler and Florian Holzapfel. "Planning, Implementation, and Execution of an Automatic First Flight of a UAV". In: *31st Congress of the International Council of the Aeronautical Science*. Belo Horizonte, Brazil: ICAS, 2018.

[161] Clyde Warsop and William Crowther. "NATO AVT-239 Task Group: Flight Demonstration of Fluidic Flight Controls on the MAGMA Subscale Demonstrator Aircraft". In: *AIAA Scitech 2019 Forum*. American Institute of Aeronautics and Astronautics, 2019. DOI: 10.2514/6.2019-0282.

[162] Donald T. Ward. *Introduction to flight test engineering*. First. Amsterdam, The Netherlands: Elsevier, 1993. ISBN: 0-444-88147-6.

[163] F. N. Stoliker. "Introduction to Flight Test Engineering". In: *RTO AGARDograph 300, Flight Test Techniques Series* 14 (2005).

[164] Warren Williams and Michael Harris. "The Challenges of Flight-Testing Unmanned Air Vehicles". In: *Systems Engineering, Test and Evaluation Conference*. Sydney, Australia, 2002.

[165] Andrew E. Pontzer, Mark D. Lower, and Jason R. Miller. "Unique Aspects of Flight Testing Unmanned Aircraft Systems". In: *RTO AGARDograph 300, Flight Test Techniques Series* 27 (2010).

[166] Johann C. Dauer, Florian-Michael Adolf, and Sven Lorenz. "Flight Testing of an Unmanned Aircraft System - A Research Perspective". In: *STO Meeting Proceedings STO-MP-SCI-269*. Ottawa, Canada: STO/NATO, 2015. ISBN: 978-92-837-2015-7. DOI: 10.14339/STO-MP-SCI-269.

[167] Lua. *Official web site of the Lua programming language*. 2017. URL: https://www.lua.org/ (visited on 05/25/2017).

[168] A. Knaus. "A technique to determine lift and drag polars in flight". In: *Journal of Aircraft* 20.7 (1983), pp. 587–593.

[169] Adrian Arustei. "Development of a System Identification Tool for Subscale Flight Testing". MA thesis. Linköping University, 2019. URL: http://urn.kb.se/resolve?urn=urn:nbn:se:liu:diva-157292.

[170] Eugene A. Morelli. "System IDentification Programs for AirCraft (SIDPAC)". In: *AIAA Atmospheric Flight Mechanics Conference*. Monterey, CA, USA: AIAA, 2002. ISBN: 978-1-62410-107-6. DOI: 10.2514/6.2002-4704.

[171] Ravindra V. Jategaonkar. "Flight Vehicle System Identification: A Time-Domain Methodology". In: *Progress in Astronautics and Aeronautics*. Second. Vol. Volume 245. Reston, VA, USA: American Institute of Aeronautics and Astronautics, 2015. ISBN: 978-1-62410-278-3. DOI: 10.2514/4.866852.

[172] Juan Carlos Cuevas González. "Implementation of an Aircraft Simulation Model for System Identification in MATLAB". MA thesis. Linköping University, 2017.

[173] Vladislav Klein and Eugene A. Morelli. *Aircraft System Identification: Theory and Practice*. First. Reston, VA, USA: AIAA, 2006.

[174] Akshay Raju Kulkarni, Carmine Varriale, Mark Voskuijl, Gianfranco la Rocca, and Leo Veldhuis. "Assessment of Sub-scale Designs for Scaled Flight Testing". In: *AIAA AVIATION Forum, 17-21 June 2019, Dallas, Texas*. AIAA Aviation 2019 Forum ; Conference date: 17-06-2019 Through 21-06-2019. United States: American Institute of Aeronautics and Astronautics Inc. (AIAA), 2019. DOI: 10.2514/6.2019-3089.

[175] A. Raju Kulkarni, G. L. Rocca, and L. L. M. Veldhuis. "Degree of similitude estimation for sub-scale flight testing". In: *AIAA Scitech 2019 Forum*. 2019. DOI: 10.2514/6.2019-1208.

[176] G. Wang et al. "Research on analytical scaling method and scale effects for subscale flight test of blended wing body civil aircraft". In: *Aerospace Science and Technology* 106 (2020). DOI: 10.1016/j.ast.2020.106114.

[177] Peter Schmollgruber et al. "Towards validation of scaled flight testing". In: *7th CEAS Air and Space Conference, First Aerospace Europe Conference*. 25-28 February, Bordeaux, France: AEC2020, 2020.

[178] T. Mandal and Y. Gu. "Pilot-vehicle system modeling using sub-scale flight experiments". In: *AIAA Modeling and Simulation Technologies Conference*. 2014. DOI: 10.2514/6.2014-1004.

Papers

The papers associated with this thesis have been removed for copyright reasons. For more details about these see:

http://urn.kb.se/resolve?urn=urn:nbn:se:liu:diva-175520

FACULTY OF SCIENCE AND ENGINEERING

Linköping Studies in Science and Technology, Dissertation No. 2127, 2021
Division of Fluid and Mechatronic Systems
Department of Management and Engineering

Linköping University
SE-581 83 Linköping, Sweden

www.liu.se

LINKÖPING
UNIVERSITY